Aus dem Fachbereich Medizin
der Johann Wolfgang Goethe-Universität
Frankfurt am Main

Institut für Biochemie I – Pathobiochemie
Direktor: Professor Dr. Bernhard Brüne

Identification of translationally deregulated proteins during inflammation-associated tumorigenesis

Dissertation
zur Erlangung des Doktorgrades der theoretischen Medizin
des Fachbereichs Medizin
der Johann Wolfgang Goethe-Universität
Frankfurt am Main

vorgelegt von

Daniela Rübsamen
(geb. Gliesing)

aus Leipzig

Frankfurt am Main, 2012

Dekan:	Prof. Dr. Josef M. Pfeilschifter
Referent:	Prof. Dr. Bernhard Brüne
Korreferent:	Prof. Dr. Wolfgang Eberhardt
Tag der mündlichen Prüfung:	06.11.2012

Index

List of figures

List of tables

Abbreviations

4EBP1	4E-binding protein 1
AD	Alzheimer´s disease
AGO	Argonaute protein
AIP2	Atrophin interaction protein 2
Akt	Protein kinase B
AML	Acute myeloid leukemia
AMY1A	Amylase alpha 1A
AP-1	Activator protein 1
APAF-1	Apoptotic peptidase activating factor 1
ARE	AU-rich element
ARE-BP	ARE binding proteins
ATP	Adenosine triphosphate
BAK	BCL2-antagonist/killer
β-Gal	β-Galactosidase
Bcl2	B-cell CLL/lymphoma 2
Bim	Pro-apoptotic bcl-2 interacting mediator of cell death
BiP	Immunoglobulin heavy-chain-binding protein
BNIP3L	Bcl2/Adenovirus E1B 19-KD protein-interacting protein 3-like
BSA	Bovine serum albumin
CBA	Cytometric bead array
Cbl-B	Casitas B-cell lymphoma B
c-Cbl	Cbl proto-oncogene
CD	Cluster of differentation
cFms	Colony stimulating factor
CHX	Cycloheximide
c-IAP	Cellular inhibitor of apoptosis protein
CM	Conditioned medium
CMT1	Charcot-Marie-Tooth syndrome Type 1
cMyc	Cellular Myc
COX-2	Cyclooxygenase 2
CrPV	Cricket paralysis virus
CsA	Cyclosporin A
Ctr	Control conditioned medium

CX32	Connexin 32
CYP24A1	Cytocrome C p450 A1
Ddx20	DEAD (Asp-Glu-Ala-Asp) box polypeptide 20
DMF	Dimethylformamide
DMSO	Dimethyl sulfoxide
DNA	Deoxyribonuceic acid
eEF	Eukaryotic elongation factor
EGR2/3	Early growth response 2/3
eIF	Eukaryotic initiation factors
EMCV	Encephalo myocarditis virus
eRF	Eukaryotic release factor
EV	Empty vector
EWS	Ewing sarcoma breakpoint region
FACS	Fluorescence activated cell sorting
fasL	Fas Ligand
FBS	Fetal bovine serum
FGF	Fibroblast growth factor
FL	*Firefly* luciferase
FLRE	FasL regulatory element
FMR	Fragile X mental retardation syndrome
FMRP	FMR protein
GADD34	Growth arrest and DNA-damage-inducible 34
GAP	GTPase activating protein
GAPDH	Glyceraldehyde-3-phosphate dehydrogenase
GCN2	General control nonrepressed 2
GDP	Guanosine diphosphate
GFRA2	GDNF family receptor alpha 2
GM-CSF	Granulocyte macrophage colony-stimulating factor
GTP	Guanosine triphosphate
h	Hour
HD	Huntington´s disease
Hif1α	Hypoxia inducible factor 1α
hnRNP	Heterogeneous nuclear ribonucleoprotein
hp	Hairpin
HuR	Human antigen R

IGF-1R	Insulin-like growth factor 1 receptor
IGF2	Insulin-like growth factor 2
IgG	Immunoglobulin G
IL	Interleukin
ILF2/3	Interleukin enhancer binding factor 2/3
IMP2/4	IGF2 mRNA-binding protein 2/4
IRES	Internal ribosome entry site
IRF2	Interferon regulatory factor 2
ITAF	IRES *trans*-acting factor
JAK	Janus kinase
JNK	JUN N-terminal kinase
KH	K-homology
L	Liter
M	Molar
m	Milli
m	Meter
m^7G	7-Methyl-gyanylic acid
MAPK	Mitogen activated protein kinase
Mcl1	Myeloid cell leukemia 1
MEK	Mitogen-activated protein kinase kinase
MHC	Major histocompatibility complex
µ	Micro
min	Minute
miRNA	MicroRNA
MKP-1	MAP kinase phosphatase 1
MNK	MAP kinase interacting kinase
mol	Molar
MPZ	Myelin protein zero
mRNA	Messenger RNA
mTOR	Mammalian target of rapamycin
n	Nano
NAB	NFGI-A-binding protein
NF45	Nuclear factor 45
NF-AT	Nuclear factor of activated T cells
NF-κB	Nuclear factor kappa-light-chain-enhancer of activated B cells

NKT	Natural killer T cells
NLS	Nuclear localization sequence
norm.	Normalized
NSP3	Non-structural protein 3
ODC	Ornithine decarboxylase
ORF	Open reading frame
$p21^{Cip1}$	p21 cyclin-dependent kinase inhibitor 1
$p27^{Kip1}$	p27 Cyclin-dependent kinase inhibitor 1
PABP	Poly(A)-binding protein
P-bodies	Processing bodies
PCBP1	Poly(rC)-binding protein 1
PCR	Polymerase chain reaction
PDCD4	Programmed cell death 4
PDK	Pyruvate dehydrogenase kinase 1
PERK	PRKR RNA-like endoplasmic reticulum kinase
PI3K	Phosphatidylinositol-3-kinase
PKC	Protein kinase C
PKR	Protein kinase R
PLAUR	Plasminogen activator urokinase receptor
PLC	Phospholipase C
pri-miRNA	Primary microRNA
PTB	Polypyrimidine tract-binding protein
PTEN	Phosphatase and tensin homolog
PUF	Pumilio/FBF
qPCR	Quantitative PCR
RBD	RNA-binding domain
RBP	RNA-binding protein
rel.	Relative
RISC	RNA-induced silencing complex
RL	*Renilla* luciferase
RLU	Relative light units
RNA	Ribonucleic acid
RNPs	Ribonucleoproteins
RPMI	Roswell Park Memorial Institute

rRNA	Ribosomal RNA
RT	Room temperature
s	Second
S6K	S6 Kinase
SDS-PAGE	Sodium dodecyl sulfate - polyacrylamide gel electrophoresis
SEM	Standard error of the mean
Sirt1	Type III histone deacetylase sirtuin 1
snoRNA	Small nucleolar RNAs
Sox10	Sex determining region Y-box 10
SUMO	Small ubiquitin-like modifier
SV40	Simian-Virus 40
TCR	T cell receptor
TGF-β	Transforming growth factor β
TIA-1	T cell restricted intracellular antigen 1
TK	Thymidine kinase
TNFR2	Tumor necrosis factor receptor 2
TNFα	Tumor necrosis factor α
TPA	12-Tetradecanoyl-phorbol-13-acetate
TRAF1	TNF receptor-associated factor 1
tRNA	Transfer RNA
Ubi	Ubiquitin
UNR	Upstream of N-ras
uORF	Upstream open reading frame
UTR	Untranslated region
UV	Ultraviolet
v	Volume
VDR	Vitamin D receptor
VEGF	Vascular endothelial growth factor
w	Weight
WT	Wildtype
XIAP	X-linked inhibitor of apoptosis
YB1	Y box binding protein 1
ZnF	Zinc finger

1 Summary

The translation of mRNAs into proteins is an elaborate and highly regulated process. Translational regulation primarily takes place at the level of initiation. During initation the eukaryotic initiation factors (eIFs) form a complex that binds to the 5'end of the mRNA to scan for a start codon. Once recognized, the ribosome is recruited to the mRNA and protein synthesis starts. Initiation of translation can basically occur via two distinct mechanisms, i.e. cap-dependent and cap-independent that is mediated via internal ribosome entry sites (IRESs). The former is mediated by a 5'cap structure composed of a 7-methylguanylate which is added to every mRNA during transcription and recruits the initiation complex. IRES-dependent translation involves elements within the 5'untranslated region (UTR) of the mRNA that mostly bind IRES *trans*-acting factors (ITAFs) which associate either with the initiation complex or with the ribosome itself and consequently allow for internal initiation of translation.

During tumorigenesis the demand for proteins is increased due to rapid cell growth, which consequently requires enhanced translation. Many factors that regulate translation are overexpressed in tumors. Moreover, signaling pathways that trigger translation or further hyperactivated by the surrounding tumor microenvironment. This environment is largely generated by infiltration of immune cells such as macrophages that secrete cytokines and other mediators to promote tumorigenesis. As the effects of inflammatory conditions on the translation of specific targets are only poorly characterized, my study aimed at identifying translationally deregulated targets during inflammation-associated tumorigenesis.

For this purpose, I cocultured MCF7 breast tumor cells with conditioned medium of activated monocyte-derived U937 macrophages (CM). Polysome profiling and microarray analysis identified 42 targets to be regulated at the level of translation. The results were validated by quantitative PCR and one target - early growth response 2 (EGR2) - was chosen for in depth analysis of the mechanism leading to its enhanced translation.

In order to identify upstream signaling molecules causing enhanced EGR2 protein synthesis the cytokine profile of CM was analyzed and the impact of several cytokines on EGR2 translation was examined. Preincubation of CM with neutralizing antibodies

revealed that lowering interleukin 6 (IL-6) had only little effect, whereas depletion of IL-1β significantly reduced EGR2 translation. This finding was corroborated by the fact that treatment with recombinant IL-1β enhanced EGR2 translation to virtually the same extend as CM. Further experiments revealed that this effect was mediated via the p38-MAPK signaling cascade.

Interestingly, I observed that the mTOR inhibitor rapamycin, which reduces cap-dependent translation, specifically stimulated EGR2 translation. This result argued for an IRES-dependent mechanism that might account for EGR2 translation. The use of bicistronic reporter assays verified this hypothesis. In line with the above mentioned results, CM, IL-1β and p38-MAPK induced EGR2-IRES activity.

Since IRESs commonly require ITAFs to mediate translation initiation, the binding of proteins to the 5'UTR was analyzed using mass spectrometry. Among others, several previously described ITAFs, such as polypyrimidine tract-binding protein (PTB) and heterogeneous nuclear ribonucleoprotein A1 (hnRNP-A1) were identified to directly bind to the EGR2-5'UTR. Furthermore, overexpression of hnRNP-A1 enhanced EGR2-IRES activity whereas a dominant negative form of hnRNP-A1 significantly decreased it, thus, showing its importance for EGR2 translation.

In summary, my data provide evidence that EGR2 expression can be controlled by IRES-dependent translational regulation, which is responsive to an inflammatory environment. The identified mechanism may not be exclusive for one target but might be representative for gene expression regulation mechanisms during tumorigenesis. This is of special interest for the treatment of cancer patients and development of more specific therapies to reduce tumor outcome.

2 Zusammenfassung

Die Translation von mRNAs in Proteine ist ein komplexer Prozess, der aufgrund seines hohen Energieverbrauchs strikt kontrolliert wird. Die Regulation findet dabei primär auf Ebene der Translationsinitiation statt. Während der Initiation bilden die eukaryotischen Initiationsfaktoren (eIFs) einen Komplex, der an das 5'Ende der mRNA bindet und die 5'untranslatierte Region (UTR) nach einem Startcodon scannt, woraufhin die ribosomalen Untereinheiten an die mRNA rekrutiert werden. Die Ribosomen vermitteln dann die eigentliche Proteinsynthese. Grundsätzlich können zwei verschiedene Arten der Initiation unterschieden werden – die Cap-abhängige sowie die Cap-unabhängige, wobei letztere über sogenannte *internal ribosome entry sites* (IRESs) vermittelt wird. Bei ersterer bindet der Initiationskomplex an die Cap-Struktur der mRNA, die aus einem N-terminalen 7-Methylguanylat besteht. Bei der IRES-vermittelten Initiation bindet der Initiationskomplex oder auch die kleine ribosomale Untereinheit direkt innerhalb der 5'UTR an die mRNA, allerdings in 3'-Distanz zur Cap-Struktur.

Während der Tumorentwicklung kommt es aufgrund des verstärkten Zellwachstums zu einem gesteigerten Bedarf an Proteinen und somit zu erhöhter Translation. Viele Faktoren, die die Translation regulieren, werden in Tumoren überexprimiert oder sind überaktiv. Bei der Aktivierung der entsprechenden Signalkaskaden spielt das Tumormilieu eine zentrale Rolle. Dieses wird insbesondere von Zellen des Immunsystems wie z.B. Makrophagen beeinflusst. Makrophagen setzen dabei Mediatoren frei, welche das Tumorwachstum begünstigen. Während tumorigene Expressionsveränderungen auf Transkriptionsebene bereits detailliert untersucht wurden, gibt es nur wenig Information über Translationsveränderungen spezifischer Proteine. Deswegen war es das Ziel dieser Studie translationell (de-)regulierte Proteine in der entzündungsinduzierten Tumorigenese zu identifizieren.

Dafür kokultivierte ich MCF7 Brustkrebszellen mit konditioniertem Medium von ausdifferenzierten U937 Makrophagen (CM). Die Translationsveränderung in den Tumorzellen wurde mit Hilfe von Polysomenfraktionierungen überprüft. Durch eine aufbauende Mikroarray Analyse wurden 42 mRNAs identifiziert, die translationell reguliert wurden. Die Ergebnisse des Mikroarrays wurden anschließend durch

quantitative PCR validiert und der Regulationsmechanismus eines Targets – *early growth response 2* (EGR2) – im Detail analysiert.

Dafür untersuchte ich den Einfluss verschiedener im CM vorhandener Zytokine auf die EGR2-Translation mittels neutralisierender Antikörper. Es stellte sich heraus, dass die Abreicherung von Interleukin 6 (IL-6) die EGR2-Translationsinduktion durch CM nur minimal verringerte, wohingegen eine Depletion von IL-1β diese signifikant inhibierte. Dieser Befund wurde dadurch unterstützt, dass eine Behandlung mit rekombinantem IL-1β eine ähnlich starke Induktion der EGR2-Translation bewirkte wie CM. Anschließende Untersuchungen ergaben, dass dieser Effekt durch die p38-MAPK Signalkaskade vermittelt wurde.

Desweiteren wurde beobachtet, dass der mTOR-Inhibitor Rapamycin, der die Cap-abhängige Translation hemmt, ebenfalls zu einer verstärkten EGR2-Translation führte. Dies ließ vermuten, dass ein IRES-vermittelter Mechanismus der Translation von EGR2 zu Grunde lag. Durch die Verwendung von bicistronischen Reporter-Vektoren wurde diese Hypothese bestätigt. Außerdem konnte ich beweisen, dass CM, IL-1β und p38-MAPK die EGR2-IRES-Aktivität in der gleichen Art beeinflussten wie bereits für die EGR2-Translation mittels Polysomenfraktionierung gezeigt. Da zelluläre IRES-Elemente oft durch sogenannte *IRES trans-acting factors* (ITAFs) induziert werden, wurden mittels Massenspektrometrie Proteine identifiziert, die an die 5'UTR von EGR2 binden. Unter anderem wurden die bereits bekannten ITAFs *polypyrimidine tract-binding protein* (PTB) und *heterogeneous nuclear ribonucleoprotein A1* (hnRNP-A1) gefunden. Abschließend konnte bewiesen werden, dass die Überexpression von hnRNP-A1 zu einer Erhöhung der EGR2-IRES-Aktivität führte, wohingegen eine dominant-negative Mutante von hnRNP-A1 diese signifikant inhibierte. Diese Ergebnisse ließen darauf schließen, dass hnRNP-A1 einen entscheidenden Einfluss auf die IRES-abhängige EGR2-Translation hat.

Zusammenfassend konnte ich einen neuen Translationsregulationsmechanismus für EGR2 identifizieren, der durch ein entzündliches Tumormikroenvironment in Tumorzellen induziert wird. Dieser Mechanismus ist möglicherweise auch auf weitere translationell regulierte Targets übertragbar. Dies ist von besonderem Interesse, da es für eine optimale Behandlung von Tumorpatienten essentiell ist die zu Grunde liegenden Regulationsmechanismen zu verstehen.

3 Introduction

3.1 Translation

The rapid adaptation of cells to changing conditions is crucial for cell survival. While most of the previous research concentrated on the modulation of gene expression via transcriptional changes, there has been increasing appreciation that likewise the translation of messenger RNAs (mRNAs) to proteins is a highly regulated process. From early embryonic development to cell differentiation and apoptosis, translation is used to quickly adjust protein levels (1-3). Deregulation of translation results in severe cell defects causing diverse maladies such as cancer, diabetes or neurodegenerative diseases (4-6). Therefore, understanding translation and its regulation is essential to prevent pathological procedures.

3.1.1 Translation initiation

The process of translation is divided into three stages – initiation, elongation and termination – each of which requires a particular set of conditions and factors. Initiation is the rate-limiting step, which involves the assembly of the translation initiation complex, including the eukaryotic initiation factors (eIFs) at the 5' untranslated region (5'UTR) of the mRNA to recruit the ribosomes (7, 8). The ribosomes translate the genetic information encoded by mRNAs into proteins and are composed of two subunits comprising ribosomal RNAs (rRNAs) and proteins called ribonucleoproteins (RNPs). The small subunit (40S) binds directly to the mRNA to allow for reading of the codons whereas the large subunit (60S) recruits the transfer RNAs (tRNAs) which are attached to amino acids (9).

Translation is a cyclic process starting with the formation of the 43S ribosome (Figure 3-1), which is comprised of eIF2, a heterotrimetic complex that contains an α-, β- and γ-domain, and the initiating methionyl tRNA ($tRNA_i^{Met}$) (10). Only in its GTP-bound state the 40S ribosomal subunit joins the complex. Simultaneously, eIF4F composed of eIF4E, eIF4A and eIF4G, attaches to the 5'UTR of the mRNA (11). In detail, eIF4E recognizes and binds to the cap-structure consisting of a 7-methyl-guanylic acid residue (m^7G). eIF4G serves as a scaffold protein for eIF4E and eIF4A. eIF4A has

helicase activity to unwind secondary structures of the 5'UTR, thereby facilitating scanning of the mRNA. Additionally, eIF3 binds to eIF4G to finally recruit the 43S ribosome. This initiation complex scans the mRNA for a start codon (AUG) in an optimal context (12). When AUG is recognized, eIF2-GTP is hydrolyzed by eIF5, a GTPase activating protein (GAP), resulting in reduced eIF2 affinity for $tRNA_i^{Met}$ and partial dissociation of eIF2-GDP from 40S subunits. Furthermore, hydrolysis of eIF5B-GTP recruits the 60S large ribosomal subunit to the complex (13), leading to the binding of $tRNA_i^{Met}$ to the peptidyl (P)-site of the ribosome. This results in the complete dissociation of the initiation complex, leaving the active 80S ribosome (40S and 60S subunit) at the initiation codon. eIF5A promotes formation of the first peptide bond and further elongation (14). The inactive eIF2-GDP is recycled to active eIF2-GTP by the nucleotide exchange factor eIF2B to allow for another round of initiation.

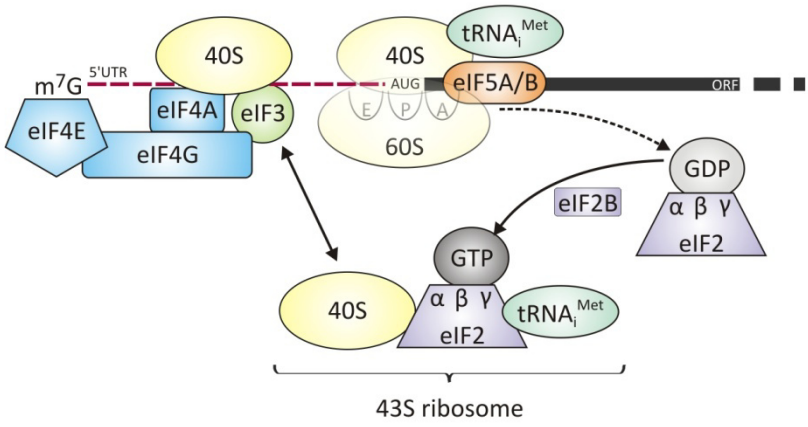

Figure 3-1: Mechanism of cap-dependent translation
During translation initiation eIF4E binds to the m^7G-cap structure of the mRNA. eIF4E is additionally associated with the scaffold protein eIF4G that binds the RNA helicase eIF4A to unwind secondary structures, thereby facilitating scanning of the genetic code. The attached eIF3 recruits the 43S ribosome containing GTP-eIF2, the 40S ribosomal subunit and $tRNA_i^{Met}$. This initiation complex scans the mRNA until the first start codon is detected. When an AUG encoding methionine is recognized, eIF2-GTP hydrolyzes to eIF2-GDP resulting in 60S ribosome recruitment thereby placing AUG to the P-site of the ribosome. Following dissociation of the initiation complex the translation process elongates. Peptide bonding is facilitated via eIF5A. eIF2B converts eIF2-GDP to eIF2-GTP. During elongation the amino acid-attached tRNA that is complementary to the next codon binds to the A-site. After correct matching is checked by eEF1A, the tRNA is transferred to the P-site where a peptide-bond is formed by the peptidyltransferase of the 60S ribosome and finally the mRNA translocates to the E-site where the empty tRNA leaves to ribosome. Abbreviations: A/P/E-site, aminoacyl/peptidyl/exit site; eEF, eukaryotic elongation factor; eIF, eukaryotic initiation factor; GPD, guanosine diphosphate; GTP, guanosine triphosphate; mRNA, messenger RNA; m^7G, 7-methyl-gyanylic acid; ORF, open reading frame; tRNA, transfer RNA; $tRNA_i^{Met}$, initiator methionyl tRNA; UTR, untranslated region.

3.1.2 Translation elongation and termination

Elongation of translation is a three step mechanism. First, the aminoacyl (A)-site of the ribosome is loaded with the appropriate tRNA consistent with the next codon of the mRNA. Each tRNA is escorted by the GTP-bound form of eukaryotic elongation factor 1A (eEF1A-GTP) which controls correct matching of the tRNA to the codon (15). In that case, eEF1A-GTP is hydrolyzed to eEF1A-GDP and leaves the ribosome. eEF1B acts as a nucleotide exchange factor to recycle GDP to GTP (16). Subsequently, the tRNA is transferred to the P-site. The 28S rRNA that belongs to the 60S ribosomal subunit and contains peptidyltransferase activity, attaches the tRNA-associated amino acid to the growing peptide chain by forming a peptide bond. Finally, the empty tRNA moves to the exit (E)-site of the ribosomes enabling the mRNA to slide to the free P-site to clear the A-site for a new tRNA (17). This translocation step is catalyzed by the hydrolysis of eEF2-GTP to eEF2-GDP (18) (Figure 3-1).

When the elongation reaches a stop codon (AUU, UAG, UGA) translation is terminated. These codons do not have complementary tRNAs, instead they are recognized by the eukaryotic release factor (eRF), which is also GTP-associated. When eRF binds to the A-site, the peptidyltransferase transfers an H_2O molecule to the peptide chain, resulting in the release of the newly synthesized protein. eRF-GTP hydrolyzes to eRF-GDP and subsequently the mRNA dissociates from the ribosome, which disassembles to be available for a new round of translation (19).

3.1.3 Regulation of translation

Translation is primarily regulated at the level of initiation rather than elongation or termination. Regulation takes place at multiple levels and is directly linked to the specificity of the regulated mRNA(s). This includes the modulation of initiation factors or ribosomal biogenesis which both affects translation in general. In contrast, RNA-binding proteins (RBPs), microRNAs (miRNAs) or the mRNA itself via upstream open reading frames (uORFs) or structural features such as hairpins or internal ribosome entry sites (IRESs) may target a particular mRNA (Figure 3-2) (20).

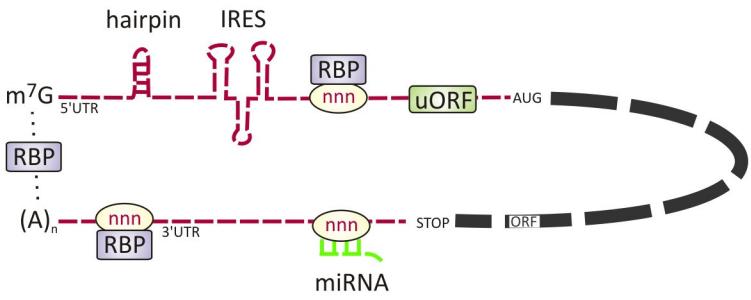

Figure 3-2: Elements that influence translation of mRNAs
The m^7G cap structure at the 5'end and the poly(A) tail at the 3'end are canonical motifs which promote translation initiation. Secondary structures block translation, whereas IRES elements induce translation cap-independently. Upstream hairpins and open reading frames are negative regulators by reducing translation of the main ORF. Yellow ovals symbolize *cis*-acting elements serving as recognition sites for RBPs that can either inhibit or enhance translation. miRNAs mediate mRNA stabilization, decay or translational inhibition. Abbreviations: IRES, internal ribosome entry; m^7G, 7-methyl-gyanylic acid; miRNA, micro RNA; RBP, RNA-binding protein; UTR, untranslated region; uORF, upstream open reading frame

3.1.3.1 Control of initiation factor activity

The phosphatidylinositol-3-kinase (PI3K) pathway is one of the best characterized pathways regulating global protein translation via phosphorylation of various initiation factors as well as the ribosome itself. Mitogenic signals such as growth factors, hormones or cytokines activate protein kinase B (PKB/Akt) by phosphatidylinositol-3-kinase (PI3K) leading to phosphorylation, and thereby activation, of mammalian target of rapamycin (mTOR) (21). In its activated state, mTOR phosphorylates the 4E-binding protein 1 (4EBP1), thereby releasing eIF4E, which allows for efficient cap-dependent translation. Inhibition of mTOR results in a block of 4EBP1 phosphorylation causing sequestration of eIF4E and a failure of initiation complex formation. Moreover, mTOR phosphorylates p70 S6 kinase ($p70^{S6K}$), which in turn phosphorylates the 40S ribosomal subunit, a critical step in translation initiation. $p70^{S6K}$ additionally facilitates the association of eIF4A with eIF4G by promoting the degradation of programmed cell death 4 (PDCD4). PDCD4 is known to inhibit the binding of eIF4A to eIF4G (22).

Another well-established mechanism of broad translation regulation is the control of active eIF2. Different kinases such as protein kinase R (PKR), PRKR RNA-like endoplasmic reticulum kinase (PERK) or general control nonrepressed 2 (GCN2) are known to phosphorylate the α-subunit of eIF2 (23). Phosphorylated eIF2 is fully capable of forming an initiation-competent 43S ribosome, but following release,

phosphorylated eIF2-GDP inhibits the guanine nucleotide exchange activity of eIF2B which is necessary for the joining of the 40S subunit. This can be reversed by the phosphatase growth arrest and DNA-damage-inducible 34 (GADD34).

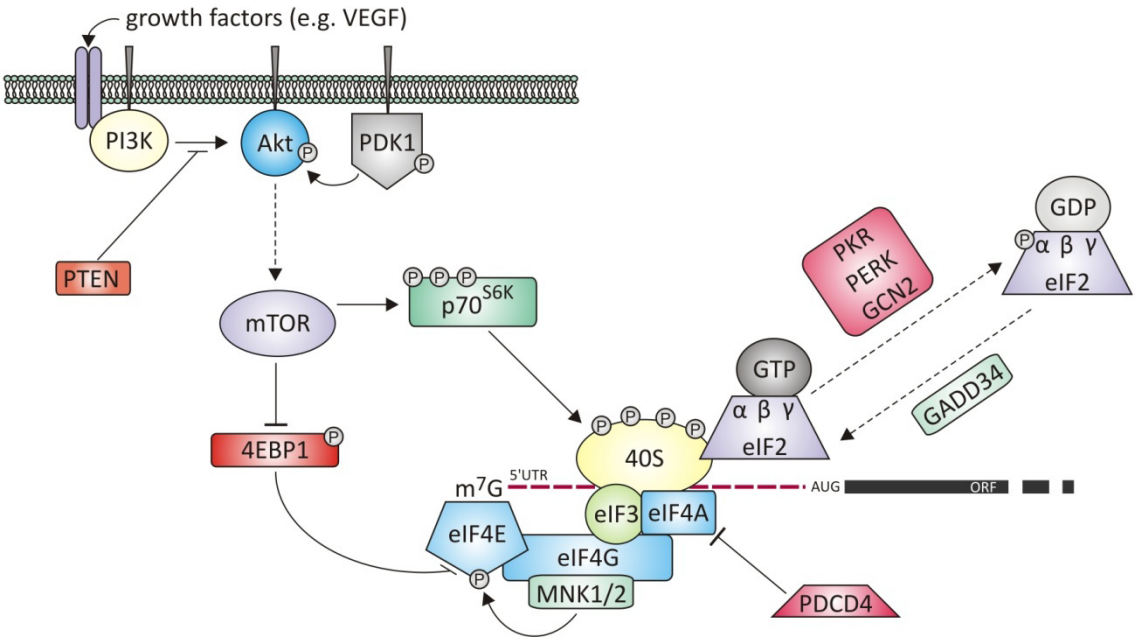

Figure 3-3: Control of initiation factor activity
Growth factors are capable of stimulating the PI3K-Akt-mTOR pathway leading to phosphorylation of $p70^{S6K}$ and 4EBP1. In the hypophosphorylated state, 4EBP1 sequesters eIF4E. When hyperphosphorylated by mTOR, eIF4E is released and binds to the cap-structure. Phosphorylated $p70^{S6K}$ induces phosphorylation of the 40S ribosomal subunit and translation is initiated. eIF2α is subject to inhibitory phosphorylation by PKR, PERK or GCN2 which can be reversed by the phosphatase GADD34. MNK1 and 2 are attached to eIF4G allowing for phosphorylation and activation of eIF4E. PDCD4 targets eIF4A by replacing it from eIF4G. Abbreviations: 4EBP1, 4E-binding protein 1; Akt, protein kinase B; eIF eukaryotic initation factor; GADD34, growth arrest and DNA-damage-inducible 34; GCN2, general control nonrepressed 2; GPD, guanosine diphosphate; GTP, guanosine triphosphate; MNK1/2, MAP kinase interacting kinase 1/2; mTOR, mammalian target of rapamycin; ORF, open reading frame; PDCD4, programmed cell death 4; PDK1, pyruvate dehydrogenase kinase 1; PERK, PRKR RNA-like endoplasmic reticulum kinase; PI3K, phosphatidylinositol-3-kinase; PKR, protein kinase R; PTEN, phosphatase and tensin homolog; S6K, S6 kinase; VEGF, vascular endothelial growth factor; UTR, untranslated region.

eIF4E itself is also subject to phosphorylation by MAP kinase interacting kinases 1 and 2 (MNK1/2). Both are associated with eIF4G which brings them into close proximity with eIF4E, thereby facilitating phosphorylation of the latter. While the phosphorylation event seems to be dispensable for normal development, it is necessary for oncogenic transformation by stimulating the translation of certain oncogenes (see 3.1.4.1) (24). This specificity is not determined by defined sequences,

but by the increased requirement for eIF4E in the translation of mRNAs with long and complex 5' UTRs. The scanning process is severely hampered by secondary structures in the 5′ UTR, i.e. a structure with a free-energy of −50 kcal/mol is sufficient to impose a strong block on scanning (25). Thus, increased availability of eIF4E and associated factors such as eIF4A enhances the translation of some tightly regulated genes, including CyclinD or cMyc (26).

3.1.3.2 Internal ribosome entry sites

As described earlier, most mRNAs utilize the cap-structure to recruit the initiation complex which facilitates scanning of the sequence for the start condon. However, some mRNAs evade the conventional scanning mechanism and at least a subset of eIFs by use of IRES elements to recruit the 40S subunit directly to the initiation region, a process referred to as internal initiation. IRESs are *cis*-acting elements within the 5'UTR of mRNAs.

IRES elements were first described for viruses, as these are able to decrease the translation of cellular mRNAs, for example via cleavage of eIF4G which accounts for inhibition of host protein synthesis, favouring cap-independent translation of viral proteins by internal initiation (27). Up to now a consensus sequence has not been identified for IRESs, instead secondary structures are considered to be responsible for the formation of an IRES element. These structures form a scaffold that contains multiple interaction sites for components of the translation apparatus, e.g. the IRES of encephalo myocarditis virus (EMCV) interacts with eIF4G (28), whereas the IRES of cricket paralysis virus (CrPV) can directly interact with the 40S ribosome without the aid of any initiation factors (29).

The first eukaryotic IRES was identified in 1991 within the 5'UTR of immunoglobulin heavy-chain-binding protein (BiP). Its translation was shown to be sustained during poliovirus infection although several initiation factors were cleaved (30). Since this initial discovery, the list of mRNAs described to contain IRES elements has been growing steadily (see Table 3-1), and *in silico* analyses estimate that up to 10% of cellular mRNAs may contain an IRES element (31). Their protein products are mostly involved in the control of cell growth, proliferation and apoptosis (32). While no common structural features have been found for cellular IRESs, it has been

hypothesized that cellular IRESs are composed of multiple short modules that include structural features as well as sites for RNA-binding proteins and the combined effect of these modules promotes internal initiation of translation (32).

Table 3-1: List of selected eukaryotic IRES containing mRNAs

mRNA	ITAF	Function	Reference
APAF-1	PTB	apoptosis	(33)
Bcl2	Dap5	cell survival	(34)
CyclinD1	hnRNP-A1	cell cycle	(35)
CyclinT1	PTB	cell cycle	(36)
c-IAP1	NF45	cell survival	(37)
cMyc	PTB, YB1, hnRNP-K/-A1	cell survival	(35, 38, 39)
FGF2	hnRNP-A1	proliferation	(40)
Hif1α	PTB	cell survival/angiogenesis	(41)
IGF-1R	PTB	proliferation	(42)
IGF2	IMP2	proliferation	(43)
IRF2	PTB	proliferation	(44)
$p27^{Kip1}$	PTB	cell cycle arrest	(45)
p53	PTB	apoptosis/cell cycle arrest	(46)
TRAF1	PTB	cell survival	(47)
VEGF	hnRNP-A1	angiogenesis	(40)
XIAP	hnRNP-A1/C1/2, La	apoptosis	(48-50)

Abbreviations: APAF-1, apoptotic peptidase activating factor 1; Bcl-2, B-cell CLL/lymphoma 2; c-IAP1, Cellular inhibitor of apoptosis protein 1; cMyc, cellular myc; Dap5, Death-associated protein 5; FGF2, fibroblast growth factor 2; Hif1α, hypoxia inducible factor 1α; hnRNP, heterogeneous nuclear ribonucleoprotein; IGF-1R, insulin-like growth factor 1 receptor; IGF2, insulin-like growth factor 2; IMP2, IGF2 mRNA-binding protein 2; IRF2, interferon regulatory factor 2; ITAF, IRES *trans*-acting factor; La, autoantigen La; NF45, nuclear factor 45; $p27^{Kip1}$, cyclin-dependent kinase inhibitor p27; PTB, polypyrimidine tract-binding protein; TRAF1, TNF receptor-associated factor 1; VEGF, VEGF, vascular endothelial growth factor; XIAP, X-linked inhibitor of apoptosis; YB1, Y box binding protein 1.

The activation of cellular IRESs predominantly arises from inhibition of cap-dependent translation. E.g. when mTOR is inhibited during hypoxia, nutrient deprivation or mitosis, hypophosphorylated 4EBP1 sequesters eIF4E, which can not bind to the cap-structure of mRNAs anymore and consequently cap-dependent translation is repressed. In order to maintain the translation of survival genes, protein synthesis switches from cap- to IRES-dependent translation. Therein different mechanisms are

known, for example via direct interaction of eIF4G or the 40S ribosome itself with the IRES (51).

However, the mere presence of an IRES within a gene does not necessarily account for translation of the mRNA during stress. In fact, IRESs themselves can be subject to regulation. For example binding of IRES *trans*-acting factors (ITAFs) results in a conformational change of the mRNA, facilitating the binding of initiation factors (Figure 3-4). Specifically, the polypyrimidine tract-binding protein (PTB) has been proposed to act as a general ITAF that is necessary for the activity of many cellular IRESs (52). Additionally, tissue-specific regulation of internal initiation has also been reported probably due to differential expression of specific ITAFs (33).

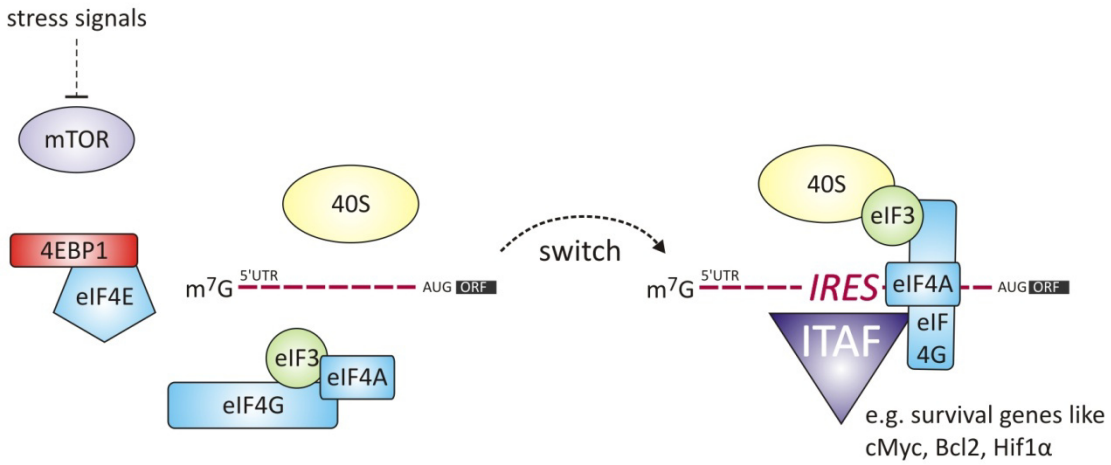

Figure 3-4: IRES-dependent initiation of translation
Stress signals lead to the inhibition of mTOR and consequently repression of cap-dependent translation. To maintain the translation of survival genes IRES elements within the 5'UTR of mRNAs can internally initiate translation. Initiation factors either bind directly to the IRES or via ITAFs which induce conformational changes of the RNA structure. Abbreviations: 4EBP1, 4E-binding protein 1; Bcl2, B-cell CLL/lymphoma 2; eIF, eukaryotic initation factor; Hif1α, hypoxia inducible factor 1α; IRES, internal ribosome entry site; ITAF, IRES *trans*-acting factor; mTOR, mammalian target of rapamycin; ORF, open reading frame; UTR, untranslated region.

Strikingly, ITAFs are predominantly located in the nucleus. However, since these proteins are known to shuttle between nucleus and cytoplasm, they can influence internal initiation. In line, it was proposed that the "nuclear experience" is important for sufficient translation via an IRES. Even though IRES-mediated translation occurs in the cytoplasm, increasing evidence has shown that gene expression steps are interconnected from transcription to translation (53).

3.1.3.3 RNA-binding proteins

Many eukaryotic mRNAs contain conserved RNA sequence motifs in their UTRs that can be targeted by RBPs. A rough distinction can be made between global and mRNA specific translational control mediated by RBPs. An important positive regulator of global translation is the poly(A)-binding protein (PABP) that associates with the 3'poly(A) tail of the mRNA. The stimulatory effect is due to the potential of PABP to interact with the 5'UTR-bound eIF4G resulting in a circularization of the mRNA (54) which facilitates ribosome recycling. Additionally, eIF4G remains tethered to the mRNA and is not needed to be recruited *de novo* from the free eIF4G pool. Therefore, PABP is sometimes denoted as canonical initiation factor.

However, RBPs usually mediate inhibition of translation rather than activation. Negative regulation by protein-RNA interactions in the 5'UTR is rare, as it is assumed that RBPs are displaced by the initiation complex during scanning (55). Since the 3'UTR of an mRNA is not scanned and - in most cases - relatively long, it offers space for regulatory elements. RBPs alter translational efficiency either directly or indirectly by bridging proteins on the mRNA. They may also tag mRNAs for rapid deadenylation or degradation. Yet, the molecular mechanisms of translational control have only been elucidated in few cases.

RBPs contain one or, more often, multiple RNA-binding domains. Some well-characterized RNA-binding domains include RNA-binding domain (RBD), K-homology (KH) domain, RGG (Arg-Gly-Gly) box, zinc finger (ZnF) Pumilio/FBF (PUF) domain and AU-rich element domain (ARE) (56). The latter interacts with AU-rich sequences in the 3'UTR to regulate localization, translation and degradation of mRNAs encoding growth-response genes, cytokines and cell cycle regulatory proteins (57).

3.1.3.4 MicroRNAs

MicroRNAs (miRNAs) are small, non-coding RNA strands composed of 21 nucleotides that bind to the 3'UTR of their target mRNAs. They control approximately 25% of all cellular mRNAs at the posttranscriptional level (58). Mammalian miRNA genes are transcribed by polymerase II from mono- and polycistronic gene clusters resulting in large primary mRNA precursors (pri-miRNAs) that contain hairpin structures

harbouring the mature miRNA as duplices (59), which are excised by the RNases Drosha and Dicer (60).

Once processed from its transcript precursor, one strand of the miRNA duplex which is complement to the target mRNA is loaded into a protein complex, referred to as RNA-induced silencing complex (RISC), including members of the Argonaute protein family (AGO) and the RNase Dicer. It acts via two distinct mechanisms, which may not be exclusive, namely repression of translation or degradation of the target mRNA. The degree of miRNA-mRNA complementarity has been considered to be a key determinant of the regulatory mechanism. Perfect complementarity allows Ago-catalyzed cleavage of the mRNA strand, whereas central mismatches exclude cleavage and promote repression of mRNA translation (61).

Repression of translation by miRNAs occurs either by inhibition of translation initiation or elongation. The former is caused by the competition between RISC and eIF4E for binding to the mRNA cap (62), stimulation of deadenylation of the mRNA tail (63) or a blockade of the association of the 60S ribosomal subunit with the 43S preinitiation complex (64). Inhibition of elongation involves the promotion of termination by RISCs that cause a drop-off of translating ribosomes during elongation (65).

Once mRNA translation is inhibited, the components that are involved in miRNA-mediated repression concentrate in processing (P)-bodies. These are suggested to be sites where mRNAs are sequestered from the translation machinery. Since P-bodies contain decapping enzymes and exonucleases, mRNAs are degraded (66). P-bodies are closely related to stress granules, which accumulate in response to various stress conditions (67) and contain nucleases. Eventually, P-bodies and stress granules are places to sort translationally inactive mRNAs for storage, reinitiation or degradation (58).

3.1.3.5 Upstream open reading frames

About 45-50% of mammalian genes encode mRNAs that have at least one upstream open reading frame (uORF) located in 5’ distance of the main protein coding ORF (68). Ribosomes associated with short uORFs (< 30 codons) resume scanning and reinitiation at downstream ORFs. With increasing length and structure of the uORF the translation of the main ORF is inhibited suggesting a time-dependent mechanism of action (69,

70). Assumably, this is due to the fact that eIF3 and eIF4G remain weakly associated with ribosomes during translation of short uORFs and these factors then promote the resumption of scanning leading to reinitiation. This semistable binding is lost after enduring scanning of the uORF preventing reinitation (71).

Another prominent mechanism of translational inhibition involves the amino acid sequence of the peptide that is encoded by the uORF which may interact with the release factor eRF1 to block polypeptide hydrolysis leading to a blockage of the ribosome at the stop codon (72). Translation can also be inhibited by the presence of a GC-rich sequence surrounding the stop codon of the uORF promoting ribosome dissociation (73).

3.1.4 Translation and disease

The regulation of translation is a central mechanism to control protein availability in the cell. Therefore, aberrant function of components of the translation machinery may provoke a variety of human diseases, including cancer and metabolic disorders.

3.1.4.1 Translation and cancer

Many cancers are caused by dysregulation of signaling pathways controlling cell growth and proliferation. Obviously, these pathways also affect translation. The most prominent example is the earlier discussed PI3K-Akt pathway which activates mTOR and is constitutively active in various tumor types promoting cellular growth, proliferation and survival (74). Hyperactivation of mTOR consequently results in enhanced translation via induction of the downstream activated initiation factors. Interestingly, the most affected targets by this mechanism are those that have long and highly structured 5'UTRs which are often found in survival genes such as CyclinD1, cMyc or ornithine decarboxylase (ODC) (75). This is due to the fact that these mRNAs have weaker ability to compete for eIF4F for either ribosome recruitment or mRNA unwinding compared to mRNAs with short 5'UTRs. Overexpression of the cap-binding protein eIF4E also accounts for this effect and has been observed in multiple tumor types (76). Moreover, the phosphorylation status of 4EBP1 is used as a prognostic

marker in endometrial cancer, especially the hyperphosphorylated, i.e. inhibited form of 4EBP1 reflects poor prognosis (77).

The helicase eIF4A has been reported to be overexpressed in hepatocellular carcinoma (78) and primary melanoma cell lines (79). Additionally, it is an important mediator of the transforming potential of other initiation factors. In line, the tumor suppressor PDCD4 acts via inhibition of eIF4A by replacing it from eIF4G (22) and is lost in certain tumors (80). While mTOR inhibitors are already in clinical use for renal cell carcinomas (81), current approaches concentrate on identifying more specific compounds to target for example PDCD4 or eIF4E (82, 83).

The development and growth of tumors is challenged by multiple stress situations such as hypoxia, nutrient deprivation or apoptosis, which would usually shut down protein synthesis due to inhibition of mTOR. Yet, it was observed that the translation of various survival genes is maintained via cap-independent that is IRES-dependent translation. This often requires high levels of eIF4G, which binds to many cellular IRESs to recruit the ribosome. Indeed, eIF4G together with 4EBP1 was found to be overexpressed in inflammatory breast cancer (84, 85). This induces a hypoxia-activated switch from cap-dependent to IRES-dependent mRNA translation promoting tumor angiogenesis and growth by inducing translation of selective mRNAs such as vascular endothelial growth factor (VEGF) and hypoxia inducible factor 1α (Hif1α). Another well investigated target to be IRES-dependently translated during tumorigenesis is the oncogene cMyc (86). 42% of patients with multiple myeloma have a C to T mutation in the cMyc-IRES sequence that results in increased cap-independent translation due to enhanced binding of the ITAF hnRNP-K (87) that facilitates IRES-dependent translation. Another strategy for tumor promotion is the circumvention of apoptosis via enhanced IRES-dependent translation of the anti-apoptotic protein X-linked inhibitor of apoptosis (XIAP) (88). Increased IRES-dependent translation of XIAP occurs in myeloma cells thereby contributing to radiation and drug resistance (89). Consequently, the development of selective inhibitors of translation is of great interest for future tumor therapy.

3.1.4.2 Translation and inflammation

Cancer is often associated with inflammation (90). Monocytes and macrophages represent an important immune cell population that infiltrates tumors and contributes to tumor progression. In invasive breast carcinomas these cells can comprise more than 50% of the total tumor mass (91). Among others, they support tumor growth by the secretion of various growth factors, such as fibroblast growth factor (FGF2) or VEGF (92). The production of such mediators can be regulated at multiple levels, including gene transcription, mRNA translation and protein degradation. FGF2 and VEGF were shown to contain IRES elements in their 5'UTR to induce protein synthesis especially under hypoxic conditions to counteract insufficient vascular supply which often occurs in growing tumors (93, 94).

Many other targets of the inflammatory response contain AREs in their 3'UTR and provide binding sites for *trans*-acting factors. Most of these mRNAs are subjected to degradation (95). However, some ARE-binding proteins (ARE-BPs) exert their function through translational repression or activation of the target mRNA. T cell restricted intracellular antigen 1 (TIA-1) binds specifically to the AREs of tumor necrosis factor α (TNFα) and cyclooxygenase 2 (COX-2) causing translational silencing (96, 97) via promoting the assembly of stress granules. Another prominent ARE-BP is Human antigen R (HuR). By binding to MAP kinase phosphatase 1 (MKP-1) mRNA to induce its translation, HuR suppresses the function of immune cells. Moreover, it targets transforming growth factor β (TGF-β) mRNA, thereby enabling advanced-stage tumor cells to escape immune recognition (98). In addition, VEGF contains an ARE in its 3'UTR which is targeted by HuR and increases VEGF mRNA stability (99). HuR also binds to the 5'UTR of certain mRNAs thereby functioning as an ITAF e.g., to induce IRES-dependent translation of XIAP (100).

Thus, targeting ARE-BPs may provide a new avenue for the development of therapeutic tools for the treatment of chronic inflammatory conditions and related cancers.

3.1.4.3 Translation and virus infection

Viruses are dependent on the host´s translational apparatus to synthesize their proteins. To gain access to the cellular translation machinery and to counteract host

defense mechanisms, they manipulate cellular signal transduction pathways to control the activity of initiation factors. Some viruses impair host translation by removing key structural elements in the mRNA, such as the cap, by inactivating eIF4F subunits or by manipulating eIF4F-binding proteins. Thus, synthesis of host defense molecules antagonizing viral replication is prevented (101). Picornavirus, for example, inhibits host translation via cleavage of eIF4G, while viral RNA translation is independent of eukaryotic initiation factors as they utilize IRES elements in their mRNAs (102).

Interestingly, some viruses (e.g., Herpes simplex) enhance cellular translation via induction of eIF4F assembly to promote proliferation of quiescent cells thereby promoting reactivation of latent virus infections (103). Furthermore, Herpes simplex virus impairs translation of selected host mRNAs by using viral encoded miRNAs, which inhibit the translation of cellular mRNAs that are required for apoptosis (104). Rotaviruses encode the non-structural protein 3 (NSP3) that binds to eIF4G and thereby prevents interaction with PABP (105). Moreover, NSP3 associates with the 3'end of rotavirus mRNA resulting in its circularization.

As described before, many strategies of regulating translation were firstly identified in viruses (e.g. IRES-dependent translation), and were later shown to be present in eukaryotic cells as well.

3.1.4.4 Translation and neurodegenerative disease

The importance of translation has also been shown for learning and memory functions of the mammalian brain (106). Consequently, it has been implicated in neuronal diseases. The fragile X mental retardation syndrome (FMR) is a disorder which is manifested by mild to severe mental retardation and connective tissue abnormalities. It is caused by mutated or weakly expressed FMR protein (FMRP), which is an RNA-binding protein that normally inhibits the translation of mRNAs whose products have critical roles in synaptic plasticity. Recently, it has been shown that FMRP binds to eIF4E, thus displacing eIF4G and inhibiting translation (107). FMRP also appears to regulate translation by acting on RISC and miRNAs such as miR-125a (108).

Activation of the eIF2α-inhibiting kinase PKR has been implicated in Alzheimer´s (AD) and Huntington´s diseases (HD). PKR was found to bind to the expanded CAG region of mutant huntingtin mRNA. CAG repeats form highly stable hairpins that bind to and

activate PKR. Its activation increases in a repeat-dependent manner (109). It was hypothesized that activation of PKR may be a common mechanism in the pathology of such trinucleotide repeat diseases and that polyglutamine diseases may include a pathological RNA mechanism in addition to the expression of toxic polyglutamine proteins (110). In AD, activated PKR has been shown to be associated with the amyloid β deposits that are thought to be the fundamental cause of the disease (111). Subsequent phosphorylation of eIF2α suggests the involvement of a stress response mechanism in HD and AD that includes the modulation and/or shutdown of protein synthesis followed by the malfunction of affected cells (112). To clarify the exact up- and downstream events of PKR activation in this context will be of utmost interest.

3.2 Early growth response 2

Early growth response 2 (EGR2, also known as Krox20) was firstly described in 1988 and belongs to the family of early growth response genes 1 to 4 (113). Their name originates from a study where they were found to be upregulated rapidly after serum stimulation of quiescent mouse fibroblasts (114). EGRs are transcription factors containing three tandem C_2H_2-type zinc fingers which bind to GCGGGGCG elements in promoter regions to regulate transcription. Although the zinc finger-binding domains of the EGR family members are virtually identical, the remaining domains differ significantly, implying unique functions for each of these transcription factors (115).

Recently, it has been proven that EGR2 functions as an E3 ligase that sumoylates its coregulators (116). Sumoylation is a posttranscriptional modification of proteins by small ubiquitin-like modifier (SUMO) and regulates many processes in eukaryotic cells such as nuclear transport, transcription, chromosome segregation and DNA repair (117). The activity of EGR family members is modulated in part by NGFI-A-binding protein 1 and 2 (NAB1/2) and DEAD (Asp-Glu-Ala-Asp) box polypeptide 20 (Ddx20) (118-120). Sumoylation of NAB2 by EGR2 modulates its transcriptional activity in a negative feedback loop.

Various functions for EGR2 have been described such as its role in the activation of T cell anergy, brain development and cell survival, which will be described in the next section.

3.2.1 EGR2 and T cells

The activation of T cells is tightly controlled by positive and negative regulatory stimuli. One negative regulatory mechanism is the induction of T cell anergy, which is characterized by a long-term hyporesponsiveness that occurs when T cells are stimulated via their T cell receptors (TCR) in the absence of an appropriate costimulation (121). EGR2 was shown to play a crucial role in this process (Figure 3-5).

EGR2 is a target gene of nuclear factor of activated T cells (NF-AT), a transcription factor that is essential for regulating immune responses (122). NF-AT is activated upon calcium influx by dephosphorylation via calcineurin whereupon it translocates into the nucleus. Macian et al. proposed that under activating conditions NF-AT cooperates with activator protein 1 (AP-1) in order to promote gene expression to enhance T cell function, e.g. through production of IL-2, IL-4 or granulocyte macrophage colony-stimulating factor (GM-CSF) (122). Under suboptimal activating conditions, i.e. in the absence of costimulatory molecules (such as CD28), expression of genes dominates that are induced by NF-AT alone (123). The expression of EGR2 meets these criteria. NF-AT was shown to bind to the promoter region of EGR2 to induce its transcription. Thus, EGR2 represents a unique negative regulatory arm of TCR-induced NF-AT activation (124).

The mechanisms whereby EGR2 triggers T cell anergy are not fully elucidated. However, recent work indicates that EGR2 induces the E3 ligase Casitas B-cell lymphoma B (CBLB) (124), which promotes the ubiquitination and subsequent degradation of key signaling components that activate T cells, such as phospholipase C (PLC) and protein kinase C (PKC) (125, 126).

Additionally, EGR2 inhibits IL-2 promoter activity. IL-2 is produced by T cells in response to antigenic or mitogenic stimulation to induce their proliferation in an autocrine loop and thus, regulates the immune response (127). T cell anergy is induced when IL-2 is absent. While EGR1 has been associated with T cell activation by promoting the upregulation of both IL-2 and the IL-2β receptor (128, 129), EGR2 was proposed to counteract this mechanism. Indeed, EGR2 together with EGR3 inhibits T cell function by blocking IL-2 production via repression of EGR1 and its co-activator NAB2 (130). IL-2 is further repressed via EGR2-dependent transcription of the type III histone deacetylase sirtuin 1 (Sirt1), a suppressor of both innate and adoptive immune

responses (131). Sirt1 subsequently mediates deacetylation and thereby repression of the transcription factors AP-1 and nuclear factor kappa-light-chain-enhancer of activated B cells (NF-κB) leading to reduced expression of IL-2 in anergic cells (132). Moreover, EGR2 binds to the *fasL* regulatory element (FLRE) in the promoter region of *fasL* and induces its transcription (133). The cell surface molecule Fas and its ligand FasL are required for the activation-induced T cell death to delete T cells that are no longer needed (134). EGR2 overexpression alone is sufficient to induce FasL. This effect is antagonized by the E3 ubiquitin ligase atrophin interaction protein 2 (AIP2) which mediates EGR2 ubiquitination and subsequent degradation, resulting in the inhibition of EGR2-driven FasL expression and thereby reducing apoptosis rates (135).

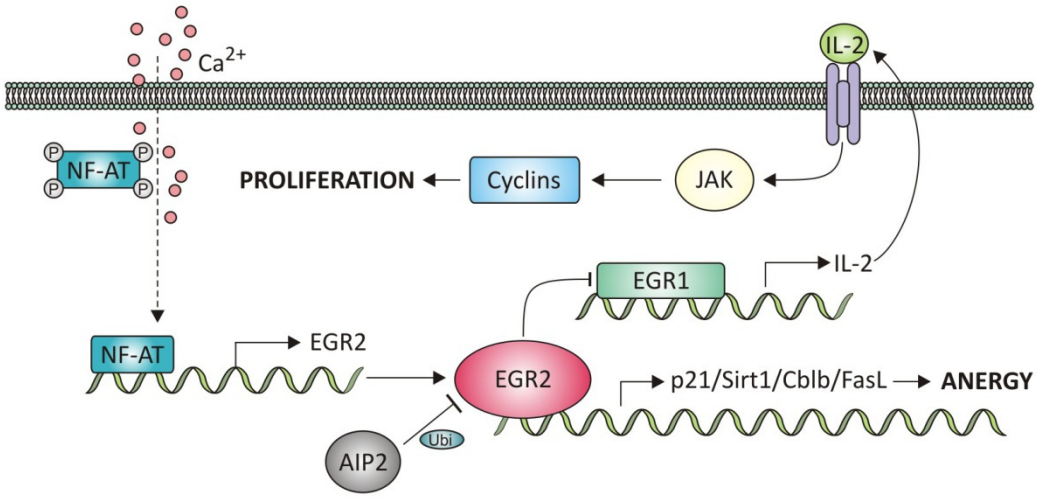

Figure 3-5: The role of EGR2 in T cell anergy
Upon calcium influx NF-AT is dephosphorylated and enters the nucleus to induce transcription of EGR2. EGR2 itself is a transcription factor for various T cell anergy-inducing genes, such as p21, Sirt1, CBLB and FasL. It also inhibits EGR1, consequently repressing IL-2. IL-2 is a potent inducer of T cell activation. Upon secretion it binds to the IL-2 receptor in an autocrine feedback loop. IL-2 receptor signals via the JAK/Stat pathway and induces transcription of the pro-proliferative Cyclins. EGR2 is degraded upon ubiquitination by AIP2. Abbreviations: AIP2, atrophin 1 interacting protein 2; CBLB, casitas B-cell lymphoma B; EGR1/2, early growth response 1/2; FasL, Fas ligand; IL-2, interleukin 2; JAK, janus kinase; NF-AT, nuclear factor of activated T-cells; p21, p21 cyclin-dependent kinase inhibitor 1; Sirt1, type III histone deacetylase sirtuin 1; Ubi, ubiquitin.

Zhu et al. showed that EGR2 controls the proliferation and tolerance of T cells via induction of p21 cyclin-dependent kinase inhibitor 1 ($p21^{Cip1}$) expression by direct binding to the promoter (136). Loss of EGR2 in T cells causes the lupuslike syndrome in mice, an autoimmune disease that is characterized by massive infiltration of

inflammatory cells into the kidney and other organs resulting in severe tissue damage. These findings again demonstrate the importance of EGR2 for the maintenance of T cell tolerance, thus, providing a potential target for the treatment of autoimmune diseases.

Another interesting observation is the requirement of EGR2 during positive selection of T cells in the thymus. T cells derive from hematopoietic stem cells in the bone marrow and infiltrate the thymus where they differentiate to thymocytes. 98% of thymocytes die during development due to selection processes ensuring that only immunocompetent T cells leave the thymus that do not have autoimmune potential. One of these steps involves the selection for T cells capable of interacting with major histocompatibility complex (MHC), referred to as positive selection. Only those thymocytes that interact with MHC-I or MHC-II will receive a "survival signal" for example via induction of pro-survival genes. Otherwise they die by apoptosis. EGR2 induces the pro-survival protein B-cell lymphoma 2 (Bcl2) during this process. Interestingly, deletion of EGR2 in thymocytes impairs positive selection, whereas simultaneous overexpression of Bcl2 rescues this defect (137). Moreover, sustained EGR2 expression is induced downstream of TCR signalling in precursor natural killer T (NKT) cells (138). In line, the absence of EGR2 significantly reduces the percentage and absolute number of NKTs at all stages of maturation (139).

3.2.2 EGR2 and myelination

Myelination of nerves is mediated by axonal signals that trigger a program of differentiation in Schwann cells to generate the myelin sheath, one of the most highly specialized cellular structures in the body allowing saltatory nerve conduction (140).

Mutations in the *EGR2* gene prevent Schwann cell development and peripheral nerve myelination in mice and lead to the development of demyelinating neuropathy (141). In humans, a hereditary defect in the *EGR2* gene causes congenital hypomyelinating neuropathy and type 1 Charcot-Marie-Tooth syndrome (CMT1) (142). CMT1 patients suffer from severe weakness, atrophy and sensory loss in distal muscles due to segmental demyelination as well as axonal loss (143).

EGR2 controls myelin protein expression directly or in conjunction with sex determining region Y-box 10 (Sox10) (144). In doing so, EGR2 promotes cell survival by

protecting cells from TGF-β-mediated cell death and induces differentiation via enhanced expression of the cell cycle inhibitor cyclin-dependent kinase inhibitor p27 ($p27^{Kip1}$), which is at least in part mediated by the activation of p38 mitogen activated protein kinase (p38-MAPK) and inhibition of the JUN N-terminal kinase (JNK) pathway (145, 146). Other putative EGR2 target genes include myelin proteins and enzymes required for synthesis of normal myelin lipids including myelin protein zero (MPZ), which is the most abundant protein component of peripheral myelin and necessary for the formation of compact myelin (147, 148).

3.2.3 EGR2 and cell survival

The role of EGR2 in the regulation of cell survival is poorly understood and studies are contradictory. EGR2 was identified to be higher expressed in endometrial cancer cell lines that overexpressed the tumor suppressor phosphatase and tensin homolog (PTEN) (149), suggesting EGR2 to be a target of the latter. In line, exogenous overexpression of EGR2 resulted in reduced colony numbers of endometrial and ovarian cancer cell lines while inhibition of EGR2 accelerated cell growth (150). The same group identified the pro-apoptotic proteins Bcl2/Adenovirus E1B 19-KD protein-interacting protein 3-like (BNIP3L) and BCL2-antagonist/killer (BAK) as direct target genes of EGR2 leading to the release of cytochrome C, as well as activation of caspase 9 and 3. EGR2 was also proposed to be a direct target gene of the tumor suppressor p53 (151) and compared to normal tissues it was found to be less expressed in a panel of tumor cell lines. However, somatic mutations in the *EGR2* gene were not observed.

In contrast, EGR2 expression was shown to be higher in uterine leiomyomata compared with matched healthy myometrial tissues (152). Interestingly, anti-apoptotic functions of EGR2 have also been described in osteoclasts (153). Macrophage colony-stimulating factor (M-CSF) induces MAPK kinase (MEK)-dependent EGR2 expression resulting in the upregulation of the pro-survival myeloid cell leukemia 1 (Mcl1), while stimulating proteasome-mediated degradation of the pro-apoptotic Bcl-2 interacting mediator of cell death (Bim) by the E3 ubiquitin ligase Cbl proto-oncogene (c-Cbl). Consequently, overexpression of EGR2 increases osteoclast survival. Contradictory, $EGR2^{+/-}$ preosteoclasts show accelerated proliferation and cell cycle progression, likely due to increased colony stimulating factor 1 receptor (cFms) expression, which is a

macrophage- and monocyte-specific growth factor (154). This suggests a role of EGR2 in the control of bone mass and a possible target in high-turnover osteoporosis.

Additionally, EGR2 was identified to be a target gene of the transcription factor SFFV proviral integration 1 (PU.1) in macrophages. In this context, EGR2 facilitates differentiation via inhibition of the miR-17-92 cluster that blocks $p21^{Cip1}$ and Bim post-transcriptionally (155). Moreover, EGR2 itself is also targeted by miR-17-92. Since miR-17-92 is often overexpressed in peripheral blood mononuclear cells of patients suffering from acute myeloid leukemia (AML), EGR2 is simultaneously downregulated and potentially causes a block in differentation.

These observations indicate an important role for EGR2 in proliferation, cell survival and apoptosis. However, only few studies have been conducted and further research is needed to clarify its impact.

3.3 Aims of the study

Deregulated translation is well appreciated to be a crucial component of cancer development and progression. However, little is known about the corresponding stimuli, especially in the context of inflammation-induced tumorigenesis. Therefore, the present study aimed at identifying translationally regulated mRNAs in cancer cells that are challenged by an inflammatory microenvironment.

For this purpose, I cocultured breast tumor cells with activated macrophages. In the first part of my work I performed polysome profiling, microarray analysis and subsequent validation to reveal genes that are regulated at the level of translation.

The second part of my project concentrated on the elucidation of the mechanism underlying the translational regulation of one chosen target. Therefore, the responsible cytokines and corresponding signaling pathways, as well as contributing RNA-binding proteins were investigated. In this context, I specifically focused on the mode of translation leading to enhanced protein synthesis of the investigated target.

This study provides new insights into the modulation of protein expression in cancer cells under inflammatory conditions, thus, expanding the comprehension of translational (dys-) regulation during physiological and pathological processes.

4 Material and Methods

4.1 Material

4.1.1 Cells

All cell lines came from LGC Standards GmbH (Wesel).

U937 cells

U937 malignant cells were derived from the pleural effusion of a 37-year-old Caucasian man with histiocytic lymphoma 1974 (156).

MCF7 cells

MCF7 human breast adenocarcinoma cells were derived from the pleural effusion of a 69-year-old Caucasian woman with metastatic mammary carcinoma in 1970 (157).

4.1.2 Bacteria

Competent bacteria strains were provided by Stratagene GmbH (Amsterdam, The Netherlands). XL1-Blue® supercompetent cells were generally used for amplification. Ligation reactions were transformed in XL10-Gold® ultracompetent cells.

4.1.3 Chemicals and reagents

All chemicals were of highest grade of purity, commercially available and usually purchased from Sigma-Aldrich (Deisenhofen), Roth (Karlsruhe) or Merck Eurolab (Darmstadt). Cell culture media, FBS GOLD and supplements came from PAA (Cölbe). Special reagents and kits are listed in the table below.

Table 4-1: Chemicals

Chemical/Kit	Provider
5’ end tag labeling kit	Axxora (Lörrach)
5x passive lysis puffer	Promega (Mannheim)
6x DNA loading dye	Invitrogen (Karlsruhe)
Absolute™ qPCR SYBR® Green Fluorescein Mix	ABgene (Hamburg)
Anti-IL-1β	R&D Systems (Wiesbaden)
Anti-IL-6	R&D Systems (Wiesbaden)

β-Galactosidase enzyme assay system	Promega (Mannheim)
Biotin maleimide label	Axxora (Lörrach)
DC protein assay kit	BioRad (Munich)
D-luciferine	AppliChem (Darmstadt)
GeneRuler	Invitrogen (Karlsruhe)
Gylcogen RNA grade	Invitrogen (Karlsruhe)
HiSpeed Plasmid Maxi Kit	Qiagen (Hilden)
Human Inflammation Kit (CBA)	BD Biosciences (Heidelberg)
IgG isotype control (mouse)	R&D Systems (Wiesbaden)
Maxima First Strand cDNA Synthesis Kit	Fermentas (St. Leon-Rot)
MEGAclear Kit	Ambion (Darmstadt)
MEGAshortscript T7 Kit	Ambion (Darmstadt)
mMESSAGE mMACHINE T7 Kit	Ambion (Darmstadt)
Nitrocellulose membrane	GE Healthcare (Munich)
NucleoSpin Gel and PCR Clean-up	MACHEREY-NAGEL (Düren)
PageRuler Prestained Protein Ladder	Fermentas (St. Leon-Rot)
Protease inhibitor mix (PIM)	Roche Diagnostics (Grenzach)
QIAprep Spin Miniprep Kit	Qiagen (Hilden)
Rapamycin	LC Laboratories (Woburn, USA)
Recombinant IL-1β	PeproTech (Hamburg)
Restriction enzymes	New England Biolabs (Frankfurt)
RNasin Plus RNAse inhibitor	Promega (Mannheim)
RNeasy Mini Kit	Qiagen (Hilden)
SB203580	Enzo Life Science (Lörrach)
T4 DNA ligase	Invitrogen (Karlsruhe)
Taq DNA Polymerase, recombinant	Invitrogen (Karlsruhe)
Triton X100	Serva (Heidelberg)

4.1.4 Antibodies

All antibodies used for Western analysis and according dilutions are listed in Table 4-2.

Table 4-2: List of Antibodies

Antibody	Provider	Dilution
Anti-Nucleolin	Santa Cruz Biotechnology (Heidelberg)	1:5000
Anti-phospho-p38	Cell signaling Technology (Frankfurt)	1:1000
Anti-p38	Cell signaling Technology (Frankfurt)	1:1000
Anti-HuR	Santa Cruz Biotechnology (Heidelberg)	1:3000
Anti-PTB	Kind gift of Anne Willis (Leicester, UK) (158)	1:1000
Anti-hnRNP-A1	Cell signaling Technology (Frankfurt)	1:1000
Anti-Actin	Sigma-Aldrich (Deisenhofen)	1:3000
Anti-rabbit/-mouse IRDye600/800	Li-COR Biosciences (Bad Homburg)	1:5000

4.1.5 Plasmids

Used plasmids are listed in Table 4-3 and Table 4-4. All vectors contain an ampicillin resistance cassette.

Table 4-3: List of reporter plasmids

Plasmid	Information	Provider
pGL3-control	Contains SV40 promoter upstream of the *firefly* luciferase encoding region	Promega (Mannheim)
pGL3-basic	Contains minimal promoter upstream of the *luciferase* encoding region	Promega (Mannheim)
pGL3-EGR2	Contains EGR2-5'UTR upstream of *firefly* luciferase	-
pRF	Contains SV40 promotor upstream of *renilla* luciferase followed by *firefly* luciferase	Addgene (Cambride, USA)
pR-EGR2-F and deletion constructs	pRF with EGR2-5'UTR inserted in the intercistronic region of *renilla* and *firefly* luciferase	-
phpRF	pRF with hairpin inserted upstream of the *renilla* luciferase to inhibit cap-dependent translation	(159)
phpR-EGR2-F	phpRF with EGR2-5'UTR inserted in the intercistronic region of *renilla* and *firefly* luciferase	-

AP-1	pGL2 expression vector containing AP-1-binding site of the collagenase promoter region upstream of *firefly* luciferase	(160)
Renilla-TK	Transfection control vector containing TK-promoter upstream of *renilla* luciferase	Promega (Mannheim)
Renilla-SV40	Transfection control vector containing SV40-promoter upstream of *renilla* luciferase	Promega (Mannheim)
β-Gal-SV40	Transfection control vector containing SV40-promoter upstream of β-galactosidase	Promega (Mannheim)

Table 4-4 List of expression plasmids

Plasmid	Information	Provider
pcDNA3.1	Expression vector for mammalien cells or *in vitro* transcription containing T7 and CMV promoter	Invitrogen (Darmstadt)
hnRNP-A1-WT	Overexpression vector for mammalian cells containing wildtype hnRNP-A1	(161)
hnRNP-A1-NLS	Overexpression vector for mammalian cells containing dominant-negative hnRNP-A1 (lacks nuclear export activity)	(161)
pDrive-hrG	Expression vector for a 300 nucleotide fraction of human reverse GAPDH containing T7 promoter	A. v. Knethen

4.1.6 Oligonucleotides

Oligonucleotides were purchased from Biomers.net (Ulm). Sequences and according annealing temperatures [°C] are presented in Table 4-5 and Table 4-6 .

Table 4-5: **Oligonucleotides for qPCR**

Target	Forward primer	Reverse primer	[°C]
GAPDH	TGCACCACCAACTGCTTAGC	GGCATGGACTGTGGTCATGAG	60
EGR2	ACGTCGGTGACCATCTTTCCCAAT´	TGCCCATGTAAGTGAAGGTCTGGT	60
CYP24A1	TTGCCAGCGATAATACGCCTCAGA	AGCAGTGAACCCTGTAGAATGCCT	60
PLAUR	TGTGGCTCATCAGACATGAGCTGT	TCATCCTTTGGACGCCCTTCTTCA	60
CBLB	TGAGCCTTGTGGGCATTTGATGTG	TTTCACAACGACAGAAAGGGCAGC	60
GFRA2	TCTCGGACATCTTCAGGCTTGCTT	TGCAGTTGTCATTCAGGTTGCAGG	60
VDR	TGAAGCGGAAGGCACTATTCACCT	ACTCCTTCATCATGCCGATGTCCA	60
AMY1A	AACAGTAACTGGTTCCCGGAAGGT	ACCCGGCCATTACCAAAGTAGTCA	60

CD44	TCGAAGAAGGTGTGGGCAGAAGAA	ATTTCCTGAGACTTGCTGGCCTCT	60
EGR3	GCTTTGTTCAGTTCGGATCGCCTT	AAACAATGAGGTGTTTGGGTCGGG	60

Table 4-6: Oligonucleotides for construction of plasmids

Target	Forward primer	Reverse primer	[°C]
EGR2-5'UTR (EcoR1/NcoI)	GGCCGAATTCGAGCAATTGATTA ATAGCTCG	TTAACCATGGTTGCTCCTCGCACA AC	69
EGR2-5'UTR (SpeI/NcoI)	GCACTAGTGAGCAATTGATTAAT AGCTCGGCG	TTAACCATGGTTGCTCCTCGCACA AC	64
EGR2-5'UTR (HindIII/NcoI)	CGGCCAAGCTTGAGCAATTGATT AATAGCTCG	TTAACCATGGTTGCTCCTCGCACA AC	62
EGR2-5'UTR (HindIII/XhoI)	CGGCCAAGCTTGAGCAATTGATT AATAGCTCG	TACTCGAGTTGCTCCTCGCACAAC C	62
EGR2-5'UTR (1-166)	GGCCGAATTCGAGCAATTGATTA ATAGCTCG	GCCCATGGATAAAAGTAGCAAAC AAGTTGCTG	62
EGR2-5'UTR (167-326)	GCGAATTCTTCTGTTGATTTTTTTT TCTTGGTGTGTGT	TTAACCATGGTTGCTCCTCGCACA AC	62
EGR2-5'UTR (1-240)	GGCCGAATTCGAGCAATTGATTA ATAGCTCG	ATCCATGGGGGATGGTATCTCCT TTTGC	60.5
pRF-FL	ATGACTTCGAAAGTTTATGATCCA GAACAAAGGAAACGG	TTACACGGCGATCTTTCCGCCCT	62

4.1.7 Buffers and solutions

Protein lysis buffer

Tris/HCl	50 mM
Sucrose	0.27 M
Na_3VO_4	1 mM
EDTA	1 mM
EGTA	1 mM
Na-β-glyercophosphate	10 mM
NaF	50 mM
Na-pyrophosphate	5 mM
Triton-X-100	1% (v/v)
protease inhibitor	1 tablet/50 mL

SDS-running buffer

Tris/HCl	25 mM
Glycine	192 mM
SDS	0.7 mM

→ Adjust pH to 8.3

4x SDS sample buffer

Tris/HCl (pH 6.8)	125 mM
SDS	2% (w/v)
Glycerol	20% (v/v)
Bromphenol blue	0.002% (w/v)
DTT	5 mM

Sodium dodecyl sulfate (SDS)-polyacrylamide gels

	12% separating gel	4% stacking gel
40% Acrylamide/Bis-acrylamide (37.5% : 1.0% w/v)	3 mL	300 µL
1.5 M Tris/HCl (pH 8.8)	2.5 mL	-
0.5 M Tris/HCl (pH 6.8)	-	750 µL
ddH_2O	4.4 mL	1.9 mL
10% (w/v) SDS	100 µL	30 µL
TEMED	10 µL	5 µL
10% (w/v) ammonium persulfate	100 µL	50 µL

Blotting buffer

Tris/HCl	25 mM
Glycine	192 mM
Methanol	20% (v/v)
→ Adjust pH to 8.3	

TBS-T (tris buffered saline with Tween)

Tris/HCl	50 mM
NaCl	140 mM
→ Adjust pH to 7.4	
Tween-20	0.05% (v/v)

Coomassie blue fixation solution

Methanol	50% (v/v)
Acetic acid	10% (v/v)
Sodium acetate	10 mM

Coomassie blue staining solution

Acetic acid	10% (v/v)
SERVA blue G	0.025% (w/v)

Coomassie blue destaining solution

Acetic acid	10% (v/v)

Polysome buffer

KCl	140 mM
Tris/HCl (pH 8.8)	20 mM
MgCl2	5 mM
NP-40	0.5% (v/v)
Heparin	0.5 mg/mL
DTT	1 mM
Cycloheximide	100 µg/mL
RNasin	100 U/mL

RNA incubation buffer

Tris/HCl (pH 7.4)	10 mM
KCl	150 mM
DTT	0.5 mM
NP-40	0.05% (v/v)
RNasin	100 U/mL

10x MOPS

MOPS	200 mM
NaAce	50 mM
EDTA	10 mM
→ Adjust pH to 7.0	

5x RNA sample buffer

EDTA	4 mM
Formaldehyde (37%)	7.2% (v/v)
Glycerol	25% (v/v)
Formamide (deion.)	31% (v/v)
10x MOPS	40% (v/v)

Denaturing agarose gel

Agarose	1% (w/v)
10x MOPS	10% (v/v)
Formaldehyde (37%)	2%(v/v)

Firefly luciferase substrate solution

Tricine	20 mM
$(MgCO_3)_4$ x $Mg(OH)_2$	1.07 mM
$MgSO_4$	2.67 mM
EDTA	100 µM
DTT	33.3 mM
ATP	530 µM
Coenzyme A lithium	0.213 mg/mL
D-luciferine	470 mM
→ adjust pH to 7.8	

Renilla luciferase substrate solution

NaCl	100 mM
Tris/HCl, pH 7.5	25 mM
CaCl2	1 mM
Coelenterazine	1 µM

4.1.8 Instruments and Software

Used instruments and software are listed in Table 4-7 and Table 4-8.

Table 4-7: Instruments

Instruments	Provider
Agilent 2100 Bioanalyzer	Agilent Technologies (Waldbronn)
AIDA Image Analyzer	Raytest (Straubenhardt)
Apollo-8 LB 912 photometer	Berthold Technologies (Bad Wildbad)
Autoclave HV 85	BPW GmbH (Süssen)
Bacteria clean bench Hera guard	Heraeus (Hanau)
Bacteria incubator B5042	Heraeus (Hanau)
Bacteria incubator Innova®44	New Brunswick Scientific (Nürtingen)
Biologic LP System	Bio-Rad Laboratories (Munich)
C1000 Thermal Cycler Realtime PCR	Bio-Rad Laboratories (Munich)
CASY	Schärfe System (Reutlingen)

Centrifuge 5415 R and 5810 R	Eppendorf (Hamburg)
LSRII Fortessa	BD Biosciences (Heidelberg)
Hera cell 150 (Lamina)	Thermo Fisher Scientific (Waltham, USA)
Hera cell 240 (Incubator)	Thermo Fisher Scientific (Schwerte)
HBI Auto Densi Flow IIC	UniEquip (Martinsried)
LabLine Orbit Shaker	Uniequip GmbH (Martinsried)
Magnetic stirrer Combimag RCH	IKA Labortechnik (Staufen)
Mastercycler	Eppendorf (Hamburg)
Microscope Axiovert 200M	Zeiss (Göttingen)
Milli-Q Synthesis	Millipore (Schwalbach)
Mini-PROTEAN Tetra Cell	Bio-Rad Laboratories (Munich)
Mithras LB940 multimode reader	Berthold Technologies (Bad Wildbad)
NanoDrop ND-1000	Peqlab Biotechnologie (Erlangen)
Odyssey infrared imaging system	Li-COR Biosciences (Bad Homburg)
Optima L-90K Ultracentrifuge	Beckman Coulter (Krefeld)
PowerPac Basic Power Supply	Bio-Rad Laboratories (Munich)
Rotator	VWR (Darmstadt)
Sub-Cell® GT electrophoresis system	Bio-Rad Laboratories (Munich)
SW 40 Ti rotor	Beckman Coulter (Krefeld)
Thermomixer 5436	Eppendorf (Hamburg)
Trans-Blot SD blotting machine	Bio-Rad Laboratories (München)
UV-Transilluminator gel	Raytest (Straubenhardt)

Table 4-8: Software

Software	**Provider**
AIDA Image Analyzer	Raytest (Straubenhardt)
AxioVision Release 4.7	Zeiss (Göttingen)
BD Biosciences FCAP software	BD Biosciences GmbH (Heidelberg)
CFX Manager	Bio-Rad Laboratories (Munich)
CorelDRAW Graphics Suite X4	Corel Corp. (Ottawa, Kanada)
Endnote	Thomson Reuters (Carlsbad, USA)
Ingenuity pathway analysis	Ingenuity Systems (Redwood City, USA)
Lasergene Core Suite	DNASTAR (Madison, USA)

LP Data View	Bio-Rad Laboratories (Munich)
Mfold	The RNA Institute (New York, USA) (162)
MikroWin 2000	Berthold Technologies (Bad Wildbad)
MSOffice 2007	Microsoft Deutschland (Unterschleißheim)
Odyssey 2.1	Chang Bioscience (Castro Valley, CA)

4.2 Methods

4.2.1 Cell biology

4.2.1.1 Cell culture

MCF7 and U937 cells were maintained in Roswell Park Memorial Institute (RPMI) medium supplemented with 10% fetal bovine serum (FBS), 100 U/mL penicillin, 100 µg/mL streptomycin, and 2 mM L-glutamine. Additionally, U937 medium contained 1 mM sodium pyruvate. Cells were kept at 37°C in a humidified atmosphere with 5% CO_2. Cell numbers were determined using the cell counter system Casy or Neubauer chamber.

4.2.1.2 Generation of conditioned medium from U937 cells

U937 monocytes ($1x10^7$ / 25 mL) were exposed to TPA (10 nM) for 48 h. The resulting adherent, activated monocyte-derived macrophages were trypsinized, pelleted and washed with PBS. For control purposes undifferentiated monocytes ($3x10^6$ / 25 mL) were incubated with DMSO (0.1%) for 48 h, pelleted by centrifugation and washed with PBS. Subsequently, control and differentiated cells were treated equally. For the generation of conditioned medium cells were reseeded at a concentration of $2x10^6$ / 5 mL. Cells were allowed to condition medium for 24 h followed by centrifugation, sterile filtration (0.45 µm filter) and storage at -80°C until further use. Conditioned medium from differentiated cells (CM) was always prepared in parallel to conditioned medium from undifferentiated cells (Ctr). All experiments were carried out in U937 medium.

4.2.1.3 Transient transfection

Transient transfection of cells with over-expression vectors and reporter plasmids was performed using the Rotifect transfection reagent (Roth, Karslruhe). For reporter analysis $5x10^4$ MCF7 cells were seeded in 24-well plates. Antibiotic-free medium was changed the next day and cells were transfected with 0.2 µg DNA for 16 h as described by the manufacturer. In brief, 0.2 µg DNA and 0.5 µL Rotifect transfection reagent were mixed each with 300 µL RPMI medium. The Rotifect mixture was added to the DNA mixture, inverted and incubated for 30 min at room temperature (RT). For co-transfection/overexpression experiments 0.2 µg reporter plasmid and 0.8 µg overexpression plasmid were used together with 1 µL Rotifect. After incubation 60 µL/well of the mixture were added to the cells. Upon 16 h incubation the medium was replaced with fresh complete cell culture medium. Luciferase activities were measured 48 h post transfection start.

For RNA transfection DNA constructs were linearized with BamHI and *in vitro* transcribed using the mMESSAGE mMACHINE T7 Kit (Ambion, Darmstadt) according to the manufacturer's protocol and purified with the MEGAclear Kit (Ambion, Darmstadt). 0.2 µg RNA were transfected as described for DNA. Luciferase activities were measured 24 h post transfection start.

4.2.1.4 Scratch assay

$2x10^5$ MCF7 cells were seeded in 24-well plates one day prior to the experiment. Scratches were administered using a 10 µL tip. After removal of medium and cell debris, cells were treated and pictures were taken at the indicated time points using an Axiovert 200M microscope (Zeiss, Göttingen).

4.2.2 Molecular biology

4.2.2.1 Polysomal fractionation

$5x10^6$ MCF7 cells were seeded in a 15 cm dish one day prior to treatment of the cells. After incubation with 100 µg/mL cycloheximide (CHX) for 10 min at 37°C, cells were harvested by scraping in 15 mL PBS/CHX (100 µg/mL) and centrifuged in a 50 mL falcon at 2000 g, 2 min at 4°C. The supernatant was discarded and the pellet washed in 1 mL

PBS/CHX and transferred to cup. After pelleting again for 30 s, 16000 rpm at 4°C, cells were lysed in 750 µL polysome buffer. After pelleting for 5 min, 16000 rpm at 4°C and transferring the supernatant to a fresh cup, 600 µL of the cytoplasmic lysate was layered onto 11 mL of a 10-50% continuous sucrose gradient (in polysome buffer). The remaining lysate was stored at -20°C for total RNA. The gradient was centrifuged at 35000 rpm for 2 h at 4°C without brake using a SW40 rotor in a Beckman ultracentrifuge. Afterwards the gradient was pumped down using Biologic LP system (Biorad, Munich). Absorbance was measured at 254 nm and recorded using LP Data View software (Biorad, Munich). Finally, 1 mL fractions were collected.

4.2.2.2 RNA isolation

RNA from sucrose gradients was precipitated with 1/10 volume sodium acetate (3 M), 1 volume isopropanol and 1 µL glycogen over night at -20°C. After centrifugation for 20 min, 16000 rpm at 4°C, supernatants were discarded and pellets were purified together with total RNA samples using the RNeasy MiniKit (Qiagen, Hilden) according to the manufacturer´s manual. RNA was eluted in 30 µL RNase-free H_2O. RNA concentration was determined using Nanodrop.

4.2.2.3 Denaturing gel-electrophoresis

For quality control of fractionated RNA, equal volumes were analyzed by denaturing agarose gel electrophoresis. For this purpose, 5 µL of each RNA fraction was incubated in RNA sample buffer containing 1 µL ethidiumbromide (1:50 of stock solution) per 20 µL sample volume for 5 min at 65°C. Samples were loaded onto a 1% denaturing agarose gel and separated at 80 V for 30 min in 1x MOPS buffer.

4.2.2.4 Reverse transcription and semiquantitative realtime PCR (qPCR)

250 to 1000 ng RNA were transcribed using the Maxima First Strand cDNA synthesis kit (Fermentas, St. Leon Roth) in 10 µL samples containing 2 µL reaction mix and 1 µL enzyme mix. Samples were incubated for 10 min at 25°C followed by 15 min at 50°C. The reaction was terminated by heating at 85°C for 5 min. The resulting cDNA was diluted 1:10 and stored at -20°C. Individual mRNAs were analyzed using qPCR. For this

purpose 4 µL cDNA were mixed with 0.4 µL Primer (10 pmol/µL each), 10 µL absolute qPCR SYBR Green Fluorescent mix (Abgene, Surrey, UK) and filled up to 20 µL with H_2O. The following thermal cycling program was used:

		50°C	2 min
	Enzyme activation	95C	15 min
40 cycles	Denaturation	95°C	15 s
	Annealing	60°C	30 s
	Extension	72°C	30 s

A melt curve was added to the program to confirm specificity of the reaction:

Denaturation	95°C	30 s
Starting temperature	72°C	30 s
Melting step	72°C to 95°C + 0.5°C per cycle	5 s

4.2.3 Construction of plasmids

4.2.3.1 Construction of pR-EGR2-F and phpR-EGR2-F

To assess the IRES activity of EGR2 its 5'UTR and according deletion constructs were inserted into pRF (Addgene, Cambridge, USA) and/or phpRF (kind gift of Prof. Anne Willis (159)) in between the *renilla* and *firefly* open reading frame.

The 5´UTR of EGR2 was amplified by PCR using 5 µL cDNA of RNA extracted from MCF7 cells and appropriate primer pairs containing extensions to obtain overhangs of the restriction sites for *EcoRI* (5') and *NcoI* (3') or *SpeI* (5') and *NcoI* (3') (see Table 4-6).

For amplification of DNA fragments, conventional PCR was performed using recombinant *Taq* DNA polymerase (Invitrogen, Karlsruhe) according to the manufacturer's protocol. Briefly, 1.25 µL forward and reverse primer (10 pmol/µL each), 1 µL dNTP mix (10 µM each NTP), 1.5 µL $MgCl_2$, 5 µL 10 x reaction buffer and 1µL *Taq* polymerase were mixed with template DNA and filled up with H_2O to 50 µL. PCRs were performed according to the following profile, while annealing temperature was dependent on the used primer pairs.

	Lid	94°C	
	Initial denaturation	94°C	3 min
5 cycles	Denaturation	94°C	45 s
	Annealing	50°C	30 s
	Extension	72°C	90 s
40 cycles	Denaturation	95°C	45 s
	Annealing	XX°C	30 s
	Extension	72°C	90 s
	Final extension	72°C	10 min

The fragment size was verified by agarose gel electrophoresis.The vector pRF was linearized using the restriction enzymes *EcoRI* and *NcoI*, whereas phpRF was linearized using *SpeI* and *NcoI* at 37°C for 4 h. The vectors as well as the PCR product were separated on 1% agarose gels using low melting agarose and cut out of the gels. DNA was isolated from the gel fragments by use of NucleoSpin Gel and PCR Clean-up Kit (Macherey & Nagel, Düren). For ligation, the vector (100 ng) and insert were incubated with a molar ratio of 1:10 together with 2 µL T4 DNA ligase buffer and 0.5 µL T4 DNA ligase in 20 µL sample volume for 1 h at RT. Afterwards 5 µL of ligation mixture was transformed into XL10-Gold® ultracompetent bacteria (see 4.2.6.1). Potential positive clones were picked, amplified in LB medium and DNA extracted by use of QIAprep Spin Miniprep Kit (Qiagen, Hilden) according to the manufacturers manual. Plasmids were digested with *EcoRI* and *NcoI* or *SpeI* and *NcoI*, respectively, to check insertion of the fragment. Correct insertion was further verified by sequencing (Seqlab, Göttingen).

4.2.3.2 Construction of pGL3-EGR2

The human EGR2-5'UTR was also cloned into the promoter-less pGL3-basic vector upstream of the *firefly* luciferase as described before using *HindIII* and *NcoI* resulting in pGL3-EGR2.

4.2.3.3 Construction of pcDNA-EGR2

For *in vitro* transcription of EGR2-5'UTR it was cloned into the pcDNA3.1(+) vector downstream of the T7-promoter using *HindIII* and *XhoI* as described before.

4.2.4 Microarray

4.2.4.1 RNA preparation

For analysis of the polysomal RNA samples, fractions 6 to 10 from the sucrose gradient were pooled. Additionally, total RNA was collected. RNA concentrations were determined using the NanoDrop spectrophotometer. RNA quality was assessed using 2100 Bioanalyzer.

4.2.4.2 Probe labeling, array hybridization and scanning

The microarray was conducted at the DKFZ Genomics and Proteomics Core Facility (Heidelberg). Therefore, biotin-labeled cRNA samples for hybridization on Illumina Human Sentrix-12 BeadChip arrays were prepared according to Illumina's recommended sample labeling procedure based on the modified Eberwine protocol (163). In brief, 250 ng total RNA was used for complementary DNA (cDNA) synthesis, followed by an amplification/labeling step (*in vitro* transcription) to synthesize biotin-labeled cRNA according to the MessageAmp II aRNA Amplification kit Biotin-16-UTP was purchased from Roche Applied Science (Penzber. The cRNA was column purified according to TotalPrep RNA Amplification Kit, and eluted in 60 µL of water. Quality of cRNA was controlled using the RNA Nano Chip Assay on an Agilent 2100 Bioanalyzer and spectrophotometrically quantified with NanoDrop.

Hybridization was performed at 58°C, in GEX-HCB buffer (Illumina, San Diego, USA) at a concentration of 100 ng cRNA/µL, unsealed in a wet chamber for 20 h. Spike-in controls for low, medium and highly abundant RNAs were added, as well as mismatch control and biotinylation control oligonucleotides. Microarrays were washed twice in E1BC buffer (Illumina, San Diego, USA) at room temperature for 5 min. After blocking for 5 min in 4 mL of 1% (wt/vol) Blocker Casein in PBS Hammarsten grade array signals were developed by 10 min incubation in 2 mL of 1 µg/mL Cy3-streptavidin solution and 1% blocking solution. After a final wash in E1BC, the arrays were dried and scanned.

Microarray scanning was done using a Beadstation array scanner, setting adjusted to a scaling factor of 1 and PMT settings at 430. Data extraction was done for all beads individually, and outliers were removed when > 2.5 MAD (median absolute deviation). All remaining data points were used for the calculation of the mean average signal for a given probe, and standard deviation for each probe was calculated.

4.2.4.3 Data analysis

Statistical analysis of the microarray was done by the Senckenberg Institute of Pathology (Faculty of Medicine, Frankfurt) with the statistical computing environment R version 2.12 (164). Additional software packages were taken from the Bioconductor project (165). The complete gene expression dataset was deposited in the Gene Expression Omnibus under accession no. GSE35022.

4.2.5 Biochemistry

4.2.5.1 SDS-PAGE/Western analysis

For Western analysis, $5x10^5$ cells were seeded in 6 cm dishes, treated as indicated, scraped in 50 µL protein lysis buffer and snap-frozen in liquid nitrogen. Cell debris was pelleted by centrifugation and the supernatant transferred to a new cup. Following protein concentration determination (see 4.2.5.2), 50 µg protein were denatured in 4xSDS sample buffer at 95°C for 5 min. Proteins were separated on 12% SDS-polyacrylamidgels and transferred onto nitrocellulose membranes. Membranes were blocked with 5% BSA in TBS-T for 1h at RT and incubated with the indicated antibodies in 5% BSA over night at 4°C (see Table 4-2). Proteins were detected using appropriate secondary antibodies (see Table 4-2) and visualized on an Odyssey infrared imaging system (Li-COR Biosciences, Bad Homburg).

4.2.5.2 Protein determination

The protein content of cell lysates was determined using the DC Protein Assay Kit, based on the Lowry method (166). Briefly, a standard dilution series of bovine serum albumin (BSA) was prepared (0.25 to 2 mg/mL). 5 µl of the 1/5 diluted samples as well

as of the standard dilution were pipetted in duplicates into a 96-well plate, 20 µL solution A followed by 200 µL of solution B were added to start the colorimetric reaction. After 10 min shaking at RT, extinction was measured at 750 nm using the Apollo reader.

4.2.5.3 Reporter assay

MCF7 cells were transiently transfected as described in 4.2.1.3 using Rotifect reagent (Roth, Karlsruhe). Cells were lysed in 100 µL passive lysis buffer (Promega, Mannheim) and frozen at -80°C. After defreezing on a shaker for 30 min at RT, *firefly* and *renilla* luciferase were on a Mithras LB 940 luminometer (Berthold, Bad Wildbad). Therefore, 20 µl of the lysate were transferred in a 96-well plate, 50 µL of the appropriate reporter assay reagent (see 4.1.7) were added automatically, plates were shaked for 2 s, and each well measured for 10 s. β-Galactosidase activity was measured using the β-Galactosidase Enzyme Assay System (Promega, Mannheim) according to the manufactures manual. To this end 25 µL of the lysate was incubated with 25 µL of 2x assay buffer for 1 h at 37°C. After a faint yellow colour has developed, the reaction is stopped by use of 75 µL 1 M sodium carbonate. Then the absorbance was read at 420 nm using Apollo reader. All reporter assays were performed in triplicates.

4.2.5.4 Cytometric Bead Array

To determine the secretion of TNFα, IL-6, IL-8, IL-1β, IL-10 and IL-12p70 by the U937 cells, Ctr and CM were analyzed using the Cytometric Bead Array (CBA) Human Inflammation Kit (BD Biosciences, Heidelberg) according to the manufacturer's manual. Samples were measured using the BD LSRFortessa flow cytometer and analyzed with BD Biosciences FCAP software (BD Biosciences, Heidelberg).

4.2.5.5 *In vitro* transcription and biotin-labeling

EGR2-5'UTR (based on NM_000399.3) and human reverse GAPDH were transcribed *in vitro* with the MEGAShortscript Transcription kit (Ambion, Darmstadt) according to the manufacturer's protocol. To this end, 2 µg of plasmid containing a T7 promotor was incubated with 2 µL T7 10x reaction buffer, 8 µL dNTPs (75 mM each) and 2 µL T7

enzyme mix in a 20 µL reaction for 4 h at 37°C. To remove DNA template, 1 mL TURBO DNase was added to the reaction mix and incubated at 37°C for additional 15 min. Denaturing agarose gel-electrophoresis (see 4.2.2.3) was used to verify the transcription. The RNA sample was filled up to 100 µL and extracted using 12.5 µL LiCl [4M] and 375 µL EtOH. Reaction was left at -80°C for 1 h, centrifuged at 16000 rpm for 10 min at 4°C and solved in 20 µL H_2O. Afterwards the transcript was biotin-labeled at the 5'end using 5'EndTag Nucleic Acid Labeling System (Axxora, Lörrach) according to the manufacturer's instructions. Briefly, 60 µg RNA were incubated with 1 µL universal reaction buffer and 1 µL alkaline phosphatase in a 10 µL reaction for 30 min at 37°C. Then 2 µL universal reaction buffer, 1 µL ATPγS, 2 µL T4 ligase and 5 µL H_2O was added and incubated for additional 30 min at 37°C. Finally, 10 µL of biotin-label (12 mg biotin-maleimide solved in 312 µL anhydrous DMF) were added and incubated for 30 min at 65°C. Following LiCl extraction as described before, the labeled transcript was ready to be used for RNA affinity chromatography.

4.2.5.6 RNA affinity chromatography

100 µL streptavidin agarose beads solution was washed 5 times in 1 mL RNA incubation buffer by centrifugation for 2 min, 3500 rpm at 4°C. Then 20 µg of biotinylated RNA were conjugated to the washed streptavidin agarose beads in 500 µL incubation buffer at 4°C for 2 h with continuous rotation. Afterwards 500 µg protein extract (lysed in incubation buffer containing 0.5% NP-40 and 160 u RNasin) were added to the beads and incubated for 1 h at 4°C on a rotator followed by 15 min at room temperature. Beads were washed 5 times with 1 mL incubation buffer, resuspended in 30 µL 4xSDS buffer and boiled for 10 min. Eluted proteins were separated by 10% SDS-PAGE.

4.2.5.7 MS analysis

MS analysis was conducted by the Bioenergetics Group (Faculty of Medicine, Frankfurt). For this purpose, SDS gels were stained with coomassie blue. Corresponding gel-lanes were cut in several slices and proteins were tryptically in-gel digested. Resulting peptides were analyzed by nano-ESI-LC-MS/MS using an LTQ-Orbitrap XL mass spectrometer and an Agilent 1200 nano-HPLC system at the front

end. Obtained mass spectra were searched against the species specific Uniprot protein database (*Homo sapiens*) using Mascot 2.2 search engine. Peptide matches were filtered by Mascot score cut-off with significance threshold at $p < 0.05$.

4.2.6 Microbiology

4.2.6.1 Transformation of bacteria by heat-shock

Bacteria were transformed with plasmid DNA by heat-shock. Therefore, 50 µL of bacteria glycerol stocks were thawed on ice, 50 to 1000 ng plasmid DNA were added and incubated for 30 min on ice. After a heat-shock for 45 s at 42°C, bacteria were incubated for another 2 min on ice. For initial growth, 450 µL of LB medium were added followed by an incubation period for 45 min at 37°C with shaking at 350 rpm. 500 µL of the bacteria solution was inoculated on a LB agar plate containing the appropriate antibiotic (100 µg/mL ampicillin) and incubated over night at 37°C to select positive plasmids carrying bacteria clones.

4.2.6.2 Bacterial culture and plasmid preparation

For preparation of plasmids a single clone from the LB agar plate was picked, transferred into 3 ml LB medium with the appropriate antibiotic and cultured over night at 37°C with shaking (220 rpm). The next day, plasmids were either isolated using QIAprep Spin Miniprep Kit (Qiagen, Hilden) according to the manufacturers manual and/or the culture was transferred into 300 mL LB medium containing the appropriate antibiotic and again shaked over night at 37°C. Isolation of plasmids was then performed according to the manufacturers protocol using the HiSpeed Plasmid Maxi Kit. DNA content was measured with the NanoDrop ND-1000.

4.2.7 Statistical analysis

Each experiment was performed at least three times. Data are presented as mean values ± SEM. Statistical analysis was performed using Student's t-test. $*p < 0.05$, $**p < 0.01$, $***p < 0.001$

5 Results

5.1 Global analysis of translational changes during inflammation

To identify targets that are regulated on the level of translation during inflammation, I established and characterized an *in vitro* system to mimic the situation of cells facing an inflammatory microenvironment. For this purpose I differentiated U937 monocytes to macrophages by treatment with 10 nM TPA for 48 h. The supernatant of differentiated U937 (CM) and undifferentiated U937 (Ctr) was collected after additional 24 h and used as treatment for the breast cancer cell line MCF7 (Figure 5-1).

Figure 5-1: Scheme of experimental setup
U937 cells were incubated with 10 nM TPA for 48 h, followed by washing and reseeding to a new dish. After additional 24 h CM was harvested and incubated on MCF7 cells. For Ctr, U937 cells were left untreated.

5.1.1 Characterization of conditioned medium

First, I wanted to investigate the characteristics of CM and Ctr with respect to inflammation and tumorigenesis and their functional consequences on MCF7 cells**.**

5.1.1.1 CM contains various pro-inflammatory cytokines

To verify that CM generates an inflammatory environment, I tested the abundance of various cytokines using CBA analysis. For this purpose CM and Ctr were generated as described before and stained with CBA inflammation kit for different cytokines that were measured by FACS. TNFα, IL-6, IL-8, IL-1β and IL-10 were significantly upregulated in CM compared to Ctr (Figure 5-2). However, the mean concentrations of TNFα (9.24 ± 2.28 pg/mL) and IL-6 (12.34 ± 3.57 pg/mL) remained at rather low concentrations in CM, whereas IL-8 (19.95 ± 21.64 ng/mL), IL-1β (91.73 ± 16.57 pg/mL) and IL-10 (204.00 ± 26.97 pg/mL) reached physiological relevant concentrations. In contrast, IL-12p70 was hardly detectable in Ctr as well as CM (0.84 ± 0.50 pg/mL).

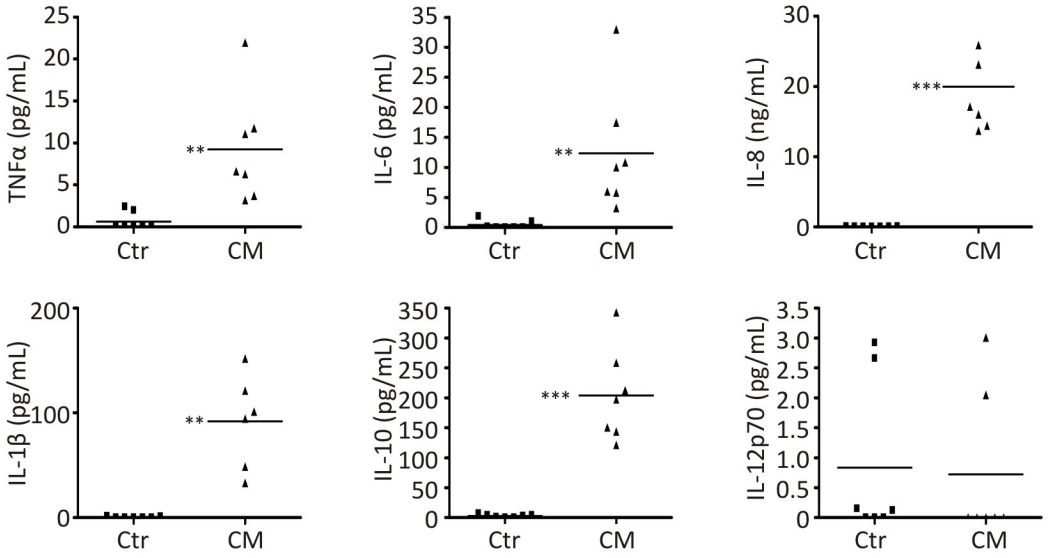

Figure 5-2: CBA of CM vs. Ctr
To determine the secretion of TNFα, IL-6, IL-8, IL-1β, IL-10 and IL-12p70 by undifferentiated and differentiated U937 cells, Ctr and CM were analyzed using CBA. Samples were measured by FACS. Horizontal bar represents mean of the different samples. ($n > 3$, $^{**}p < 0.01$)

These data provide evidence, that CM indeed generates an inflammatory microenvironment by the secretion of various proinflammatory cytokines and can be used for further experiments.

5.1.1.2 CM induces AP-1 transactivation and tumor cell migration

To determine whether CM induces tumorigenic effects in MCF7 cells, I measured the activity of the transformation marker AP-1 using a reporter plasmid that contains an AP-1-binding site of the collagenase promoter region (160). For this purpose, MCF7 cells were transfected with the reporter plasmid together with a *renilla* luciferase containing vector as transfection control and treated for 24 h with normal RPMI medium (NM), Ctr or CM, respectively. As depicted in Figure 5-3, CM induced a significant transactivation of AP-1 up to 4.5 ± 0.40 fold in comparison to NM, whereas Ctr had no effect.

As an increase in AP-1 activity indicates a pro-tumorigenic effect of CM on MCF7 cells, I additionally wanted to test its impact on another functional endpoint, i.e. tumor cell migration using scratch wound healing assays. For this purpose cells were seeded in high density and after attachment of the cells a scratch was administered through the

confluent cells. Migration of MCF7 was markedly increased after 4 h treatment with CM, whereas Ctr did not influence the migration compared to NM.

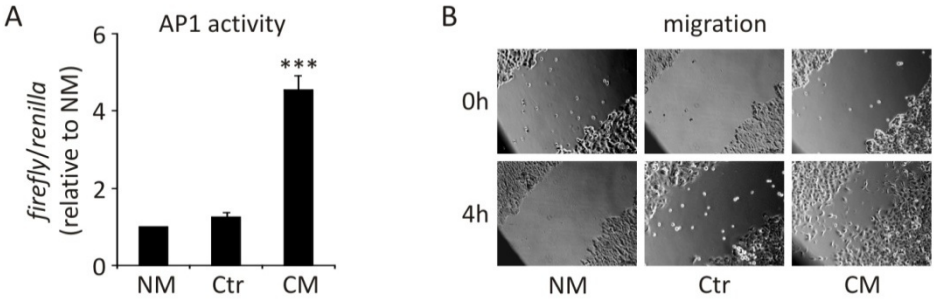

Figure 5-3: CM has pro-tumorigenic potential
(A) MCF7 cells were co-transfected with an AP-1 *firefly* reporter and a *renilla* luciferase plasmid 16 h prior to treatment with NM, Ctr or CM for 24 h. AP-1 activity was normalized to *renilla* luciferase and presented relative to NM treated cells. All data are given as means ± SEM (n > 3, ***p < 0.001). (B) MCF7 cells were subjected to a scratch wound assay. After administration of the scratch, medium was changed to NM, Ctr or CM. Wound closure was examined after 4 h.

In summary, enhanced AP-1 transactivation as well as the increased migration is indicative for the induction of a tumor-promoting programm in MCF7 cells that was provoked after treatment with CM, which generates a proinflammatory environment.

5.1.2 Establishment of polysomal fractionation

As the aim of my study was to identify proteins that are regulated at the translational level, I established the method of polysomal fractionation. For this technique cytoplasmic lysates were generated and layered on a sucrose gradient. Subsequent ultracentrifugation led to sedimentation of mRNAs according to their ribosome occupancy.

The UV profile of cellular lysates that were subjected to polysomal fractionation as shown in Figure 5-4 started with a high peak that contained small RNAs such as transfer RNAs (tRNAs) or small nucleolar RNAs (snoRNAs) and ribonucleoproteins (RNPs) leading to high absorption. The profile then dropped and peaks could be detected for the 40S, 60S and 80S ribosomes as indicated. Then the profile dropped again and changed over to smoothly rising peaks representing enhanced ribosome loading (polysomes). The ribosome distribution was further confirmed by visualizing the 28S rRNA which belongs to the large ribosomal subunit and the 18S rRNA that is part of the small ribosomal subunit. To this end, RNA was isolated from single fractions

and subjected to denaturing agarose gel-electrophoresis. The distribution of the two rRNAs fitted very well to the UV profile, thus confirming the validity of using polysomal fraction for the investigation of translational changes.

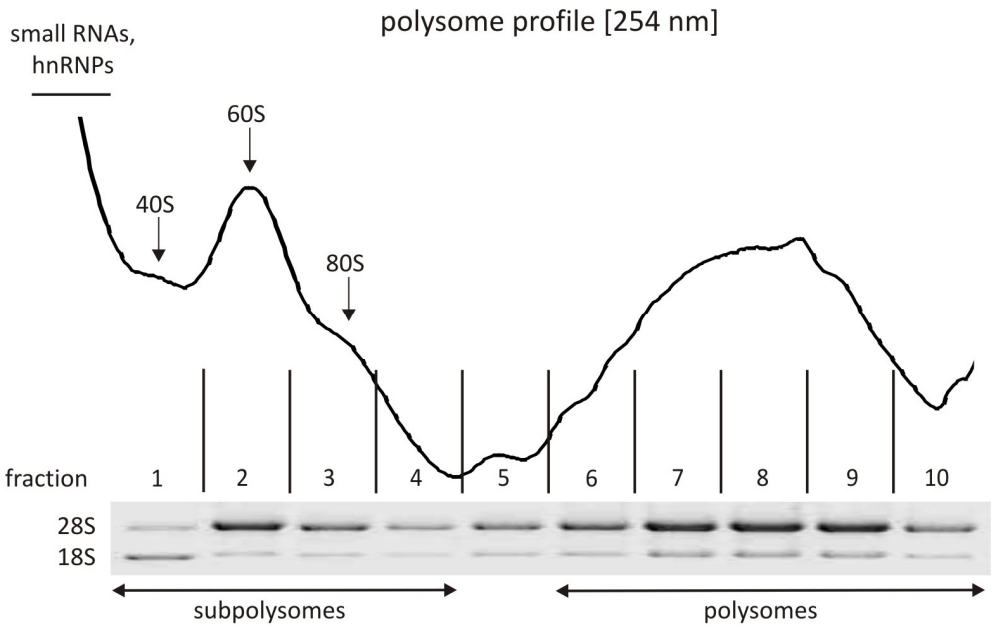

Figure 5-4: UV profile of MCF7 cells after polysomal fractionation
MCF7 cells were subjected to polysomal fractionation and the absorbance was measured at 254 nm. RNA was isolated from single fractions and equal volumes were analyzed using denaturing agarose gel-electrophoresis. 28S and 18S rRNAs were visualized with ethidiumbromide.

5.1.3 Microarray

For identification of genes that are regulated on polysome level during inflammation, I conducted a microarray in cooperation with the Genomics and Proteomics Core Facility (DKFZ, Heidelberg) and the Senckenberg Institute of Pathology (Faculty of Medicine, Frankfurt). For this purpose MCF7 cells were treated for 4 h with CM or Ctr, followed by polysomal fractionation. Fractions 6 to 10 were pooled and subjected to microarray analysis by use of a whole genome BeadChip array (Illumina). In parallel, microarray analysis of total mRNA was performed.

5.1.3.1 Microarray results of total changes

Initially, I analyzed changes of total mRNA expression in response to CM. 144 genes were found to be more than 2 fold upregulated on total mRNA level (Table 5-1), whereas only 13 genes were more than 2 fold downregulated (Table 5-2).

Table 5-1: List of genes that were more than 2 fold upregulated on total level

Gene	Fold change	Gene	Fold change	Gene	Fold change
PHLDA1	18,8	LOC649095	3,2	MAP2K3	2,5
EGR1	14,7	FLRT3	3,2	RPL7L1	2,5
SERPINE1	13,0	CD83	3,1	SDCBP	2,4
IL24	12,0	NFKBIA	3,1	VCL	2,4
F2RL1	8,6	TMEM2	3,1	ZC3H12A	2,4
TNFRSF21	8,6	IL4R	3,1	ABCC3	2,4
IL8	8,2	SOX9	3,1	HPS3	2,4
KCNF1	8,2	PMEPA1	3,0	FURIN	2,4
RASD1	7,9	BHLHB2	3,0	GJB2	2,4
IL8	7,7	ANKRD57	3,0	KRT16	2,4
ZNF365	7,3	SERPINB8	3,0	PTPRE	2,3
DUSP5	7,1	PLEK2	3,0	LOC728014	2,3
TNFRSF11B	7,0	THBS1	2,9	MYADM	2,3
IL24	7,0	LIF	2,9	ATP1B1	2,3
MALL	6,7	ZNF275	2,9	PLAUR	2,3
TM4SF1	6,6	VCL	2,9	IRF2BP2	2,3
ITGA2	6,5	JUNB	2,8	TMEM158	2,3
ERRFI1	6,5	ZFP36L2	2,8	ITGB2	2,2
STAMBPL1	5,9	CEBPB	2,8	CXCR4	2,2
LRRC8C	5,9	SLC4A7	2,8	DKFZP761P0423	2,2
SPRY4	5,7	PMEPA1	2,8	DSG2	2,2
F2RL1	5,6	DOK7	2,8	FLJ13236	2,2
MAFF	5,6	SPHK1	2,8	DDB1	2,2
IL1RL1	5,3	TRIB1	2,8	SDCCAG1	2,2
DUSP4	5,0	TNFRSF12A	2,7	SPRED2	2,2
KIAA1199	4,7	PRPF40A	2,7	ZYX	2,2
CCL2	4,6	CCNA1	2,7	RBMS1	2,2
NUAK2	4,6	HBEGF	2,7	RBMS1	2,2
FOSL1	4,2	NUAK2	2,7	MPZL2	2,2
LTB	4,0	ARNT2	2,7	BAZ1A	2,1
PMEPA1	4,0	IFNGR2	2,7	QPCT	2,1
FHL2	3,9	ALDH1A3	2,7	NOL6	2,1
TNFAIP8	3,9	OSMR	2,6	TNFRSF10A	2,1
ELL2	3,9	KRT80	2,6	LHFPL2	2,1
STX11	3,7	PALLD	2,6	ZSWIM4	2,1
IER3	3,7	LONRF2	2,6	MGC3020	2,1
EGFR	3,6	IGF2BP2	2,6	EIF2C2	2,1
SMAD3	3,6	BIRC3	2,6	JUN	2,1
CLDN1	3,6	RELB	2,6	NDE1	2,1
ITGAV	3,5	MCL1	2,6	GNL3L	2,1
ZSWIM4	3,5	ZYX	2,5	ADORA2A	2,1
FOXO1	3,4	ETS2	2,5	ZFP36	2,1
ATF3	3,4	FRMD6	2,5	CSNK1E	2,1
SH3TC1	3,4	MYEOV	2,5	ARTN	2,0
TNF	3,4	TNFAIP3	2,5	ALDH1A3	2,0
SERPINB8	3,3	RGS16	2,5	HS.60257	2,0
FHL2	3,3	CCRN4L	2,5	FOXC1	2,0
FBXO32	3,2	ATP1B1	2,5	NFKB1	2,0

Table 5-2: List of genes that were more than 2 fold downregulated

Gene	Fold change	Gene	Fold change	Gene	Fold change
ZNF823	-2,0	PPP2R3C	-2,3	RTN4RL1	-2,7
TRERF1	-2,1	HS.193406	-2,4	ID2	-3,3
CKAP2L	-2,1	AIFM2	-2,5	FAM46B	-4,6
CDC42EP4	-2,2	RPRM	-2,6	CYP1A1	-4,6
SEMA3F	-2,3				

To elucidate molecular mechanisms and pathways that are induced in MCF7 cells upon treatment with CM, the complete target list was subjected to pathway analysis using Ingenuity software. Table 5-3 provides an overview of the obtained results with the amount of associated molecules. Within the associated network functions inflammatory and cancer responses were enriched. Similarly, cancer emerged as a disease relevant function and molecular changes were also indicative of tumorigenic changes (i.e. cell growth, proliferation and cellular movement). The data also provided evidence, that IL-6, TNFR2 and IL-10 signaling pathways were likely to be activated in our setting.

Table 5-3: Results of Ingenuity pathway analysis of total changes

Associated network functions	**Molecules**
Cell death, proliferation, inflammatory response	39
Inflammatory response and disease	32
Cancer, cell cycle	17
Molecular and cellular functions	
Cell death	53
Cellular growth and proliferation	56
Cellular movement	34
Diseases and disorders	
Cancer	65
Reproductive system disease	43
Dermatological diseases	21

Signaling pathways	Molecules
IL-6 signaling	9/98
TNFR2 signaling	6/32
IL-10 signaling	7/72

These results support the concept that TPA-activated U937 monocyte-derived macrophages induce a pro-tumorigenic and inflammatory response in MCF7 cells.

5.1.3.2 Microarray results of polysomal changes

For identification of those mRNAs that are regulated at the level of translation, I compared the changes in mRNA abundance in the polysomal as well as in the total RNA.

The targets that significantly changed in the polysome-associated portion but not on total level were considered as translationally regulated. Using these criteria 42 genes were identified (Table 5-4). Specifically, 25 genes were translationally upregulated, whereas 17 genes were downregulated. Among these mRNAs early growth response 2 (EGR2), plasminogen activator urokinase receptor (PLAUR), mitogen-activated protein kinase kinase kinase 5 (MAP3K5), GDNF family receptor alpha 2 (GFRA2) and Cas-Br-M (murine) ecotropic retroviral transforming sequence b (CBLB) showed the strongest translational induction (2.5 to 7.0 fold), while aquaporin 11 (AQP11), FYVE, RhoGEF and PH domain containing 3 (FGD3), ring finger protein 214 (RNF214), Fanconi anemia, complementation group E (FANCE) and leucine rich repeat containing 20 (LRRC20) displayed the strongest translational repression (-2.2 and -2.7 fold).

Table 5-4: Heatmap of translationally regulated genes

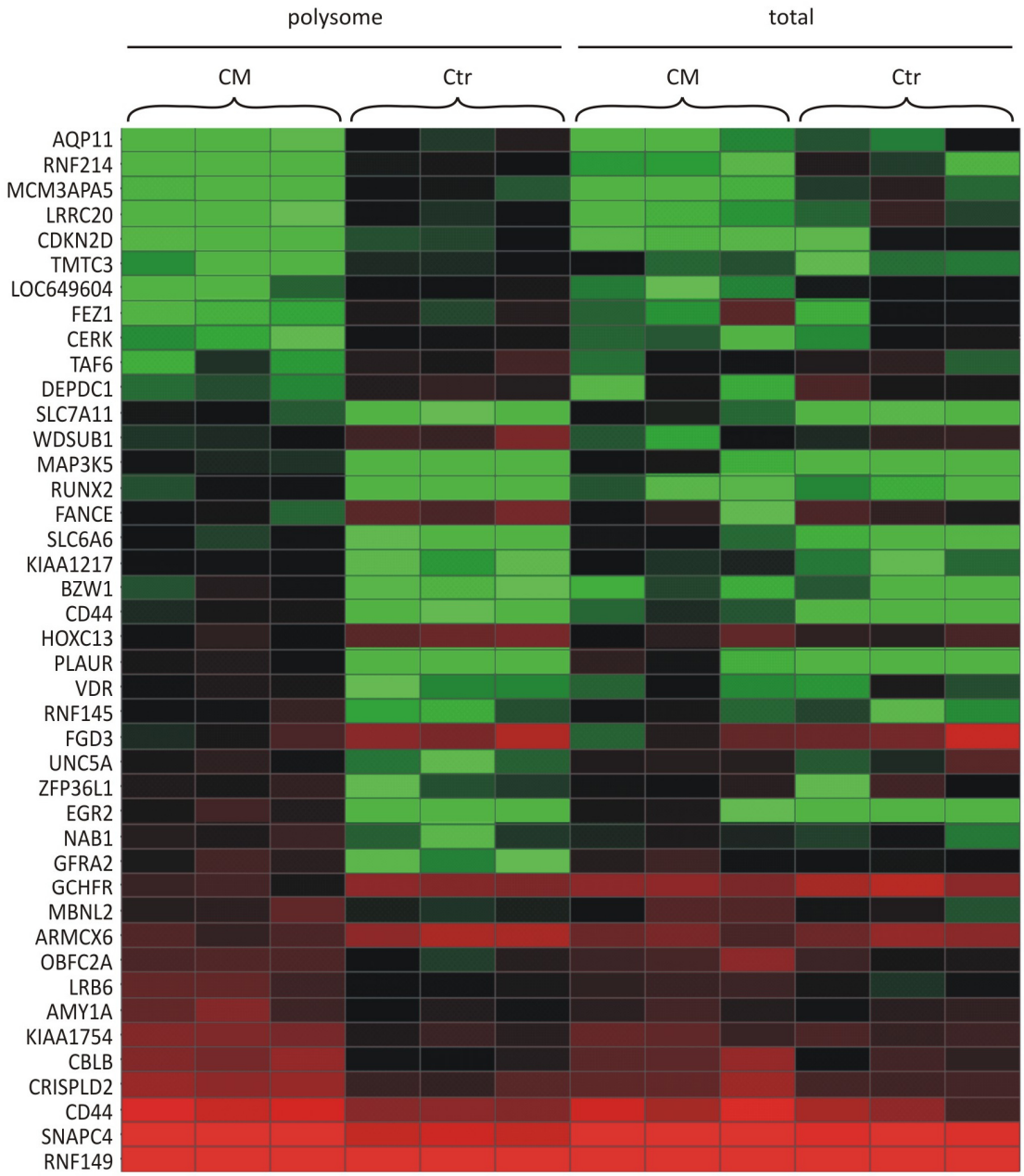

5.1.3.3 Validation of microarray results

After accomplishing the microarray, the first task was to validate the obtained results by semiquantitative realtime PCR (qPCR). For this purpose targets were selected based on their magnitude of regulation but also by considering their functional relevance. I performed again polysomal fractionation with MCF7 cells that were treated for 4 h with CM or Ctr, respectively, and compared the changes in pooled polysomal fractions 6 to 10 to the changes on total RNA level by use of qPCR with primers against selected targets.

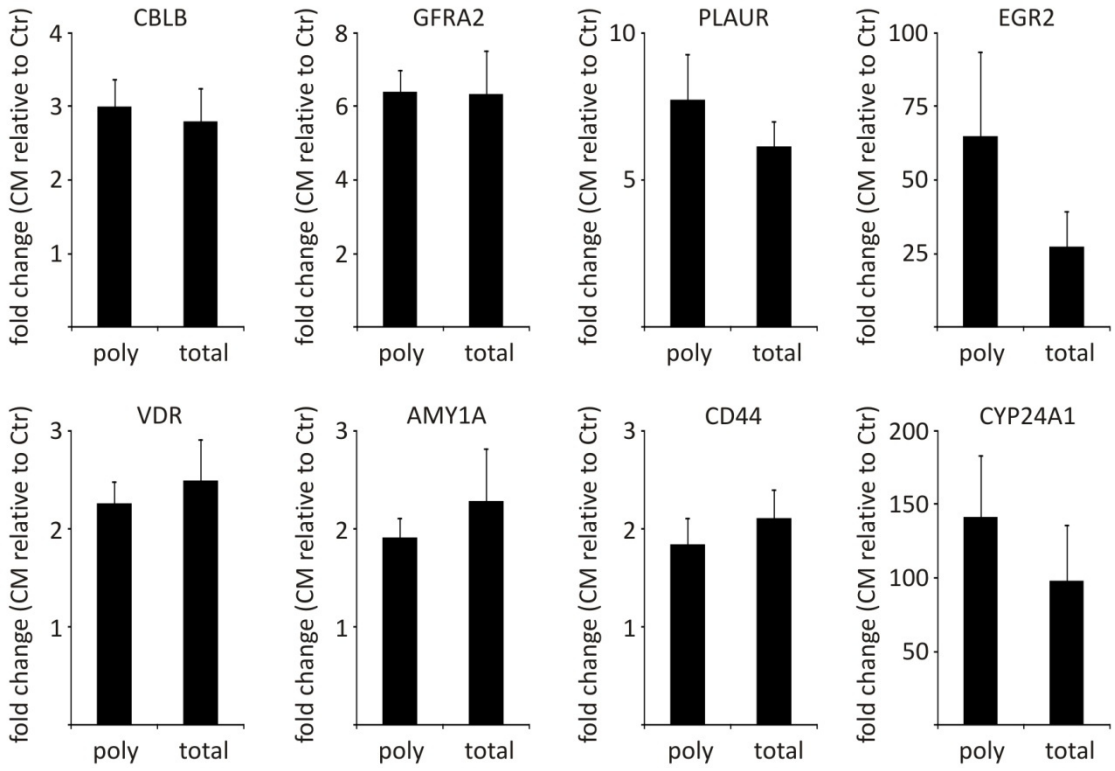

Figure 5-5: Comparison of poly vs. total change
MCF7 cells were treated with CM or Ctr for 4 h and subjected to polysomal fractionation. Fractions 6 to 10 were pooled (poly). In parallel, total RNA was isolated. Expression of mRNAs was tested by qPCR and normalized to GAPDH. Data are shown as fold inductions relative to Ctr. Values are mean values ± SEM, n > 3.

Surprisingly, in contrast to the results of the microarray analysis, all of the 8 tested mRNAs changed in expression not only on polysomal but also on total RNA level upon CM treatment (Figure 5-5). CBLB, GFRA2, vitamin D receptor (VDR), alpha-amylase 1A (AMY1A) and cluster of differentiation (CD44) changed on both levels to a similar extend and therefore have to be considered to be predominantly transcriptionally regulated. Notably, PLAUR, EGR2 and cytochrome P 24A1 (CYP24A1) showed higher changes in the polysomes than in total RNA, thus indicating an upregulation on transcriptional as well as on translational level.

In order to investigate the translational changes of EGR2, PLAUR and CYP24A1 in more detail, I conducted polysomal fractionation with CM and Ctr treated MCF7 cells and analyzed the distribution of the target mRNAs in single fractions relative to total RNA within the whole gradient.

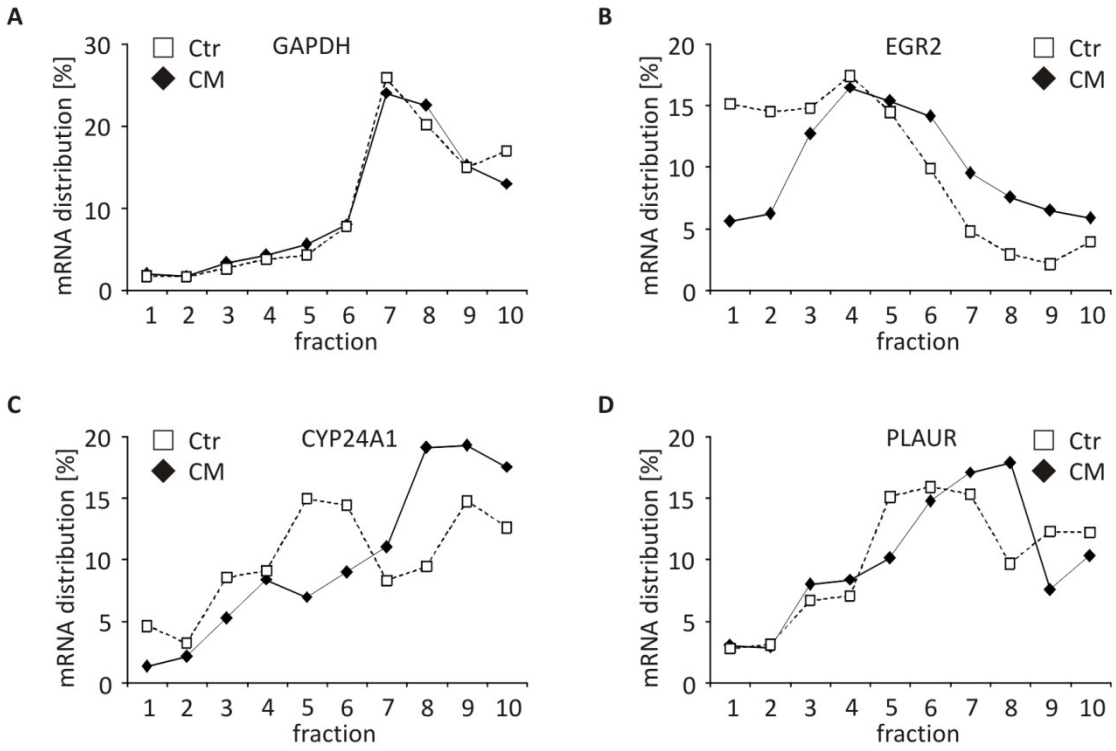

Figure 5-6: Distribution of mRNAs in single fractions
MCF7 cells were treated with CM or Ctr for 4 h and subjected to polysomal fractionation. RNA was isolated from single fractions and the distribution of mRNA in single fractions was measured relative to total RNA using qPCR with primers for GAPDH (A), EGR2 (B), CYP24A1 (C) and PLAUR (D). Data are representative for at least 3 experiments.

The mRNA distribution of glyceraldehyde-3-phosphate dehydrogenase (GAPDH) did not change when comparing Ctr to CM treatment, thus proving that CM did not induce a general change in translation (Figure 5-6A). For EGR2 mRNA distribution a dramatic drop in monosomal fractions 1 to 3 could be observed upon CM treatment, whereas it markedly increased in the polysomal fractions 6 to 10 (Figure 5-6B) indicating that the mRNA moves from monosomes to polysomes. The mRNA distribution of CYP24A1 changed in a similar way but not to the same extend as EGR2 (Figure 5-6C), i.e. CYP24A1 mRNA was more abundant in fractions 5 and 6 under control conditions and increased in fractions 7 to 10 after CM treatment. In contrast, I could not observe a consistent movement from monosomes to polysomes for PLAUR (Figure 5-6D). These data indicate that EGR2 and CYP24A1 translation is specifically induced under inflammatory conditions.

In further experiments I concentrated on the investigation of the translational regulation of EGR2 since this target showed the strongest and most reliable induction.

5.2 Mechanism of EGR2 translation

5.2.1 EGR2 translation is significantly upregulated upon CM

First I wanted to check whether the translational upregulation of EGR2 was significant. To allow for statistical evaluation, the relative amount of GAPDH and EGR2 mRNA was analyzed in single fractions (Figure 5-7A). Then the ratio of CM to Ctr was calculated in each fraction (Figure 5-7B).

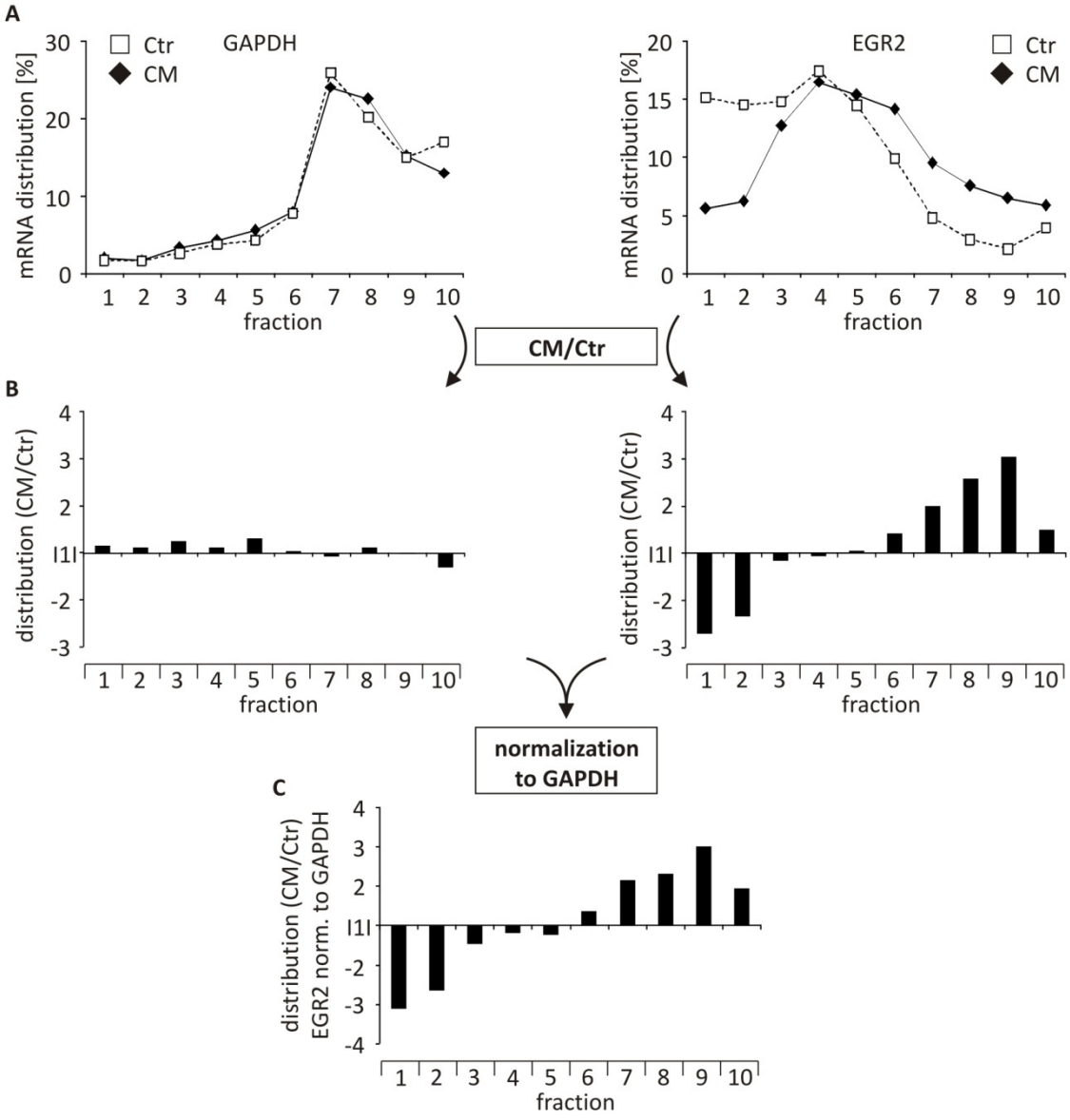

Figure 5-7: Calculation of target mRNA distribution changes

(A) MCF7 cells were treated with CM (black diamonds, solid line) or Ctr (white squares, dashed line) for 4 h and subjected to polysomal fractionation. RNA was isolated from single fractions and was analyzed using qPCR. The mRNA distribution over the isolated fractions was calculated for GAPDH (left panel) and EGR2 (right panel). (B) The ratio of mRNA distribution of CM to Ctr was calculated to visualize stimulus-dependent changes. (C) The CM/Ctr ratio of EGR2 was normalized to the GAPDH ratio.

Since the mRNA distribution of GAPDH did not change in response to CM, GAPDH distribution was chosen as normalization control (Figure 5-7C).

Combining all experiments revealed that GAPDH mRNA distribution did not change (Figure 5-8A), whereas EGR2 mRNA significantly decreased in all monosomal fractions 1 to 4 and increased in all polysomal fractions 6 to 10 (Figure 5-8B). Specifically, the mean EGR2 mRNA distribution across all polysomal fractions increased to 196 ± 13% relative to Ctr, thus supporting enhanced translation.

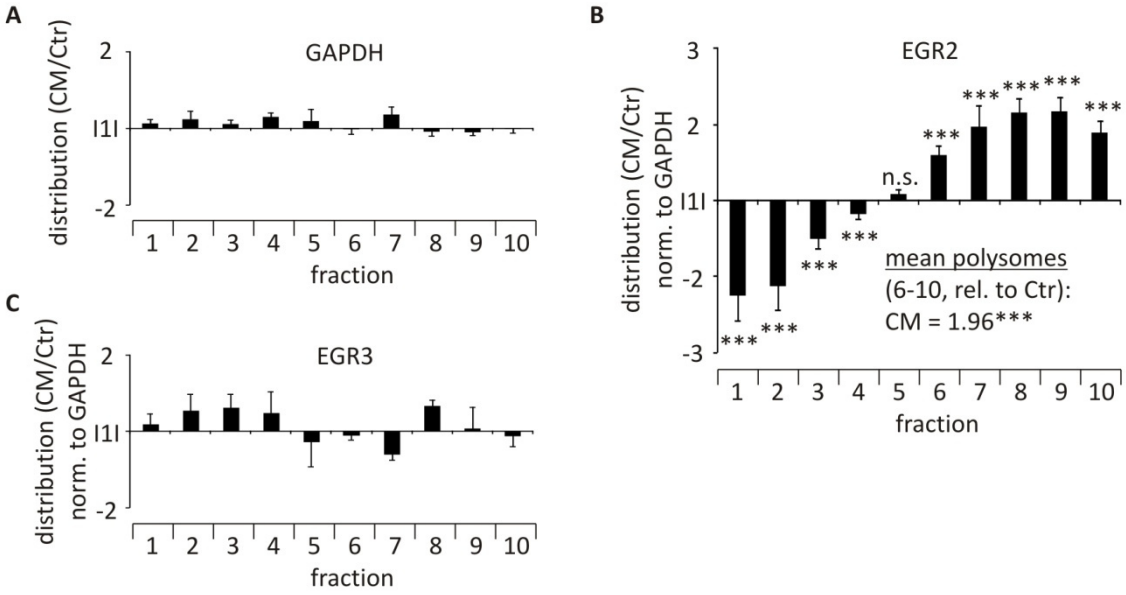

Figure 5-8: EGR2 mRNA distribution significantly changes upon CM

MCF7 cells were treated with CM or Ctr for 4 h and subjected to polysomal fractionation. Changes of mRNA distribution induced by CM relative to Ctr were analyzed using qPCR for GAPDH (A), EGR2 (B) and EGR3 (C). Data are presented as means ± SEM (n > 3, ***p < 0.001). EGR2 and EGR3 distributions are normalized to GAPDH distribution. Mean polysomal change (fractions 6 to 10) of EGR2 upon CM was calculated relative to Ctr.

For control purposes, I determined changes in the mRNA distribution of the related EGR3, which was not identified to be translationally regulated in the microarray analysis. As expected no significant changes could be observed for EGR3 mRNA distribution in response to CM (Figure 5-7C). These data again demonstrate that EGR2 translation is specifically induced under inflammatory conditions.

5.2.2 Impact of IL-1β and IL-6 on EGR2 translation

Next, I wanted to identify which factor(s) in CM account for the translational upregulation of EGR2.

5.2.2.1 Blocking IL-1β but not IL-6 impairs EGR2 translation

In 5.1.1.1 the abundance of several cytokines in Ctr and CM was already shown. Besides others, IL-6 and IL-1β were identified to be elevated in CM compared to Ctr. As IL-6 and the IL-1β-related IL-1α were previously shown to play a role in the regulation of translation of certain target mRNAs (167, 168), I investigated the impact of these cytokines on EGR2 translation. To this end, I depleted IL-6 and IL-1β in CM by preincubating CM with IL-1β or IL-6 neutralizing antibodies or with an IgG isotype control for 1 h at 37°C. MCF7 cells were incubated with the resulting CMs or Ctr for 4 h followed by polysomal fractionation.

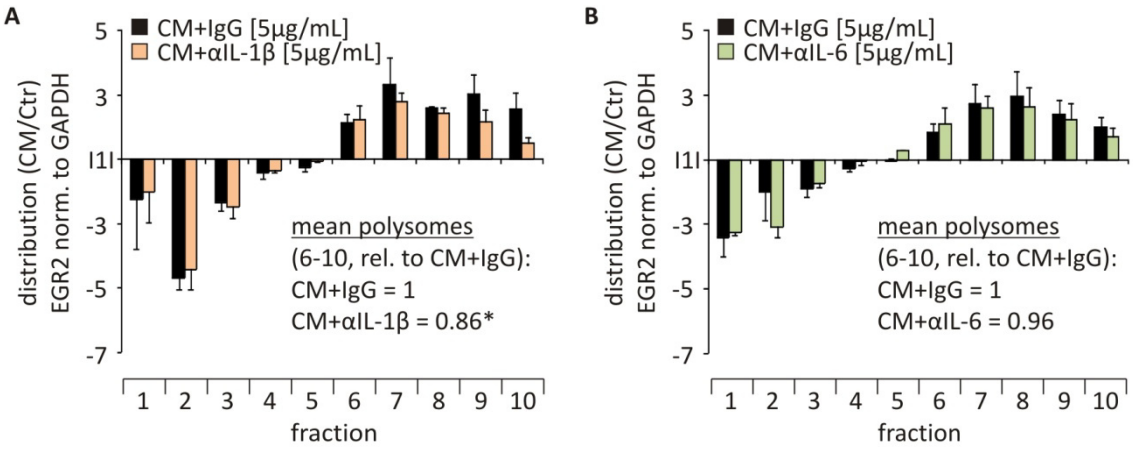

Figure 5-9: Impact of IL-6 or IL-1β on EGR2 translation
CM was pre-treated with IgG control [5 µg/mL], neutralizing IL-1β antibody [5 µg/mL] (A) or neutralizing IL-6 antibody [5 µg/mL] (B) for 1 h at 37°C. Then MCF7 cells were incubated with the respective CMs for 4 h, followed by polysomal fractionation. Changes of EGR2 mRNA distribution induced by CM+IgG compared to Ctr are shown in black bars, those induced by CM+αIL-1β are shown in orange bars and those induced by CM+αIL-6 are shown in green bars. Mean polysomal distribution (fractions 6 to 10) of EGR2 upon CM+αIL-1β or αIL-6 was calculated relative to CM+IgG. Data are presented as means ± SEM ($n \geq 3$, $^*p < 0.05$).

In response to the IL-1β depleted CM, EGR2 mRNA distribution to the polysomal fractions was lower compared to the IgG control CM (Figure 5-9A). Importantly, comparing polysomal fractions 6 to 10 of MCF7 cells treated with IL-1β-depleted CM

with those treated with IgG control CM, revealed a significant decrease in the mean polysomal distribution of EGR2 to 86 ± 3%.

In contrast, preincubation with neutralizing IL-6 antibody barely changed the translational induction by CM+IgG (Figure 5-9B). Pooling of polysomal fractions 6 to 10 decreased the polysomal distribution of EGR2 to 96 ± 3% of the control.

These findings support an involvement of IL-1β in the process causing enhanced translation of EGR2, whereas IL-6 seems not to be relevant.

5.2.2.2 Recombinant IL-1β induces EGR2 translation

To determine whether IL-1β induces EGR2 translation on its own, I treated MCF7 cells with recombinant IL-1β (50 ng/mL) for 4 h and conducted polysomal fractionation. Recombinant IL-1β caused a marked shift of EGR2 mRNA into the polysomes (Figure 5-10). Specifically, mean EGR2 mRNA distribution across all polysomal fractions significantly increased in the polysomes to 164 ± 11% relative to the control.

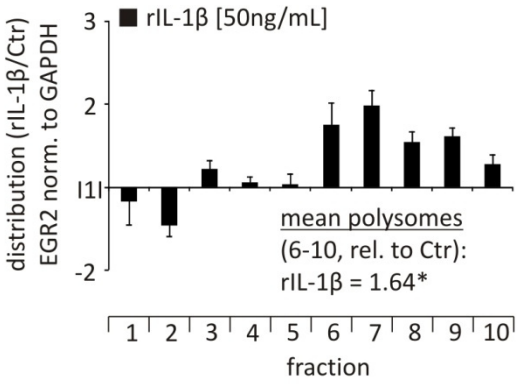

Figure 5-10: Impact of recombinant IL-1β on EGR2 translation
MCF7 cells were treated with recombinant human IL-1β [50 ng/mL] for 4 h followed by polysomal fractionation. IL-1β-induced changes in EGR2 mRNA distribution relative to Ctr were analyzed using qPCR and normalized to GAPDH. Mean polysomal changes (fractions 6 to 10) of EGR2 in response to rIL-1β were calculated relative to Ctr. Data are presented as means ± SEM (n ≥ 3, *p < 0.05).

Taken together, these data strongly suggest that IL-1β suffices to induce EGR2 translation. Moreover, IL-1β appears to contribute to the induction of EGR2 translation in response to conditioned medium from activated monocyte-derived macrophages.

5.2.3 Impact of p38-MAPK on EGR2 translation

Next, I aimed at understanding the signaling cascades linking EGR2 translation and IL-1β.

5.2.3.1 p38-MAPK is activated in response to CM

IL-1β is known to induce p38-MAPK signaling via phosphorylation of the latter (169). Accordingly, I found that p38-MAPK is rapidly, but transiently phosphorylated in MCF7 cells in response to IL-1β treatment (Figure 5-11A). Interestingly, the same phosphorylation pattern was observed upon treatment with CM, whereas Ctr did not affect phosphorylation, i.e. activation of p38-MAPK (Figure 5-11), thus proving that p38-MAPK is indeed activated upon CM treatment.

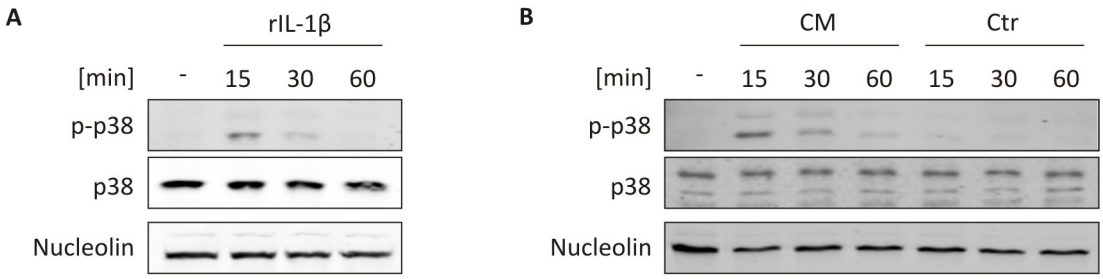

Figure 5-11: CM induces phosphorylation of p38-MAPK
MCF7 cells were treated for 15, 30 and 60 min with human recombinant IL-1β [50 ng/mL] (A) or CM and Ctr (B). Whole-cell extracts were subjected to Western analysis and probed with the indicated antibodies. Blots are representative for at least 3 independent experiments.

5.2.3.2 Inhibition of p38-MAPK impairs EGR2 translation

In further experiments, I examined whether the activation of the p38-MAPK pathway accounts for enhanced translation of EGR2. Therefore, I treated MCF7 cells with CM in combination with the p38-MAPK inhibitor SB203580 [10 µM] and performed polysomal fractionation.

Inhibition of p38-MAPK increased EGR2 mRNA distribution in monosomal fractions and decreased its distribution in polysomal fractions as compared to CM-treated cells. Specifically, the mean distribution of EGR2 mRNA across all polysomal fractions 6 to 10 was significantly lower when p38-MAPK was inhibited (84 ± 1% compared to CM-

alone) (Figure 5-12A). Hence, CM-induced EGR2 translation is partially inhibited by blocking p38-MAPK activity.

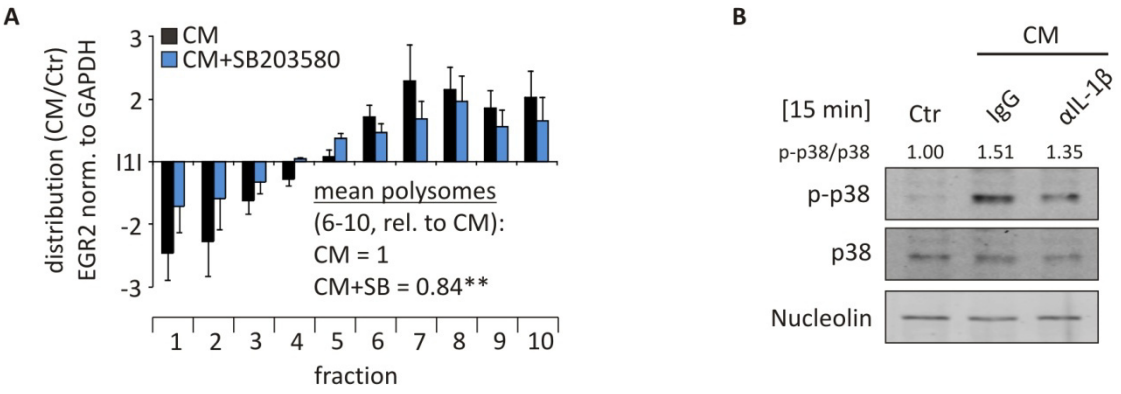

Figure 5-12: Inhibition of p38-MAPK impairs EGR2 translation
(A) MCF7 cells were treated for 4 h with Ctr, CM alone (black bars) or in combination with SB203580 [10 µM] (blue bars). Using polysomal fractionation und qPCR, changes of EGR2 mRNA distribution were analyzed relative to Ctr. Data were normalized to GAPDH. Mean polysomal change (fractions 6 to 10) of EGR2 upon CM+SB was calculated relative to CM. Data are presented as means ± SEM ($n \geq 3$, $^{**}p < 0.01$). (B) MCF7 cells were treated for 15 min with Ctr and CM pre-treated with IgG or IL-1β neutralizing antibody as described before. Whole-cell extracts were subjected to Western analysis and probed with the indicated antibodies followed by densitometric analysis. Levels of phospho-p38 were normalized to total p38 and are presented relative to Ctr. Blot is representative for at least 3 independent experiments.

To verify that IL-1β contributed to activation of p38-MAPK in response to CM, I employed again CM depleted for IL-1β by a neutralizing antibody and tested the activation, i.e. phosphorylation status, of p38-MAPK using Western analysis. Indeed, neutralizing IL-1β attenuated CM-induced phosphorylation of p38-MAPK (Figure 5-12B).

In summary, these results indicate that IL-1β increases EGR2 translation in a p38-MAPK-dependent manner.

5.2.4 EGR2 is translated in an IRES-dependent manner

As described in detail in 3.1.1, translation can be initiated in a cap-dependent or cap-independent manner, for example via IRES elements. Therefore, I aimed at determining the mode of translation of EGR2 under inflammatory conditions.

5.2.4.1 *In silico* analysis of EGR2-5'UTR

As translation of individual mRNAs is often regulated via their 5'UTRs (170), I first analyzed the 5'UTR of EGR2. The 5'UTR of EGR2 proved to be relatively long being composed of 326 nucleotides (Figure 5-13A).

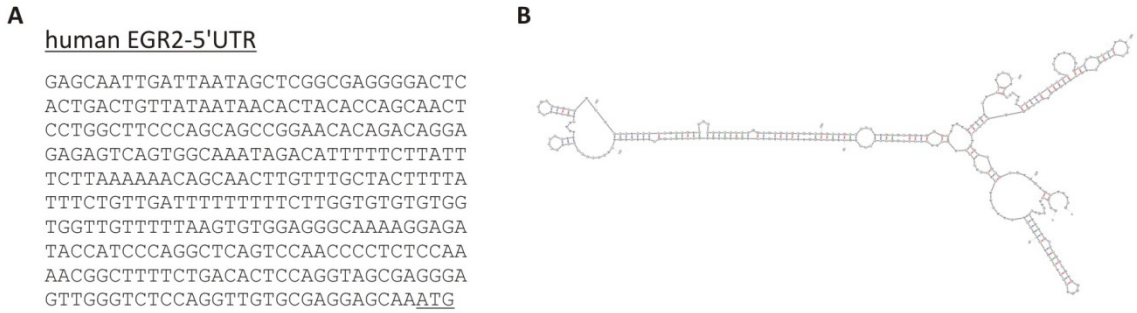

Figure 5-13: EGR2-5'UTR is long and highly structured
(A) Sequence of human EGR2-5'UTR. (B) Predicted structure of the human EGR2-5'UTR using *mfold*.

To determine potential structures within the 5'UTR of EGR2, I used the online software *mfold* for an *in silico* structure analysis (162), which predicted a secondary structure containing various loops with a minimal free energy of -89.40 kcal/mol (Figure 5-13B). As described in 3.1.3.1, a structure with a free-energy of −50 kcal/mol is sufficient to block UTR scanning (25). The EGR2-5'UTR can therefore be considered as highly structured.

These findings imply that the 5'UTR of EGR2 is presumably a target of regulational control.

5.2.4.2 Rapamycin induces EGR2 translation

Next, I tested whether inhibition of cap-dependent translation in general has an impact on EGR2 translation. For this purpose, I treated MCF7 cells with the mTOR inhibitor rapamycin to inhibit cap-dependent translation.

As expected, polysomal distribution of GAPDH increased in monosomal fractions and decreased in polysomal fractions in response to rapamycin, indicative for an mRNA being translated cap-dependently (Figure 5-14A). Therefore, GAPDH could not be used for normalization when EGR2 mRNA distribution was analyzed. Interestingly,

translation of EGR2 appeared to be enhanced under these conditions, supporting a cap-independent mechanism of EGR2 translation (Figure 5-14B).

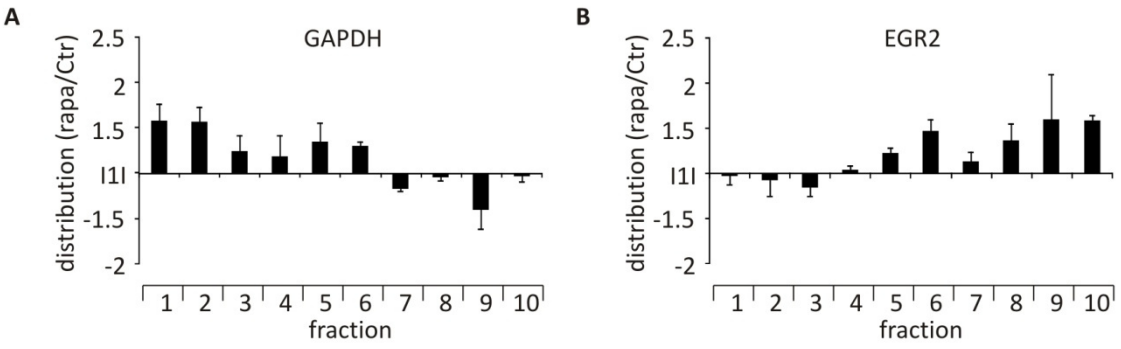

Figure 5-14: Rapamycin leads to altered GAPDH and EGR2 translation
MCF7 cells were treated with rapamycin [100 nM] for 4 h and subjected to polysomal fractionation. RNA from single fractions was isolated. GAPDH (A) and EGR2 (B) mRNA distribution was analyzed using qPCR. Data are not normalized and presented as means ± SEM (n = 3).

Taken together, the long and structured 5'UTR as well as the enhanced translation under conditions of inhibited cap-dependent translation support the assumption that EGR2 mRNA might be translated in a cap-independent, e.g. in an IRES-dependent manner.

5.2.4.3 EGR2 contains an IRES element

To determine if an IRES element is present within the 5'UTR of EGR2, I used the bicistronic reporter plasmids pRF and phpRF containing both, a *renilla* and a downstream *firefly* luciferase gene. These constructs express *renilla* luciferase in a cap-dependent manner, whereas the downstream *firefly* luciferase is only translated when a functional IRES element is present intercistronically (Figure 5-15A). In addition, phpRF contained a hairpin sequence that was inserted upstream of the *renilla* luciferase open reading frame to minimize cap-dependent translation and inhibit reinitiation of translation (Figure 5-15B). To determine the presence of an IRES within the 5'UTR of EGR2, EGR2-5'UTR was inserted into the intercistronic regions of pRF and phpRF, resulting in pR-EGR2-F and phpR-EGR2-F, respectively.

Cells transiently transfected with pRF or pR-EGR2-F in combination with the β-Galactosidase transfection control showed similar relative *renilla* activities (Figure 5-15A). In contrast, the relative *firefly* activity was significantly higher in the presence

of EGR2-5'UTR (11.79 ± 2.27 fold relative to pRF). The same is true for the hairpin containing construct where I observed a 7.12 ± 0.61 fold induction of *firefly* luciferase compared to phpRF, whereas the *renilla* activity remained at equal levels (Figure 5-15B).

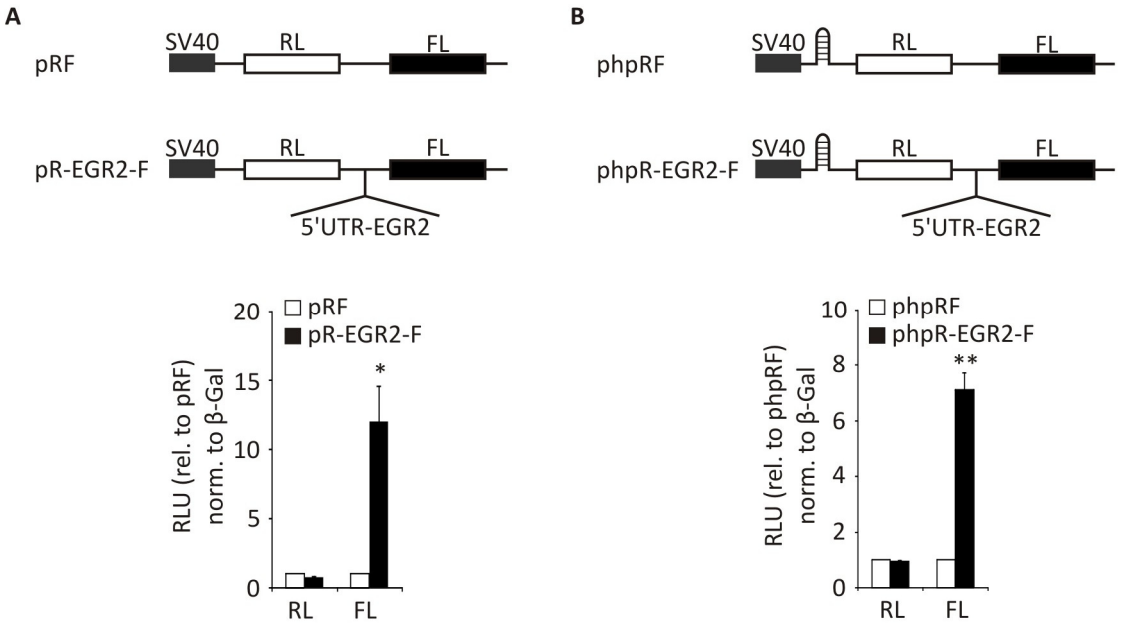

Figure 5-15: Identification of an IRES element in the 5'UTR of EGR2
Scheme of bicistronic constructs pRF (A) and phpRF (B) used for reporter assays. Vectors were co-transfected with SV40-β-Gal plasmid into MCF7 cells. 24 h after transfection *renilla* and *firefly* activities were measured and normalized to β-Galactosidase activity. Data are presented as means ± SEM (n > 3, **p < 0.01) relative to the empty vector.

The identification of IRES elements has been controversially discussed in literature (171), thus, it is crucial to exclude false positive identification of IRES elements that could arise from cryptic promoter activity or cryptic splicing.

In an attempt to rule out cryptic promoter activity, I introduced the EGR2-5'UTR into the promoterless pGL3-basic vector, resulting in pGL3-EGR2.

Insertion of EGR2-5'UTR did not enhance *firefly* activity in transiently transfected MCF7 cells compared to the pGL3-basic parent vector (Figure 5-16A). The positive control containing an SV40 promoter referred to as pGL3-SV40 showed a strong relative luciferase activity compared to the promoterless vector.

As cryptic splicing events may cause the excision of the intercistronic region and/or the formation of fusion proteins that exhibit *renilla* and *firefly* activities, I next tested whether the bicistronic plasmid generates an mRNA transcript of the expected size.

Specifically, the full length transcript of the phpR-EGR2-F (R-EGR2-F) was predicted to contain 2933 nucleotides, whereas the phpRF control vector was expected to produce a transcript (RF) of 2587 nucleotides. For this purpose, I treated mRNA isolated from cells transfected with either phpRF or phpR-egr2-F with DNase to remove residual contaminations of the plasmid DNA.

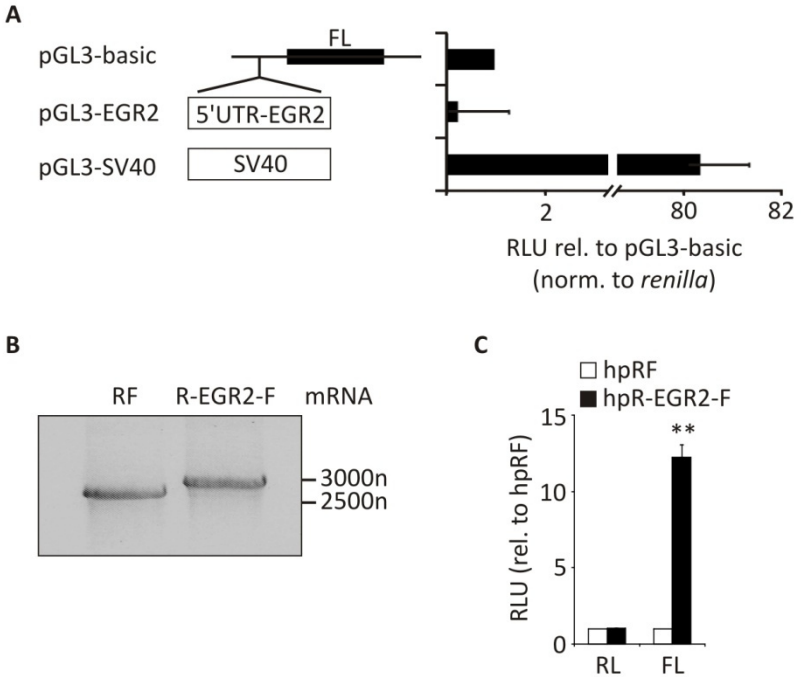

Figure 5-16: EGR2-5'UTR does not contain cryptic promoters or splice sites
(A) MCF7 cells were co-transfected with the indicated reporter constructs and SV40-*renilla* plasmid. 48 h after transfection *firefly* activity was measured and normalized to *renilla* activity. Data are presented as means ± SEM (n > 3). (B) RNA isolated from cells transfected with phpRF or phpR-EGR2-F was DNase treated. cDNA was synthesized and PCR was performed with specific primers to amplify full length RL or R-EGR2-L mRNAs. PCR products were visualized via agarose gel electrophoresis. Data are representative for at least 3 independent experiments. (C) *In vitro* transcribed mRNA of the indicated reporter plasmids was transfected into MCF7 cells. 24 h after transfection *renilla* and *firefly* activities were measured. Data are presented as means ± SEM (n > 3, **p < 0.01) relative to hpRF.

PCR with primers that specifically bind to the 5'end of *renilla* and 3'end of *firefly* open reading frames to amplify the full length RL or R-EGR2-L mRNAs resulted in a single product of the expected size for each vector (Figure 5-16B).

Finally, I used *in vitro* transcribed, capped mRNA instead of DNA for transfection of the indicated constructs to exclude any cryptic promoter or splicing events since transfected mRNA does not enter the nucleus where splicing occurs. While *renilla* luciferase signals remained at similar levels, *firefly* activity was again enhanced to 12.3

± 0.83 fold when comparing hpR-egr2-F mRNA to hpRF mRNA (Figure 5-16C).

These data strongly support the presence of a functional IRES element within the 5'UTR of EGR2.

5.2.4.4 Localization of the EGR2-IRES element within the 5'UTR

To determine the exact localization of the IRES element within the EGR2-5'UTR, I cloned deletion constructs containing different fragments of the 5'UTR and inserted them into the bicistronic reporter construct. These constructs were transfected into MCF7 cells and the IRES activity was measured by calculating the ratio of *firefly* to *renilla* luciferase activities (Figure 5-17).

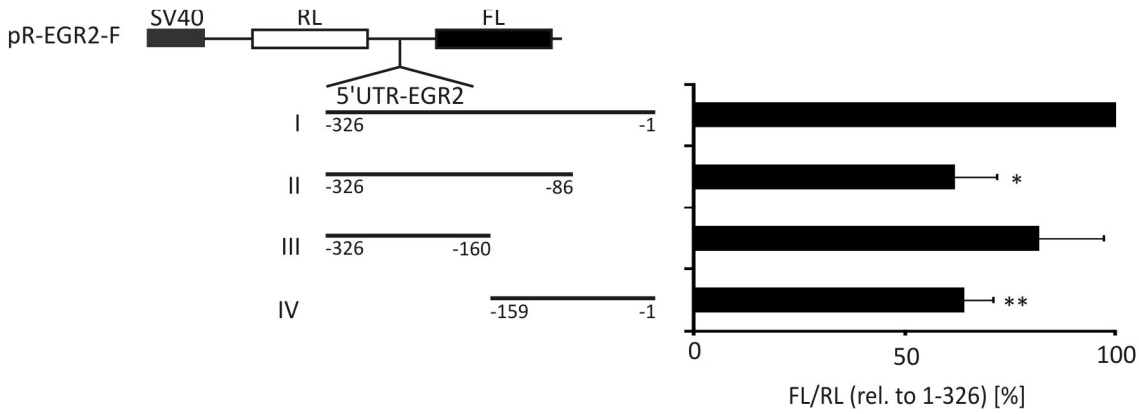

Figure 5-17: Full length EGR2-5'UTR is required for full IRES activity

The deletion constructs II to IV of the EGR2-5'UTR were inserted into the bicistronic reporter plasmid as indicated and transfected into MCF7 cells. IRES activity was calculated as ratio of *firefly* luciferase to *renilla* luciferase and is given relative to construct I (full length EGR2-5'UTR). Data are presented as means ± SEM (n > 3, *p < 0.05, **p < 0.01).

While the reduction of EGR2-IRES activity of construct III to 82 ± 15% of the full length construct I was not significant, insertion of the constructs II and IV led to a significant decrease of EGR2-IRES activity down to 62 ± 10% and 64 ± 7% of the full length. However, from these constructs it was not reasonable to define a specific region in the 5'UTR that is responsible for the IRES activity. Thus, I assume that the entire 5'UTR of EGR2 appears to be necessary for maintaining full IRES activity.

5.2.4.5 CM and IL-1β induce EGR2-IRES activity p38-MAPK-dependently

In the following experiments, I determined whether the IRES element of EGR2 also responds to CM. For this purpose, I transfected the hairpin containing phpR-EGR2-F construct into MCF7 cells and treated them for 24 h with CM or Ctr. As predicted, IRES activity of phpR-EGR2-F transfected cells was significantly induced in response to CM up to 2.30 ± 0.22 fold compared to Ctr (Figure 5-18A).

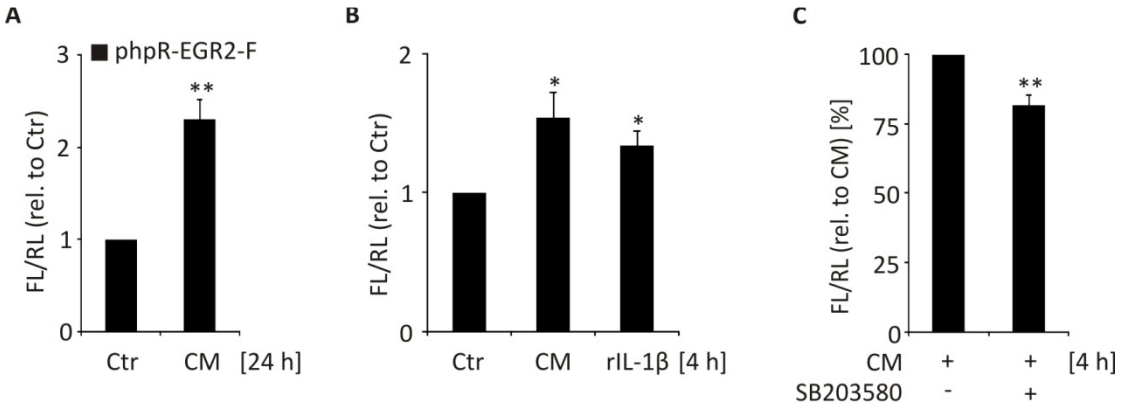

Figure 5-18: CM and IL-1β enhance EGR2-IRES activity
MCF7 cells were transfected with phpR-EGR2-F and treated with Ctr or CM for 24 h (A), with Ctr, CM or rIL-1β [50 ng/µL] for 4 h (B) or for 4 h with CM or CM containing SB203580 [10 µM] (C). EGR2-IRES activity was calculated as ratio of *firefly* luciferase to *renilla* luciferase. Data are presented as means ± SEM (n > 3, *p < 0.05, **p < 0.01).

In the next set of experiments, I aimed at determining if the CM-induced IRES activity was also dependent on IL-1β and p38-MAPK activation. To this end, cells were again transfected with phpR-EGR2-F. As seen in (Figure 5-18B), treatment with CM for 4 h led to a significant 1.5 ± 0.18 fold increase of EGR2-IRES activity. Similarly, treatment with recombinant IL-1β alone resulted in a 1.34 ± 0.11 fold IRES activation compared to Ctr treated cells. Importantly, CM-induced IRES activity was significantly reduced by the p38-MAPK inhibitor SB203580 to 82 ± 4% (Figure 5-18C).

Thus, I conclude that within an inflammatory environment, IL-1β and p38-MAPK contribute to EGR2-IRES-dependent translation.

5.2.5 Various ITAFs bind to the 5'UTR of EGR2

As described in 3.1.3.3, IRES-dependent translation commonly requires IRES *trans*-acting factors (ITAFs) that bind to the mRNA to recruit initiation factors and ribosomal

subunits to the mRNA. Therefore, I wanted to identify factors that bind to the 5'UTR of EGR2.

5.2.5.1 Identification of proteins that bind to EGR2-5'UTR

To detect proteins bound to RNAs, the method of streptavidin-tethered RNA-affinity purification is commonly used. For this purpose, I transcribed the 5'UTR of EGR2 *in vitro* and conjugated a biotin-label at the 5'end. This labeled transcript was then incubated with streptavidin agarose beads and protein lysates of CM-treated MCF7 cells. After elution and electrophoretic separation, proteins bound to the 5'UTR of EGR2 were visualized by silver staining (Figure 5-19A) and analyzed by mass spectrometry in cooperation with the Molecular Bioenergetics Group (Faculty of Medicine, Frankfurt).

A

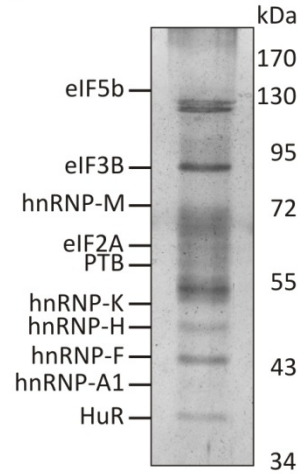

B

	CM and Ctr (195)	CM only (40)	Ctr only (84)
Initiation factors	2, 3, 5		
hnRNPs	M, L, A1, K, AB, U, A2B1, D, A0	A3	CL1, Q
ITAFs	PTB, ILF2, HuR, EWS	IMP2	
others	ILF3	IMP4	

Figure 5-19: Identification of proteins that bind to EGR2-5'UTR
(A) Lysates of CM-treated MCF7 cells were incubated with *in vitro* transcribed, biotinylated EGR2-5'UTR. After immunoprecipitation using streptavidin agarose beads, bound proteins were separated via SDS-PAGE and visualized using silver staining. Individual proteins were identified by mass spectrometric analysis of gel slices. Positions of identified proteins are shown on the left side, protein molecular weight markers are shown on the right side. (B) Overview of selected targets that bound to EGR2-5'UTR identified by mass spectrometry

Figure 5-19B lists selected targets that were identified by mass spectrometry and that were previously described to be involved in translational control (full list see section 8). A number of hnRNPs and initiation factors were identified to bind to the 5'UTR of EGR2, which did not precipitate in the control reaction using non-biotinylated RNA.

Interestingly, among the EGR2-5'UTR-binding proteins, I found PTB and hnRNP-A1, which were previously shown to act as ITAFs associated with enhanced translation of target mRNAs (38, 40, 172).

To ensure a RNA specific binding of these proteins to the EGR2-5'UTR, the interaction was further verified via RNA-affinity purification followed by Western analysis including a control RNA of similar length (300 nucleotides) encoding human reverse GAPDH (hrG). Indeed, PTB, hnRNP-A1 and HuR bound to EGR2-5'UTR but not to the control (Figure 5-20A). Thus, I can ascertain a specific binding of these proteins to the EGR2-5'UTR but not to other RNAs. However, I could not observe a differential binding when comparing CM and Ctr treated MCF7 lysates (Figure 5-20B).

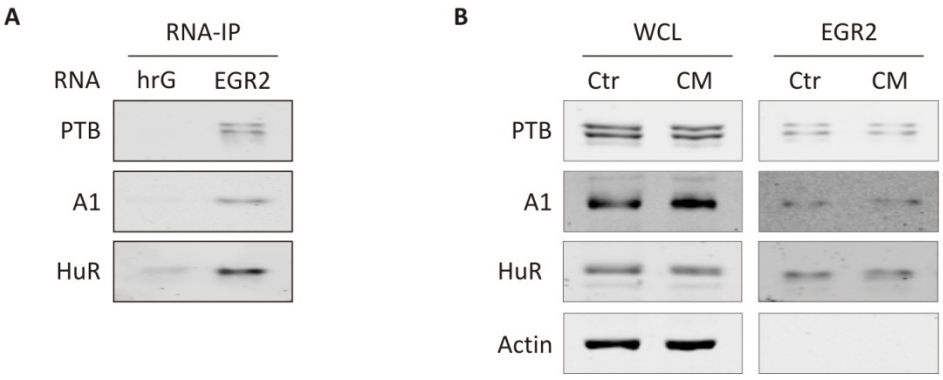

Figure 5-20 Specific binding of ITAFs to EGR2-5'UTR
(A) Lysates of CM-treated MCF7 cells were incubated with *in vitro* transcribed, biotinylated EGR2-5'UTR or human reverse GAPDH (hrG) RNA, before immunoprecipitation of proteins using streptavidin agarose beads. Bound proteins were subjected to Western analysis and probed with the indicated antibodies. Blots are representative for at least 3 independent experiments. (B) Lysates of Ctr or CM-treated MCF7 cells were incubated with *in vitro* transcribed, biotinylated EGR2-5'UTR before immunoprecipitation of proteins using streptavidin agarose beads. Bound proteins were subjected to Western analysis and probed with the indicated antibodies. For whole cell lysates 10% of input was used. Blots are representative for at least 3 independent experiments.

These data provide evidence that several ITAFs indeed bind to the 5'UTR of EGR2, which might influence the EGR2-IRES activity.

5.2.5.2 Overexpression of hnRNP-A1 enhances EGR2-IRES activity

Since hnRNP-A1 was identified to bind to the 5'UTR of EGR2 and it is already known to act as an ITAF, I wanted to test whether overexpression of hnRNP-A1 is sufficient to induce the IRES activity of EGR2. To this end, wildtype hnRNP-A1 (A1-WT) as well as a

dominant negative form of hnRNP-A1 (A1-NLS) were transiently overexpressed in phpR-EGR2-F transfected MCF7 cells and the IRES activity was measured.

Overexpression of A1-WT led to a significant 1.8 ± 12 fold upregulation of EGR2-IRES activity compared to the empty vector control (EV), whereas the dominant-negative form of A1, which is supposed to inhibit endogenous hnRNP-A1 by sequestration to the nucleus, significantly decreased the IRES activity to 0.79 ± 12 fold of the empty vector (Figure 5-21A). Overexpression of the constructs was confirmed by Western analysis (Figure 5-21B).

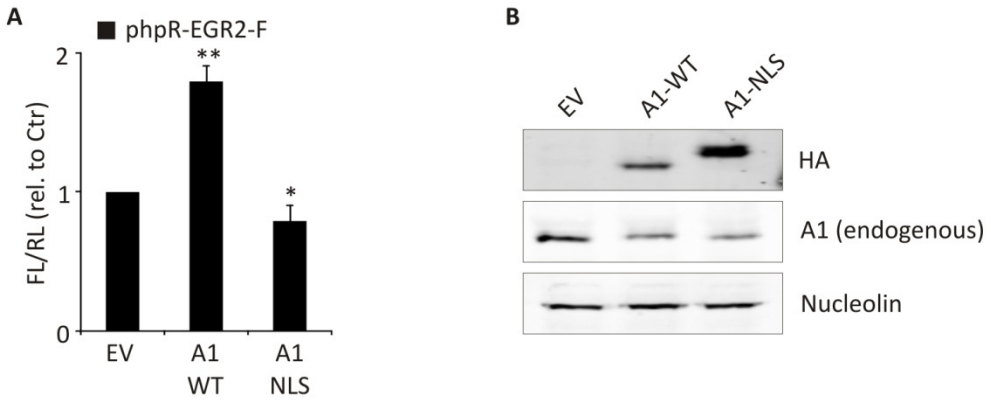

Figure 5-21: hnRNP-A1 overexpression leads to enhanced EGR2-IRES activity

MCF7 cells were co-transfected with phpR-EGR2-F and pcDNA3.1 (EV), wildtype hnRNP-A1 (A1-WT) or dominant negative hnRNP-A1 (A1-NLS). 48 h after transfection cells were harvested and luciferase activities were measured. IRES activity was calculated as described before and is given relative to EV. Data are presented as means ± SEM ($n > 3$, $*p < 0.05$, $**p < 0.01$). (B) MCF7 cells were transfected with the indicated constructs. Whole-cell extracts were generated, subjected to Western analysis and probed with the indicated antibodies. Blot is representative for at least 3 independent experiments.

From these data I conclude, that EGR2 contains an IRES element within its 5'UTR which can be activated by inflammatory stimuli dependent on p38-MAPK activity and hnRNP-A1 availability, in turn enhancing translation of EGR2.

6 Discussion

Translation is a sophisticated and tightly regulated process that enables post-transcriptional control of gene expression. The regulation of translation offers the possibility of a rapid response to external stimuli, without invoking nuclear pathways for mRNA synthesis, processing and transport. Besides, given the huge amount of energy needed for protein synthesis (2 ATP and 2 GTP molecules per each peptide bond, see 3.1) it is pivotal to monitor this process.

The essential idea of translational control is that gene expression is regulated by the efficient use of one mRNA strand for protein synthesis. This may take place at multiple levels, which include targeting of structural features of the mRNA, stimulating *trans*-acting protein or RNA factors or modulating the activity of the translational apparatus all of which mostly affect translation initiation. While these processes are triggered by a variety of stimuli including mitogens, hormones, nutrients and stress signals, especially in the context of cancer progression (23, 173-175), little is known about the effect of inflammatory mediators on translational regulation. It is widely accepted that an inflammatory microenvironment is an essential component of tumors (176) and can be used in cancer immunotherapy to augment the response to chemotherapy (177, 178). However, in some cases, inflammation can diminish the beneficial effects of therapy (179). Therefore, it is crucial to understand regulatory mechanism at all levels – including translation – caused by inflammatory signals in tumor cells. To this end the present study aimed at identifying translationally deregulated targets during inflammation-associated tumorigenesis. In depth analysis of the regulation of one specific target – EGR2 – provides information about a potential general strategy for regulating protein levels.

6.1 Validation of the *in vitro* cell system

The first task of the project was to establish an *in vitro* cell system that mimics the situation of tumor cells that are exposed to an inflammatory microenvironment. For this purpose, I used human U937 monocytes that were differentiated to macrophages by TPA treatment. U937 is a histiocytic lymphoma cell line that is widely used for the investigation of macrophages especially in the context of tumor-associated

inflammation (180, 181). To ensure that U937 cells generate an inflammatory environment in my setting, CBA analysis of the supernatant of differentiated U937 cells (CM) was performed. Indeed, of the six cytokines tested, the pro-inflammatory cytokines TNFα, IL-6, IL-8 and IL-1β and the anti-inflammatory cytokine IL-10 were significantly elevated compared to supernatants of undifferentiated cells (Ctr), whereas IL-12p70 could not be detected in both supernatants. Thus, it was proven that U937 cells secrete pro- and anti-inflammatory mediators and that the secretion profile changes after differentiation. Since only one timepoint was tested, i.e. 24 h after 48 h differentiation, it is not clear whether these cytokines show different concentrations after shorter or longer incubation times due to altered expression or stability. To clarify the exact type of macrophage generated upon TPA-treatment of U937 cells, in depth analysis of the secretion and surface marker profiles would be required.

For the investigation of translational changes in tumor cells, the breast cancer cell line MCF7 was chosen. Breast cancers are highly infiltrated by macrophages which often correlates with poor prognosis (182). Moreover, MCF7 cells are estrogen receptor positive indicating that their invasive potential is only moderate as the estrogen receptor is often lost during tumor progression (183). This provided the opportunity to investigate changes in the tumorigenic potential. Indeed, I could show that CM has a pro-tumorigenic impact on MCF7 cells, since it induced the activity of the transformation marker AP-1, which is a dimeric transcription factor complex that regulates genes involved in cell proliferation, differentiation, apoptosis, angiogenesis and tumor invasion (184). In line, enhanced migration could be observed. Additionally, it was shown previously that CM strongly reduces protein levels of the tumor suppressor PDCD4 (185, 186). Taken together, these data indicate that CM induces a pro-tumorigenic program in MCF7 cells. Further support for this conclusion comes from the microarray analysis of total RNA from 4 h CM-treated compared to Ctr-treated MCF7 cells. Pathway analysis revealed that pro-tumorigenic and anti-apoptotic networks were activated. Moreover, a strong inflammatory response was induced in MCF7 cells.

To identify those genes, which are regulated on the translational level, I conducted microarray analysis of polysome-bound mRNA. The polysomal mRNA is that portion of the RNA that is associated with more than one ribosome, i.e. the polysomes. On

average, ribosomes appear once every 80-100 nucleotides with a limit of one per 30–40 nucleotides due to packing constraints (187). The more ribosomes bind to the mRNA, the more efficient is the translation and the more protein is synthesized from one mRNA strand. In order to isolate polysome-bound mRNA the technique of polysomal fractionation was used, which involves the separation of the mRNA on a sucrose gradient according to its sedimentation after ultracentrifugation. This method is the most flexible and powerful tool for diagnosing and investigating translational changes. For global identification of translational changes, the polysomal RNA was pooled and analyzed using microarray. Due to the fact that mRNAs that change in abundance, that is for example via enhanced transcription, are expected to similarly increase in the polysomes and monosomes, the results of the total RNA changes were compared with the polysomal changes. In fact, only those genes that showed a stronger change in the polysomes than on total RNA level were considered to be translationally regulated. 42 targets were found to meet these criteria. Some of them were already shown to be subject to post-transcriptional regulation such as CYP24A1 (188), PLAUR (189) and CD44 (190). Validation of 8 selected targets confirmed the microarray results.

To take a closer look on the translational status of specific mRNAs, I analyzed their distribution in single fractions. When translation initiation is enhanced the polysomes become larger (= more ribosomes per mRNA → more mRNA abundant in later fractions). The same is true in the case of elongation inhibition, since initiation still occurs normally and the ribosomes accumulate at the mRNA, thereby shifting it to later fractions within the polysomes.

To distinguish an increase in translation initiation from a decrease in elongation, the amount of mRNA in the subpolysomes, which are presented by nonactive mRNPs and monosomes, has to be considered. If an mRNA does not shift within the polysomes but from subpolysomal to polysomal fractions, translation initiation is enhanced. This applied to the mRNA distribution change of EGR2 that showed the highest change in polysomes, hence, this target was chosen for further investigation.

6.2 Involved pathways of EGR2 translation

So far regulation of EGR2 is only poorly understood. Some studies suggested transcriptional activation for EGR2. The most prominent transcription factor identified to date is NF-AT, which induces EGR2 expression during T cell anergy induction (122). p53 has also been described to directly bind to the EGR2 promotor to induce its transcription (151). A recent report identified miR-17-92 to bind to the 3'UTR of EGR2 and to reduce EGR2 levels in murine macrophages during leukemogenesis (155). The authors assume this effect was either caused by enhanced destabilization of EGR2 mRNA or decreased translation, yet without experimental verification. However, by use of polysomal fractionation, I could prove that EGR2 translation is significantly enhanced in breast cancer cells that are challenged with a pro-inflammatory microenvironment generated by CM. This effect was at least in part mediated by IL-1β that is present in CM. Notably, depletion of IL-1β via neutralizing antibodies did not fully repress and, similarly, treatment with recombinant IL-1β did not completely recover induction of EGR2 translation compared to CM. Therefore, it is likely that other factors might contribute to the induction of EGR2 translation as well. I additionally tested the effect of neutralizing IL-6 in CM but only a minimal inhibition could be observed. It would be of great interest to examine whether simultaneous neutralization of IL-1β, IL-6 and/or other cytokines acted synergistically on EGR2 translation.

Since IL-1β is known to induce phosphorylation and thereby activation of p38-MAPK (169, 191), I assessed the p38-MAPK activity in my system. I observed strong phosphorylation of p38-MAPK upon CM or IL-1β treatment after 15 min already whereas Ctr had no effect. This effect was transient, i.e. phosphorylation decreased again after 30 min and was back to control levels after 1 h. In line, neutralization of IL-1β in CM diminished p38-MAPK phosphorylation, thereby verifying that IL-1β is responsible for the CM-induced p38-MAPK activation. To determine whether p38-MAPK activation also accounts for EGR2 translation, I used the p38-MAPK inhibitor SB203580 in polysomal fractionation experiments (192). I observed a significant decrease of EGR2 translation when p38-MAPK was inhibited, thus proving that p38-MAPK contributes to the translational activation of EGR2. Notably, translation of EGR2 was assessed after 4 h whereas p38-MAPK phosphorylation was almost absent after

1 h CM treatment already. This discrepancy may be due to the fact, that while p38-MAPK activation is typically transient, various downstream signaling events might be required until EGR2 translation is activated. Again p38-MAPK inhibition could not fully inhibit EGR2 translation, implying the involvement of additional signaling pathways in this process.

6.3 IRES-dependent EGR2 translation

While IL-1β was previously shown to suppress IRES-dependent translation of thrombomodulin (193), no translation-inducing function of IL-1β has been identified so far. Recently, IL-1α was reported to activate translation of mRNAs such as IκBζ and IL-6 (168). Moreover, IRES-dependent translation of pro-survival genes like cMyc was shown to be p38-MAPK-dependent, which was activated by IL-6 (194, 195). IRES-dependent translation is often activated under stress situations such as nutrient deprivation and hypoxia when mTOR and subsequently cap-dependent translation is repressed (32). Interestingly, I observed enhanced EGR2 translation upon rapamycin-treatment, which is a specific mTOR inhibitor (196). Thus, I concluded that an IRES-dependent mechanism may account for EGR2 translation. In order to identify IRES elements within the 5'UTR of target mRNAs, bicistronic reporter plasmids were used (referred to as phpRF and phpR-EGR2-F), which contain two ORFs and the 5'UTR of interest inserted in between. Specifically, the potential IRES element is flanked by an upstream *renilla* luciferase, which is translated cap-dependently, whereas the downstream *firefly* luciferase can only be translated when an IRES element is located intercistronically to induce translation internally (30). The plasmid used in this study additionally contained a hairpin structure generated by a palindromic sequence upstream of the *renilla* luciferase to reduce cap-dependent translation and read-through across the *renilla* termination codon. Insertion of the EGR2-5'UTR indeed resulted in a strong induction of *firefly* activity indicating an IRES-dependent mechanism of translation. This finding was also supported by the fact that CM and IL-1β-treatment induced IRES activity while inhibition of p38-MAPK reduced it. Notably, all effects that were observed via polysomal fractionation and subsequent analysis of EGR2 mRNA distribution were also observed when testing EGR2-IRES activity via luciferase assays.

The use of bicistronic reporter plasmids for the identification of IRES elements has been questioned because of the potential presence of cryptic promoters or splice sites within 5'UTRs, which may lead to *firefly* expression from a monocistronic mRNA (171). Cryptic splicing is of special interest since the *renilla* luciferase contains a splice donor site which might induce splicing events when the inserted 5'UTR contains a suitable splice acceptor site (197). Indeed, an accurate re-examination of some predicted IRES containing sequences such as XIAP revealed that their first identification might have been false-positive due to the generation of aberrant monocistronic transcripts (198). However, the occurrence of cryptic splicing or promoter activities does not necessarily exclude the presence of IRES elements. Sherill et al. could prove that while the Bcl2-5'UTR contains both an alternatively spliced intron and a minor promoter, an IRES element was still attributable to enhanced translation of Bcl2 (199). Therefore, stringent test procedures are required to clarify this issue. One unequivocal proof of principle is the transfection of *in vitro* transcribed mRNA from the bicistronic reporter plasmid (200). Since transfected mRNA does not enter the nucleus it is neither transcribed nor spliced. Transfection of hpR-EGR2-F mRNA led to even higher induction of *firefly* luciferase as compared to transfected DNA. Additionally DNase-treated RNA was extracted from transfected cells and cDNA synthesized. PCR with primers to amplify the full length bicistronic mRNA revealed that shortened constructs, which might occur from cryptic splicing, were not present. Finally, EGR2-5'UTR was inserted into the promoterless monocistronic pGL3-basic vector and transfected into MCF7 cells. No induction of *firefly* activity could be observed, thus, cryptic promoter activity was ruled out. These important control experiments clearly excluded that cryptic promoters or splicing events accounted for the proposed EGR2-IRES activity in the bicistronic luciferase assays. Thus, I could unambiguously proof the presence of an IRES element within the 5'UTR of EGR2.

6.4 Impact of ITAFs on EGR2 translation

Cellular IRES-mediated translation is typically less efficient than the best studied cases of viral IRES-mediated translation (201). However, an increasing body of evidence indicates that cellular IRESs have two major functions. First, they support robust translation of cellular mRNAs under a variety of physiological conditions, such as

mitosis, when cap-dependent translation is compromised. Second, they support low levels of translation initiation for cellular IRES containing mRNAs with highly structured 5'UTRs. These are incompatible with efficient scanning under normal physiological conditions when cap-dependent translation is fully active (202). In fact, it was previously shown that CM induces the PI3K-mTOR-pathway, thus proving that mTOR and subsequent cap-dependent translation is not generally inhibited in my system (185). Accordingly, the translation efficiency of the housekeeping gene *GAPDH* does not change upon treatment with CM. Hence, I conclude that the activation of IRES-dependent EGR2 translation mediated by CM is not due to the induction of stress signaling pathways that generally shut down cap-dependent translation thereby favoring IRES-dependent translation. Instead, induction of specific factors that facilitate EGR2 protein synthesis in an IRES-dependent manner appears rational.

This is further corroborated by the observation that the 5'UTR of EGR2 is relatively long containing 326 nucleotides and highly structured as predicted by use of *mfold,* which calculated a secondary structure with a minimal free energy of -89.40 kcal/mol. A structure with a free-energy of -50 kcal/mol is sufficient to block UTR scanning and indicates the need for additional factors (25). Conventional scanning from the 5'end is not efficient for most IRES containing cellular mRNAs because their 5'UTRs are typically long, GC-rich and highly structured. Accordingly, the activity of cellular IRES elements strongly depends on the availability and interaction of their corresponding IRES *trans*-acting factors (ITAFs). By use of RNA pulldown and subsequent mass spectrometry analysis 319 proteins were found to bind to the 5'UTR of EGR2. Among various translation initiation factors as well as heterogeneous nuclear ribonucleoproteins (hnRNPs) some previously described ITAFs were found namely PTB, hnRNP-A1 and HuR. Their binding to the EGR2-5'UTR was highly specific since pulldown with GAPDH RNA did not show an interaction with any of these proteins.

Interestingly, overexpression of wildtype hnRNP-A1 significantly enhanced whereas a dominant negative form (hnRNP-A1-NLS) diminished EGR2-IRES activity. The NLS-construct contains the bipartitebasic-type NLS of hnRNP-K fused in frame with the N-terminus of an hnRNP-A1 mutant (A1-G274A), which lacks both nuclear import and export activities. It was proven that the nucleus-localized NLS-A1 mutant has the

potential to compete with wild-type hnRNP-A1 for binding to and nuclear export of mRNAs thereby sequestering it to the nucleus (161).

However, I could not observe a differential expression or binding affinity when comparing CM- or Ctr-treated protein lysates indicating that CM does not alter hnRNP-A1 protein levels. Yet, the mechanisms responsible for regulating ITAF concentration and activity have not been fully defined. Several studies have suggested that the subcellular distribution of ITAFs is an important determinant for IRES activity (202). Since whole cell lysates were prepared for the RNA pulldown and protein expression experiments, a difference in the localization of hnRNP-A1 would not have been taken into consideration. Moreover, hnRNP-A1 has been shown to be regulated via phosphorylation of its M9 peptide domain by p38-MAPK which subsequently caused enhanced IRES-dependent translation of cMyc (167, 194). Whether hnRNP-A1 is phosphorylated before it binds to its target mRNA or *vice versa* is not clear. Because of the lack of commercially available phospho-hnRNP-A1 antibodies the phosphorylation status of hnRNP-A1 was not determined. On account of the fact that the IRES activity of EGR2 is also dependent on p38-MAPK signaling, I conclude that phosphorylation and/or localization events of hnRNP-A1 are likely to be the mechanism of action for regulating the influence of hnRNP-A1 on the translation of EGR2.

Besides hnRNP-A1, PTB was also found to bind to EGR2-5'UTR. This was not surprising given the fact that PTB is considered to be a general ITAF for most of the identified cellular IRESs so far (52). PTB plays a role in the recruitment of the ribosome to the mRNA (203). PTB often needs co-factors to bind to the 5'UTR such as poly(rC)-binding protein 1 (PCBP1) or upstream of N-ras (UNR) which cause a conformational change allowing PTB to bind and to recruit the ribosome (204, 205). Strikingly, PCBP1 was also identified by mass spectrometry to bind to the 5'UTR of EGR2 (see Table 8-3). The consensus sequence for PTB-mediated ribosome recruitment is $(CCU)_n$ (52). Interestingly, two CCU elements are located within the EGR2-5'UTR namely at position -258 and -69. The generation of different deletion constructs of the EGR2-5'UTR in the bicistronic vector with either the one or the other CCU deleted led to a reduction of the IRES activity for each construct but none of the two could completely abolish IRES activity. Probably, one PTB-binding site is sufficient to maintain IRES activity. Determination of the IRES activity when both potential PTB-binding sites are deleted or

mutated could give further insights into the impact of PTB on EGR2 translational regulation. Additionally, knockdown of PTB or hnRNP-A1 and subsequent polysomal fractionation could support the involvement of one or both of these factors in the ribosomal loading onto the EGR2 mRNA.

The function of HuR on IRES activity is not clear, yet. While one report described HuR as an inducer of XIAP-IRES activity (100), another study proved its inhibitory potential on $p27^{Kip1}$-IRES activity (206). In line, IL-1β-mediated repression of thrombomodulin-IRES activity was also mediated via enhanced binding of HuR (193). It was also shown that hnRNP-C competes with HuR for binding to the IGF-IR-5'UTR to enhance IRES-mediated translation initiation (207). Whether HuR regulates the IRES activity of EGR2 remains to be elucidated for example via knockdown and/or overexpression experiments. Interestingly, Papadopoulou et al. recently described a complex comprising a number of hnRNPs and HuR to interact with mRNAs (208). Since many hnRNPs were identified to bind to the EGR2-5'UTR, changes in its binding complexes might account for the translational regulation of EGR2 as well.

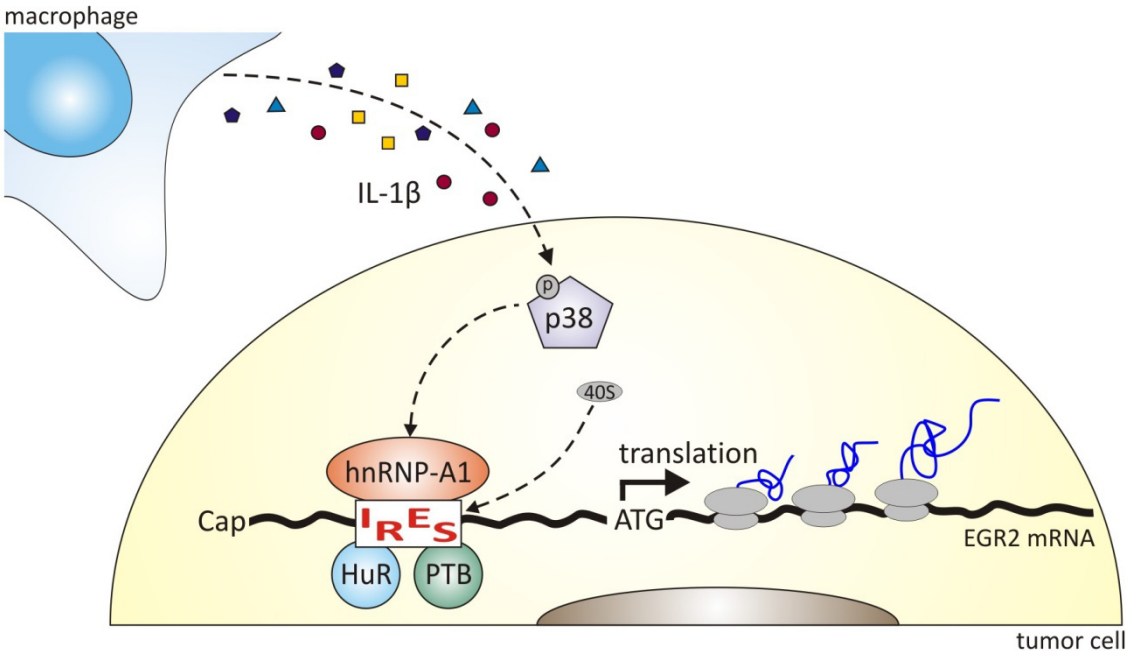

Figure 6-1: Mechanism of EGR2 translation

Macrophages secrete cytokines such as IL-1β that induce a signaling cascade leading to p38-MAPK induction and subsequent binding of ITAFs such as PTB or hnRNP-A1 to an IRES element within the 5'UTR of EGR2. IRES-dependent translation is induced and ribosomes are recruited to the mRNA to mediate protein synthesis.

Abbreviations: 40S, 40S ribosomal subunit; EGR2, early growth response 2; hnRNP, heterogeneous nuclear ribonucleoprotein; HuR, human antigen R; IL, interleukin; IRES, internal ribosome entry site; ITAF, IRES *trans*-acting factor; mRNA, messenger ribonucleic acid; p, phospho group; p38, p38 mitogen activated protein kinase; PTB, polyprimidine tract-binding protein.

6.5 Therapeutic opportunities and concluding remarks

Functionally, EGR2 was described as a transcription factor belonging to the early growth response gene family, that are activated immediately after serum addition (113). It was shown to be crucial for hindbrain development (209) and recently proposed to exert E3 SUMO ligase activity (116). Furthermore, EGR2 was identified as an important regulator of T cell tolerance by inhibiting IL-2 production, thereby promoting a TCR-induced negative regulatory program. Its role in the regulation of cell proliferation is controversial. EGR2 was shown to be induced in cells overexpressing the tumor suppressor PTEN (149) implying anti-proliferative effects. On the opposite, it also appears to induce the anti-apoptotic protein Mcl1 and to stimulate proteasomal degradation of the pro-apoptotic protein Bim (153) denoting pro-survival functions. Thus, while EGR2 translation is enhanced under conditions which I and others have shown to be pro-tumorigenic (185, 186), the function of EGR2 in this setting remains to be elucidated. However, the proposed mechanism in this study for regulating EGR2 protein levels may not be exclusive for MCF7 cells. In fact, it will be of utmost interest to assess whether IRES-dependent translation of EGR2 might play a role in the induction of T cell anergy as well and if this mechanism could be relevant for clinical applications. Regulating T cell anergy is important for blocking tumor-induced tolerance in cancers or during the immunosuppressive treatment of transplantation patients. With respect to the latter, cyclosporin A (CsA) is a potent clinically relevant immunosuppressive agent which blocks NF-AT activation by inhibiting calcineurin. Consequently, T cell activation is blocked. Thus, transplantation patients must remain on CsA therapy indefinitely. Unfortunately, CsA has severe side effects such as nephrotoxicity and hepatotoxicity (210). Alternatively, pharmacological agents that block T cell activation but leave EGR2 induction intact might have the added benefit of promoting T cell tolerance. The specific induction of IRES-dependent translation of EGR2, for example via activation of p38-MAPK and/or hnRNP-A1, might support this effect. Interestingly, rapamycin is also in clinical use for transplantation patients with less side effects than CsA (211). As I could observe enhanced EGR2 translation upon treatment with rapamycin, one until now unknown mechanism of exerting its beneficial effects might be the induction of EGR2 translation thereby promoting T cell anergy. Additionally, EGR2 was proposed to be a good target in cancer therapy to

evade tumor-induced immune tolerance (124). In this case, inhibition of factors that specifically promote EGR2 translation might be advantageous, such as chemically blocking p38-MAPK or neutralizing IL-1β, while at the same time leaving TCR-induced T cell activation intact. Notably, rapamycin is in clinical trial for cancer therapy as well (81). This might have the disadvantageous side effect of inducing EGR2 translation thereby facilitating T cell anergy. Therefore, co-treatment with compounds that inhibit EGR2 as mentioned above would be potentially required.

Mutations in the human *EGR2* gene have been associated with peripheral myelinopathies, including Charcot-Marie-Tooth disease (CMT). Dominant neuropathy-associated mutations of EGR2 have been identified in all three zinc fingers of the DNA-binding domain and these mutations either result in decreased protein expression or impaired DNA-binding (142). Interestingly, mutations in the 5'UTR of Connexin 32 (CX32) have also been linked to CMT. It was proven that CX32 contains an IRES whose function is abolished after insertion of a mutation resulting in reduced protein synthesis (212). Up to now the identification of mutations in the *EGR2* gene concentrates on the open reading frame or promoter region. In the light of the identified translational component of EGR2 regulation it might also be advisable to scan the 5'UTR for mutations in the future and check whether the IRES activity is affected.

In summary, the presented data provide evidence for a novel mechanism of EGR2 regulation via enhanced IRES-dependent translation under pro-inflammatory conditions. This effect is mediated by IL-1β and p38-MAPK activation. The exact characterization and identification of missing signaling events, especially regarding the regulation of ITAF activity upon inflammatory stimuli, opens multiple opportunities for further studies. In depths analyses of the regulation of EGR2 will be of interest for conditions where T cell activation should be therapeutically altered such as transplantations or tumor immunotherapies. Moreover, the described mechanism may not be exclusive for one target but supports the understanding of regulation of gene expression in the context of inflammation-associated tumorigenesis.

7 References

1. Richter, J.D. and Lasko, P. (2011) Translational control in oocyte development. Cold Spring Harb Perspect Biol, 3, a002758.
2. Lewis, S.M. and Holcik, M. (2005) IRES in distress: translational regulation of the inhibitor of apoptosis proteins XIAP and HIAP2 during cell stress. Cell Death Differ, 12, 547-553.
3. Krichevsky, A.M., Metzer, E. and Rosen, H. (1999) Translational control of specific genes during differentiation of HL-60 cells. J Biol Chem, 274, 14295-14305.
4. Scheper, G.C., van der Knaap, M.S. and Proud, C.G. (2007) Translation matters: protein synthesis defects in inherited disease. Nat Rev Genet, 8, 711-723.
5. Chang, R.C., Yu, M.S. and Lai, C.S. (2006) Significance of molecular signaling for protein translation control in neurodegenerative diseases. Neurosignals, 15, 249-258.
6. Bilanges, B. and Stokoe, D. (2007) Mechanisms of translational deregulation in human tumors and therapeutic intervention strategies. Oncogene, 26, 5973-5990.
7. Silvera, D., Formenti, S.C. and Schneider, R.J. (2010) Translational control in cancer. Nat Rev Cancer, 10, 254-266.
8. Sonenberg, N. and Hinnebusch, A.G. (2009) Regulation of translation initiation in eukaryotes: mechanisms and biological targets. Cell, 136, 731-745.
9. Pestova, T.V., Lorsch, J.R. and Hellen, C.U.T. (2007) "The Mechanism of Translation Initiation in Eukaryotes" In Mathews, M. B., Sonenberg, N. and Hershey, J. W. B. (eds.), Translational Control in Biology and Medicine. Cold Spring Harbor Laboratory Press, New York, pp. 87-128.
10. Proud, C.G. (2005) eIF2 and the control of cell physiology. Semin Cell Dev Biol, 16, 3-12.
11. Jackson, R.J., Hellen, C.U. and Pestova, T.V. (2010) The mechanism of eukaryotic translation initiation and principles of its regulation. Nat Rev Mol Cell Biol, 11, 113-127.
12. Kozak, M. (1991) Structural features in eukaryotic mRNAs that modulate the initiation of translation. J Biol Chem, 266, 19867-19870.
13. Lee, J.H., Pestova, T.V., Shin, B.S., Cao, C., Choi, S.K. and Dever, T.E. (2002) Initiation factor eIF5B catalyzes second GTP-dependent step in eukaryotic translation initiation. Proc Natl Acad Sci U S A, 99, 16689-16694.
14. Henderson, A. and Hershey, J.W. (2011) The role of eIF5A in protein synthesis. Cell Cycle, 10, 3617-3618.
15. Carvalho, M.D., Carvalho, J.F. and Merrick, W.C. (1984) Biological characterization of various forms of elongation factor 1 from rabbit reticulocytes. Arch Biochem Biophys, 234, 603-611.
16. Slobin, L.I. and Moller, W. (1978) Purification and properties of an elongation factor functionally analogous to bacterial elongation factor Ts from embryos of Artemia salina. Eur J Biochem, 84, 69-77.
17. Spahn, C.M., Gomez-Lorenzo, M.G., Grassucci, R.A., Jorgensen, R., Andersen, G.R., Beckmann, R., Penczek, P.A., Ballesta, J.P. and Frank, J. (2004) Domain movements of elongation factor eEF2 and the eukaryotic 80S ribosome facilitate tRNA translocation. EMBO J, 23, 1008-1019.

18. Taylor, D.J., Frank, J. and Kinzy, T.G. (2007) "Structure and Function of the Eukaryotic Ribosome and Elongation Factors" In Michael B. Mathews, N. S., John W.B. Hershey (ed.), Translational Control in Biology and Medicine. Cold Spring Harbor Laboratory Press, New York, pp. 59-85.
19. Caskey, T., Scolnick, E., Tompkins, R., Goldstein, J. and Milman, G. (1969) Peptide chain termination, codon, protein factor, and ribosomal requirements. Cold Spring Harb Symp Quant Biol, 34, 479-488.
20. Gebauer, F. and Hentze, M.W. (2004) Molecular mechanisms of translational control. Nat Rev Mol Cell Biol, 5, 827-835.
21. Ma, X.M. and Blenis, J. (2009) Molecular mechanisms of mTOR-mediated translational control. Nat Rev Mol Cell Biol, 10, 307-318.
22. Yang, H.S., Jansen, A.P., Komar, A.A., Zheng, X., Merrick, W.C., Costes, S., Lockett, S.J., Sonenberg, N. and Colburn, N.H. (2003) The transformation suppressor Pdcd4 is a novel eukaryotic translation initiation factor 4A binding protein that inhibits translation. Mol Cell Biol, 23, 26-37.
23. Wek, R.C., Jiang, H.Y. and Anthony, T.G. (2006) Coping with stress: eIF2 kinases and translational control. Biochem Soc Trans, 34, 7-11.
24. Hou, J., Lam, F., Proud, C. and Wang, S. (2012) Targeting Mnks for cancer therapy. Oncotarget, 3, 118-131.
25. van der Velden, A.W. and Thomas, A.A. (1999) The role of the 5' untranslated region of an mRNA in translation regulation during development. Int J Biochem Cell Biol, 31, 87-106.
26. Silva, R.L. and Wendel, H.G. (2008) MNK, EIF4E and targeting translation for therapy. Cell Cycle, 7, 553-555.
27. Jang, S.K., Krausslich, H.G., Nicklin, M.J., Duke, G.M., Palmenberg, A.C. and Wimmer, E. (1988) A segment of the 5' nontranslated region of encephalomyocarditis virus RNA directs internal entry of ribosomes during in vitro translation. J Virol, 62, 2636-2643.
28. Kolupaeva, V.G., Pestova, T.V., Hellen, C.U. and Shatsky, I.N. (1998) Translation eukaryotic initiation factor 4G recognizes a specific structural element within the internal ribosome entry site of encephalomyocarditis virus RNA. J Biol Chem, 273, 18599-18604.
29. Wilson, J.E., Pestova, T.V., Hellen, C.U. and Sarnow, P. (2000) Initiation of protein synthesis from the A site of the ribosome. Cell, 102, 511-520.
30. Macejak, D.G. and Sarnow, P. (1991) Internal initiation of translation mediated by the 5' leader of a cellular mRNA. Nature, 353, 90-94.
31. Spriggs, K.A., Stoneley, M., Bushell, M. and Willis, A.E. (2008) Re-programming of translation following cell stress allows IRES-mediated translation to predominate. Biol Cell, 100, 27-38.
32. Stoneley, M. and Willis, A.E. (2004) Cellular internal ribosome entry segments: structures, trans-acting factors and regulation of gene expression. Oncogene, 23, 3200-3207.
33. Mitchell, S.A., Spriggs, K.A., Coldwell, M.J., Jackson, R.J. and Willis, A.E. (2003) The Apaf-1 internal ribosome entry segment attains the correct structural conformation for function via interactions with PTB and unr. Mol Cell, 11, 757-771.

34. Marash, L., Liberman, N., Henis-Korenblit, S., Sivan, G., Reem, E., Elroy-Stein, O. and Kimchi, A. (2008) DAP5 promotes cap-independent translation of Bcl-2 and CDK1 to facilitate cell survival during mitosis. Mol Cell, 30, 447-459.
35. Jo, O.D., Martin, J., Bernath, A., Masri, J., Lichtenstein, A. and Gera, J. (2008) Heterogeneous nuclear ribonucleoprotein A1 regulates cyclin D1 and c-myc internal ribosome entry site function through Akt signaling. J Biol Chem, 283, 23274-23287.
36. Bushell, M., Stoneley, M., Kong, Y.W., Hamilton, T.L., Spriggs, K.A., Dobbyn, H.C., Qin, X., Sarnow, P. and Willis, A.E. (2006) Polypyrimidine tract binding protein regulates IRES-mediated gene expression during apoptosis. Mol Cell, 23, 401-412.
37. Graber, T.E., Baird, S.D., Kao, P.N., Mathews, M.B. and Holcik, M. (2009) NF45 functions as an IRES trans-acting factor that is required for translation of cIAP1 during the unfolded protein response. Cell Death Differ, 17, 719-729.
38. Cobbold, L.C., Wilson, L.A., Sawicka, K., King, H.A., Kondrashov, A.V., Spriggs, K.A., Bushell, M. and Willis, A.E. (2010) Upregulated c-myc expression in multiple myeloma by internal ribosome entry results from increased interactions with and expression of PTB-1 and YB-1. Oncogene, 29, 2884-2891.
39. Evans, J.R., Mitchell, S.A., Spriggs, K.A., Ostrowski, J., Bomsztyk, K., Ostarek, D. and Willis, A.E. (2003) Members of the poly (rC) binding protein family stimulate the activity of the c-myc internal ribosome entry segment in vitro and in vivo. Oncogene, 22, 8012-8020.
40. Bonnal, S., Pileur, F., Orsini, C., Parker, F., Pujol, F., Prats, A.C. and Vagner, S. (2005) Heterogeneous nuclear ribonucleoprotein A1 is a novel internal ribosome entry site trans-acting factor that modulates alternative initiation of translation of the fibroblast growth factor 2 mRNA. J Biol Chem, 280, 4144-4153.
41. Schepens, B., Tinton, S.A., Bruynooghe, Y., Beyaert, R. and Cornelis, S. (2005) The polypyrimidine tract-binding protein stimulates HIF-1alpha IRES-mediated translation during hypoxia. Nucleic Acids Res, 33, 6884-6894.
42. Giraud, S., Greco, A., Brink, M., Diaz, J.J. and Delafontaine, P. (2001) Translation initiation of the insulin-like growth factor I receptor mRNA is mediated by an internal ribosome entry site. J Biol Chem, 276, 5668-5675.
43. Dai, N., Rapley, J., Angel, M., Yanik, M.F., Blower, M.D. and Avruch, J. (2011) mTOR phosphorylates IMP2 to promote IGF2 mRNA translation by internal ribosomal entry. Genes Dev, 25, 1159-1172.
44. Dhar, D., Venkataramana, M., Ponnuswamy, A. and Das, S. (2009) Role of polypyrimidine tract binding protein in mediating internal initiation of translation of interferon regulatory factor 2 RNA. PLoS One, 4, e7049.
45. Cho, S., Kim, J.H., Back, S.H. and Jang, S.K. (2005) Polypyrimidine tract-binding protein enhances the internal ribosomal entry site-dependent translation of p27Kip1 mRNA and modulates transition from G1 to S phase. Mol Cell Biol, 25, 1283-1297.
46. Grover, R., Ray, P.S. and Das, S. (2008) Polypyrimidine tract binding protein regulates IRES-mediated translation of p53 isoforms. Cell Cycle, 7, 2189-2198.
47. Yang, L., Gu, L., Li, Z. and Zhou, M. (2010) Translation of TRAF1 is regulated by IRES-dependent mechanism and stimulated by vincristine. Nucleic Acids Res, 38, 4503-4513.

48. Lewis, S.M., Veyrier, A., Hosszu Ungureanu, N., Bonnal, S., Vagner, S. and Holcik, M. (2007) Subcellular relocalization of a trans-acting factor regulates XIAP IRES-dependent translation. Mol Biol Cell, 18, 1302-1311.
49. Holcik, M., Gordon, B.W. and Korneluk, R.G. (2003) The internal ribosome entry site-mediated translation of antiapoptotic protein XIAP is modulated by the heterogeneous nuclear ribonucleoproteins C1 and C2. Mol Cell Biol, 23, 280-288.
50. Holcik, M. and Korneluk, R.G. (2000) Functional characterization of the X-linked inhibitor of apoptosis (XIAP) internal ribosome entry site element: role of La autoantigen in XIAP translation. Mol Cell Biol, 20, 4648-4657.
51. Chappell, S.A. and Mauro, V.P. (2003) The internal ribosome entry site (IRES) contained within the RNA-binding motif protein 3 (Rbm3) mRNA is composed of functionally distinct elements. J Biol Chem, 278, 33793-33800.
52. Mitchell, S.A., Spriggs, K.A., Bushell, M., Evans, J.R., Stoneley, M., Le Quesne, J.P., Spriggs, R.V. and Willis, A.E. (2005) Identification of a motif that mediates polypyrimidine tract-binding protein-dependent internal ribosome entry. Genes Dev, 19, 1556-1571.
53. Keene, J.D. (2007) RNA regulons: coordination of post-transcriptional events. Nat Rev Genet, 8, 533-543.
54. Imataka, H., Gradi, A. and Sonenberg, N. (1998) A newly identified N-terminal amino acid sequence of human eIF4G binds poly(A)-binding protein and functions in poly(A)-dependent translation. EMBO J, 17, 7480-7489.
55. Paraskeva, E., Gray, N.K., Schlager, B., Wehr, K. and Hentze, M.W. (1999) Ribosomal pausing and scanning arrest as mechanisms of translational regulation from cap-distal iron-responsive elements. Mol Cell Biol, 19, 807-816.
56. Lunde, B.M., Moore, C. and Varani, G. (2007) RNA-binding proteins: modular design for efficient function. Nat Rev Mol Cell Biol, 8, 479-490.
57. Audic, Y. and Hartley, R.S. (2004) Post-transcriptional regulation in cancer. Biol Cell, 96, 479-498.
58. Wehner, K.A. and Sarnow, P. (2007) "Regulation of mRNA Molecules by MicroRNAs" In Mathews, M. B., Sonenberg, N. and Hershey, J. W. B. (eds.), Translational Control in Biology and Medicine. Cold Spring Harbor Laboratory Press, New York, pp. 297-318.
59. Lee, Y., Kim, M., Han, J., Yeom, K.H., Lee, S., Baek, S.H. and Kim, V.N. (2004) MicroRNA genes are transcribed by RNA polymerase II. EMBO J, 23, 4051-4060.
60. Kim, V.N. (2005) MicroRNA biogenesis: coordinated cropping and dicing. Nat Rev Mol Cell Biol, 6, 376-385.
61. Carthew, R.W. and Sontheimer, E.J. (2009) Origins and Mechanisms of miRNAs and siRNAs. Cell, 136, 642-655.
62. Mathonnet, G., Fabian, M.R., Svitkin, Y.V., Parsyan, A., Huck, L., Murata, T., Biffo, S., Merrick, W.C., Darzynkiewicz, E., Pillai, R.S. *et al.* (2007) MicroRNA inhibition of translation initiation in vitro by targeting the cap-binding complex eIF4F. Science, 317, 1764-1767.
63. Giraldez, A.J., Mishima, Y., Rihel, J., Grocock, R.J., Van Dongen, S., Inoue, K., Enright, A.J. and Schier, A.F. (2006) Zebrafish MiR-430 promotes deadenylation and clearance of maternal mRNAs. Science, 312, 75-79.

64. Chendrimada, T.P., Finn, K.J., Ji, X., Baillat, D., Gregory, R.I., Liebhaber, S.A., Pasquinelli, A.E. and Shiekhattar, R. (2007) MicroRNA silencing through RISC recruitment of eIF6. Nature, 447, 823-828.
65. Petersen, C.P., Bordeleau, M.E., Pelletier, J. and Sharp, P.A. (2006) Short RNAs repress translation after initiation in mammalian cells. Mol Cell, 21, 533-542.
66. Sheth, U. and Parker, R. (2003) Decapping and decay of messenger RNA occur in cytoplasmic processing bodies. Science, 300, 805-808.
67. Anderson, P. and Kedersha, N. (2008) Stress granules: the Tao of RNA triage. Trends Biochem Sci, 33, 141-150.
68. Calvo, S.E., Pagliarini, D.J. and Mootha, V.K. (2009) Upstream open reading frames cause widespread reduction of protein expression and are polymorphic among humans. Proc Natl Acad Sci U S A, 106, 7507-7512.
69. Luukkonen, B.G., Tan, W. and Schwartz, S. (1995) Efficiency of reinitiation of translation on human immunodeficiency virus type 1 mRNAs is determined by the length of the upstream open reading frame and by intercistronic distance. J Virol, 69, 4086-4094.
70. Kozak, M. (2001) Constraints on reinitiation of translation in mammals. Nucleic Acids Res, 29, 5226-5232.
71. Poyry, T.A., Kaminski, A. and Jackson, R.J. (2004) What determines whether mammalian ribosomes resume scanning after translation of a short upstream open reading frame? Genes Dev, 18, 62-75.
72. Janzen, D.M., Frolova, L. and Geballe, A.P. (2002) Inhibition of translation termination mediated by an interaction of eukaryotic release factor 1 with a nascent peptidyl-tRNA. Mol Cell Biol, 22, 8562-8570.
73. Hinnebusch, A.G. (1997) Translational regulation of yeast GCN4. A window on factors that control initiator-trna binding to the ribosome. J Biol Chem, 272, 21661-21664.
74. Engelman, J.A. (2009) Targeting PI3K signalling in cancer: opportunities, challenges and limitations. Nat Rev Cancer, 9, 550-562.
75. Koromilas, A.E., Lazaris-Karatzas, A. and Sonenberg, N. (1992) mRNAs containing extensive secondary structure in their 5' non-coding region translate efficiently in cells overexpressing initiation factor eIF-4E. EMBO J, 11, 4153-4158.
76. De Benedetti, A. and Graff, J.R. (2004) eIF-4E expression and its role in malignancies and metastases. Oncogene, 23, 3189-3199.
77. Castellvi, J., Garcia, A., Ruiz-Marcellan, C., Hernandez-Losa, J., Peg, V., Salcedo, M., Gil-Moreno, A. and Ramon y Cajal, S. (2009) Cell signaling in endometrial carcinoma: phosphorylated 4E-binding protein-1 expression in endometrial cancer correlates with aggressive tumors and prognosis. Hum Pathol, 40, 1418-1426.
78. Shuda, M., Kondoh, N., Tanaka, K., Ryo, A., Wakatsuki, T., Hada, A., Goseki, N., Igari, T., Hatsuse, K., Aihara, T. *et al.* (2000) Enhanced expression of translation factor mRNAs in hepatocellular carcinoma. Anticancer Res, 20, 2489-2494.
79. Eberle, J., Krasagakis, K. and Orfanos, C.E. (1997) Translation initiation factor eIF-4A1 mRNA is consistently overexpressed in human melanoma cells in vitro. Int J Cancer, 71, 396-401.

80. Wei, N.A., Liu, S.S., Leung, T.H., Tam, K.F., Liao, X.Y., Cheung, A.N., Chan, K.K. and Ngan, H.Y. (2009) Loss of Programmed cell death 4 (Pdcd4) associates with the progression of ovarian cancer. Mol Cancer, 8, 70.
81. Wander, S.A., Hennessy, B.T. and Slingerland, J.M. (2011) Next-generation mTOR inhibitors in clinical oncology: how pathway complexity informs therapeutic strategy. J Clin Invest, 121, 1231-1241.
82. Blees, J.S., Schmid, T., Thomas, C.L., Baker, A.R., Benson, L., Evans, J.R., Goncharova, E.I., Colburn, N.H., McMahon, J.B. and Henrich, C.J. (2010) Development of a high-throughput cell-based reporter assay to identify stabilizers of tumor suppressor Pdcd4. J Biomol Screen, 15, 21-29.
83. Moerke, N.J., Aktas, H., Chen, H., Cantel, S., Reibarkh, M.Y., Fahmy, A., Gross, J.D., Degterev, A., Yuan, J., Chorev, M. *et al.* (2007) Small-molecule inhibition of the interaction between the translation initiation factors eIF4E and eIF4G. Cell, 128, 257-267.
84. Braunstein, S., Karpisheva, K., Pola, C., Goldberg, J., Hochman, T., Yee, H., Cangiarella, J., Arju, R., Formenti, S.C. and Schneider, R.J. (2007) A hypoxia-controlled cap-dependent to cap-independent translation switch in breast cancer. Mol Cell, 28, 501-512.
85. Silvera, D., Arju, R., Darvishian, F., Levine, P.H., Zolfaghari, L., Goldberg, J., Hochman, T., Formenti, S.C. and Schneider, R.J. (2009) Essential role for eIF4GI overexpression in the pathogenesis of inflammatory breast cancer. Nat Cell Biol, 11, 903-908.
86. Spriggs, K.A., Cobbold, L.C., Jopling, C.L., Cooper, R.E., Wilson, L.A., Stoneley, M., Coldwell, M.J., Poncet, D., Shen, Y.C., Morley, S.J. *et al.* (2009) Canonical initiation factor requirements of the Myc family of internal ribosome entry segments. Mol Cell Biol, 29, 1565-1574.
87. Chappell, S.A., LeQuesne, J.P., Paulin, F.E., deSchoolmeester, M.L., Stoneley, M., Soutar, R.L., Ralston, S.H., Helfrich, M.H. and Willis, A.E. (2000) A mutation in the c-myc-IRES leads to enhanced internal ribosome entry in multiple myeloma: a novel mechanism of oncogene de-regulation. Oncogene, 19, 4437-4440.
88. Holcik, M., Yeh, C., Korneluk, R.G. and Chow, T. (2000) Translational upregulation of X-linked inhibitor of apoptosis (XIAP) increases resistance to radiation induced cell death. Oncogene, 19, 4174-4177.
89. Desplanques, G., Giuliani, N., Delsignore, R., Rizzoli, V., Bataille, R. and Barille-Nion, S. (2009) Impact of XIAP protein levels on the survival of myeloma cells. Haematologica, 94, 87-93.
90. Hanahan, D. and Weinberg, R.A. (2011) Hallmarks of cancer: the next generation. Cell, 144, 646-674.
91. O'Sullivan, C. and Lewis, C.E. (1994) Tumour-associated leucocytes: friends or foes in breast carcinoma. J Pathol, 172, 229-235.
92. Leek, R.D., Lewis, C.E., Whitehouse, R., Greenall, M., Clarke, J. and Harris, A.L. (1996) Association of macrophage infiltration with angiogenesis and prognosis in invasive breast carcinoma. Cancer Res, 56, 4625-4629.
93. Vagner, S., Gensac, M.C., Maret, A., Bayard, F., Amalric, F., Prats, H. and Prats, A.C. (1995) Alternative translation of human fibroblast growth factor 2 mRNA occurs by internal entry of ribosomes. Mol Cell Biol, 15, 35-44.

94. Stein, I., Itin, A., Einat, P., Skaliter, R., Grossman, Z. and Keshet, E. (1998) Translation of vascular endothelial growth factor mRNA by internal ribosome entry: implications for translation under hypoxia. Mol Cell Biol, 18, 3112-3119.
95. Zhang, T., Kruys, V., Huez, G. and Gueydan, C. (2002) AU-rich element-mediated translational control: complexity and multiple activities of trans-activating factors. Biochem Soc Trans, 30, 952-958.
96. Piecyk, M., Wax, S., Beck, A.R., Kedersha, N., Gupta, M., Maritim, B., Chen, S., Gueydan, C., Kruys, V., Streuli, M. *et al.* (2000) TIA-1 is a translational silencer that selectively regulates the expression of TNF-alpha. EMBO J, 19, 4154-4163.
97. Dixon, D.A., Balch, G.C., Kedersha, N., Anderson, P., Zimmerman, G.A., Beauchamp, R.D. and Prescott, S.M. (2003) Regulation of cyclooxygenase-2 expression by the translational silencer TIA-1. J Exp Med, 198, 475-481.
98. Srikantan, S. and Gorospe, M. (2011) HuR function in disease. Front Biosci, 17, 189-205.
99. Levy, N.S., Chung, S., Furneaux, H. and Levy, A.P. (1998) Hypoxic stabilization of vascular endothelial growth factor mRNA by the RNA-binding protein HuR. J Biol Chem, 273, 6417-6423.
100. Durie, D., Lewis, S.M., Liwak, U., Kisilewicz, M., Gorospe, M. and Holcik, M. (2010) RNA-binding protein HuR mediates cytoprotection through stimulation of XIAP translation. Oncogene, 30, 1460-1469.
101. Mohr, I.J., Pe'ery, T. and Matthews, M.B. (2007) "Protein Synthesis and Translational Control during Viral Infection" In Mathews, M. B., Sonenberg, N. and Hershey, J. W. B. (eds.), Translational Control in Biology and Medicine. Cold Spring Harbor Laboratory Press, New York, pp. 545-600.
102. Haghighat, A., Svitkin, Y., Novoa, I., Kuechler, E., Skern, T. and Sonenberg, N. (1996) The eIF4G-eIF4E complex is the target for direct cleavage by the rhinovirus 2A proteinase. J Virol, 70, 8444-8450.
103. Arias, C., Walsh, D., Harbell, J., Wilson, A.C. and Mohr, I. (2009) Activation of host translational control pathways by a viral developmental switch. PLoS Pathog, 5, e1000334.
104. Sullivan, C.S. and Ganem, D. (2005) MicroRNAs and viral infection. Mol Cell, 20, 3-7.
105. Piron, M., Vende, P., Cohen, J. and Poncet, D. (1998) Rotavirus RNA-binding protein NSP3 interacts with eIF4GI and evicts the poly(A) binding protein from eIF4F. EMBO J, 17, 5811-5821.
106. Klann, E. and Richter, J.D. (2007) "Translational Control of Synaptic Plasticity and Learning and Memory" In Mathews, M. B., Sonenberg, N. and Hershey, J. W. B. (eds.), Translational Control in Biology and Medicine. Cold Spring Harbor Laboratory Press, New York, pp. 485-506.
107. Napoli, I., Mercaldo, V., Boyl, P.P., Eleuteri, B., Zalfa, F., De Rubeis, S., Di Marino, D., Mohr, E., Massimi, M., Falconi, M. *et al.* (2008) The fragile X syndrome protein represses activity-dependent translation through CYFIP1, a new 4E-BP. Cell, 134, 1042-1054.
108. Muddashetty, R.S., Nalavadi, V.C., Gross, C., Yao, X., Xing, L., Laur, O., Warren, S.T. and Bassell, G.J. (2011) Reversible inhibition of PSD-95 mRNA translation by miR-125a, FMRP phosphorylation, and mGluR signaling. Mol Cell, 42, 673-688.

109. Tian, B., White, R.J., Xia, T., Welle, S., Turner, D.H., Mathews, M.B. and Thornton, C.A. (2000) Expanded CUG repeat RNAs form hairpins that activate the double-stranded RNA-dependent protein kinase PKR. RNA, 6, 79-87.
110. Peel, A.L. (2004) PKR activation in neurodegenerative disease. J Neuropathol Exp Neurol, 63, 97-105.
111. Chang, R.C., Wong, A.K., Ng, H.K. and Hugon, J. (2002) Phosphorylation of eukaryotic initiation factor-2alpha (eIF2alpha) is associated with neuronal degeneration in Alzheimer's disease. Neuroreport, 13, 2429-2432.
112. Chang, R.C., Suen, K.C., Ma, C.H., Elyaman, W., Ng, H.K. and Hugon, J. (2002) Involvement of double-stranded RNA-dependent protein kinase and phosphorylation of eukaryotic initiation factor-2alpha in neuronal degeneration. J Neurochem, 83, 1215-1225.
113. Joseph, L.J., Le Beau, M.M., Jamieson, G.A., Jr., Acharya, S., Shows, T.B., Rowley, J.D. and Sukhatme, V.P. (1988) Molecular cloning, sequencing, and mapping of EGR2, a human early growth response gene encoding a protein with "zinc-binding finger" structure. Proc Natl Acad Sci U S A, 85, 7164-7168.
114. Sukhatme, V.P., Kartha, S., Toback, F.G., Taub, R., Hoover, R.G. and Tsai-Morris, C.H. (1987) A novel early growth response gene rapidly induced by fibroblast, epithelial cell and lymphocyte mitogens. Oncogene Res, 1, 343-355.
115. O'Donovan, K.J., Tourtellotte, W.G., Millbrandt, J. and Baraban, J.M. (1999) The EGR family of transcription-regulatory factors: progress at the interface of molecular and systems neuroscience. Trends Neurosci, 22, 167-173.
116. Garcia-Gutierrez, P., Juarez-Vicente, F., Gallardo-Chamizo, F., Charnay, P. and Garcia-Dominguez, M. (2011) The transcription factor Krox20 is an E3 ligase that sumoylates its Nab coregulators. EMBO Rep, 12, 1018-1023.
117. Gareau, J.R. and Lima, C.D. (2010) The SUMO pathway: emerging mechanisms that shape specificity, conjugation and recognition. Nat Rev Mol Cell Biol, 11, 861-871.
118. Russo, M.W., Sevetson, B.R. and Milbrandt, J. (1995) Identification of NAB1, a repressor of NGFI-A- and Krox20-mediated transcription. Proc Natl Acad Sci U S A, 92, 6873-6877.
119. Svaren, J., Sevetson, B.R., Apel, E.D., Zimonjic, D.B., Popescu, N.C. and Milbrandt, J. (1996) NAB2, a corepressor of NGFI-A (Egr-1) and Krox20, is induced by proliferative and differentiative stimuli. Mol Cell Biol, 16, 3545-3553.
120. Gillian, A.L. and Svaren, J. (2004) The Ddx20/DP103 dead box protein represses transcriptional activation by Egr2/Krox-20. J Biol Chem, 279, 9056-9063.
121. Zheng, Y., Zha, Y. and Gajewski, T.F. (2008) Molecular regulation of T-cell anergy. EMBO Rep, 9, 50-55.
122. Rao, A., Luo, C. and Hogan, P.G. (1997) Transcription factors of the NFAT family: regulation and function. Annu Rev Immunol, 15, 707-747.
123. Macian, F., Garcia-Cozar, F., Im, S.H., Horton, H.F., Byrne, M.C. and Rao, A. (2002) Transcriptional mechanisms underlying lymphocyte tolerance. Cell, 109, 719-731.
124. Safford, M., Collins, S., Lutz, M.A., Allen, A., Huang, C.T., Kowalski, J., Blackford, A., Horton, M.R., Drake, C., Schwartz, R.H. *et al.* (2005) Egr-2 and Egr-3 are negative regulators of T cell activation. Nat Immunol, 6, 472-480.

125. Mueller, D.L. (2004) E3 ubiquitin ligases as T cell anergy factors. Nat Immunol, 5, 883-890.
126. Harris, J.E., Bishop, K.D., Phillips, N.E., Mordes, J.P., Greiner, D.L., Rossini, A.A. and Czech, M.P. (2004) Early growth response gene-2, a zinc-finger transcription factor, is required for full induction of clonal anergy in CD4+ T cells. J Immunol, 173, 7331-7338.
127. Smith, K.A. and Cantrell, D.A. (1985) Interleukin 2 regulates its own receptors. Proc Natl Acad Sci U S A, 82, 864-868.
128. Decker, E.L., Skerka, C. and Zipfel, P.F. (1998) The early growth response protein (EGR-1) regulates interleukin-2 transcription by synergistic interaction with the nuclear factor of activated T cells. J Biol Chem, 273, 26923-26930.
129. Lin, J.X. and Leonard, W.J. (1997) The immediate-early gene product Egr-1 regulates the human interleukin-2 receptor beta-chain promoter through noncanonical Egr and Sp1 binding sites. Mol Cell Biol, 17, 3714-3722.
130. Collins, S., Lutz, M.A., Zarek, P.E., Anders, R.A., Kersh, G.J. and Powell, J.D. (2008) Opposing regulation of T cell function by Egr-1/NAB2 and Egr-2/Egr-3. Eur J Immunol, 38, 528-536.
131. Gao, B., Kong, Q., Kemp, K., Zhao, Y.S. and Fang, D. (2012) Analysis of sirtuin 1 expression reveals a molecular explanation of IL-2-mediated reversal of T-cell tolerance. Proc Natl Acad Sci U S A, 109, 899-904.
132. Yeung, F., Hoberg, J.E., Ramsey, C.S., Keller, M.D., Jones, D.R., Frye, R.A. and Mayo, M.W. (2004) Modulation of NF-kappaB-dependent transcription and cell survival by the SIRT1 deacetylase. EMBO J, 23, 2369-2380.
133. Mittelstadt, P.R. and Ashwell, J.D. (1999) Role of Egr-2 in up-regulation of Fas ligand in normal T cells and aberrant double-negative lpr and gld T cells. J Biol Chem, 274, 3222-3227.
134. Green, D.R., Droin, N. and Pinkoski, M. (2003) Activation-induced cell death in T cells. Immunol Rev, 193, 70-81.
135. Chen, A., Gao, B., Zhang, J., McEwen, T., Ye, S.Q., Zhang, D. and Fang, D. (2009) The HECT-type E3 ubiquitin ligase AIP2 inhibits activation-induced T-cell death by catalyzing EGR2 ubiquitination. Mol Cell Biol, 29, 5348-5356.
136. Zhu, B., Symonds, A.L., Martin, J.E., Kioussis, D., Wraith, D.C., Li, S. and Wang, P. (2008) Early growth response gene 2 (Egr-2) controls the self-tolerance of T cells and prevents the development of lupuslike autoimmune disease. J Exp Med, 205, 2295-2307.
137. Lauritsen, J.P., Kurella, S., Lee, S.Y., Lefebvre, J.M., Rhodes, M., Alberola-Ila, J. and Wiest, D.L. (2008) Egr2 is required for Bcl-2 induction during positive selection. J Immunol, 181, 7778-7785.
138. Seiler, M.P., Mathew, R., Liszewski, M.K., Spooner, C., Barr, K., Meng, F., Singh, H. and Bendelac, A. (2012) Elevated and sustained expression of the transcription factors Egr1 and Egr2 controls NKT lineage differentiation in response to TCR signaling. Nat Immunol, 13, 264-271.
139. Lazarevic, V., Zullo, A.J., Schweitzer, M.N., Staton, T.L., Gallo, E.M., Crabtree, G.R. and Glimcher, L.H. (2009) The gene encoding early growth response 2, a target of the transcription factor NFAT, is required for the development and maturation of natural killer T cells. Nat Immunol, 10, 306-313.
140. Mirsky, R. and Jessen, K.R. (1996) Schwann cell development, differentiation and myelination. Curr Opin Neurobiol, 6, 89-96.

141. Topilko, P., Schneider-Maunoury, S., Levi, G., Baron-Van Evercooren, A., Chennoufi, A.B., Seitanidou, T., Babinet, C. and Charnay, P. (1994) Krox-20 controls myelination in the peripheral nervous system. Nature, 371, 796-799.
142. Warner, L.E., Mancias, P., Butler, I.J., McDonald, C.M., Keppen, L., Koob, K.G. and Lupski, J.R. (1998) Mutations in the early growth response 2 (EGR2) gene are associated with hereditary myelinopathies. Nat Genet, 18, 382-384.
143. Suter, U. and Scherer, S.S. (2003) Disease mechanisms in inherited neuropathies. Nat Rev Neurosci, 4, 714-726.
144. Jones, E.A., Jang, S.W., Mager, G.M., Chang, L.W., Srinivasan, R., Gokey, N.G., Ward, R.M., Nagarajan, R. and Svaren, J. (2007) Interactions of Sox10 and Egr2 in myelin gene regulation. Neuron Glia Biol, 3, 377-387.
145. Hossain, S., de la Cruz-Morcillo, M.A., Sanchez-Prieto, R. and Almazan, G. (2012) Mitogen-activated protein kinase p38 regulates krox-20 to direct schwann cell differentiation and peripheral myelination. Glia, 60, 1130-1144.
146. Parkinson, D.B., Bhaskaran, A., Droggiti, A., Dickinson, S., D'Antonio, M., Mirsky, R. and Jessen, K.R. (2004) Krox-20 inhibits Jun-NH2-terminal kinase/c-Jun to control Schwann cell proliferation and death. J Cell Biol, 164, 385-394.
147. Greenfield, S., Brostoff, S., Eylar, E.H. and Morell, P. (1973) Protein composition of myelin of the peripheral nervous system. J Neurochem, 20, 1207-1216.
148. Giese, K.P., Martini, R., Lemke, G., Soriano, P. and Schachner, M. (1992) Mouse P0 gene disruption leads to hypomyelination, abnormal expression of recognition molecules, and degeneration of myelin and axons. Cell, 71, 565-576.
149. Matsushima-Nishiu, M., Unoki, M., Ono, K., Tsunoda, T., Minaguchi, T., Kuramoto, H., Nishida, M., Satoh, T., Tanaka, T. and Nakamura, Y. (2001) Growth and gene expression profile analyses of endometrial cancer cells expressing exogenous PTEN. Cancer Res, 61, 3741-3749.
150. Unoki, M. and Nakamura, Y. (2001) Growth-suppressive effects of BPOZ and EGR2, two genes involved in the PTEN signaling pathway. Oncogene, 20, 4457-4465.
151. Yokota, I., Sasaki, Y., Kashima, L., Idogawa, M. and Tokino, T. (2010) Identification and characterization of early growth response 2, a zinc-finger transcription factor, as a p53-regulated proapoptotic gene. Int J Oncol, 37, 1407-1416.
152. Yin, P., Navarro, A., Fang, F., Xie, A., Coon, J.S., Richardson, C. and Bulun, S.E. (2011) Early growth response-2 expression in uterine leiomyoma cells: regulation and function. Fertil Steril, 96, 439-444.
153. Bradley, E.W., Ruan, M.M. and Oursler, M.J. (2008) Novel pro-survival functions of the Kruppel-like transcription factor Egr2 in promotion of macrophage colony-stimulating factor-mediated osteoclast survival downstream of the MEK/ERK pathway. J Biol Chem, 283, 8055-8064.
154. Gabet, Y., Baniwal, S.K., Leclerc, N., Shi, Y., Kohn-Gabet, A.E., Cogan, J., Dixon, A., Bachar, M., Guo, L., Turman, J.E., Jr. *et al.* (2010) Krox20/EGR2 deficiency accelerates cell growth and differentiation in the monocytic lineage and decreases bone mass. Blood, 116, 3964-3971.
155. Pospisil, V., Vargova, K., Kokavec, J., Rybarova, J., Savvulidi, F., Jonasova, A., Necas, E., Zavadil, J., Laslo, P. and Stopka, T. (2011) Epigenetic silencing of the

oncogenic miR-17-92 cluster during PU.1-directed macrophage differentiation. EMBO J, 30, 4450-4464.
156. Sundstrom, C. and Nilsson, K. (1976) Establishment and characterization of a human histiocytic lymphoma cell line (U-937). Int J Cancer, 17, 565-577.
157. Soule, H.D., Vazguez, J., Long, A., Albert, S. and Brennan, M. (1973) A human cell line from a pleural effusion derived from a breast carcinoma. J Natl Cancer Inst, 51, 1409-1416.
158. Spriggs, K.A., Cobbold, L.C., Ridley, S.H., Coldwell, M., Bottley, A., Bushell, M., Willis, A.E. and Siddle, K. (2009) The human insulin receptor mRNA contains a functional internal ribosome entry segment. Nucleic Acids Res, 37, 5881-5893.
159. Coldwell, M.J., Mitchell, S.A., Stoneley, M., MacFarlane, M. and Willis, A.E. (2000) Initiation of Apaf-1 translation by internal ribosome entry. Oncogene, 19, 899-905.
160. Li, J.J., Westergaard, C., Ghosh, P. and Colburn, N.H. (1997) Inhibitors of both nuclear factor-kappaB and activator protein-1 activation block the neoplastic transformation response. Cancer Res, 57, 3569-3576.
161. Iervolino, A., Santilli, G., Trotta, R., Guerzoni, C., Cesi, V., Bergamaschi, A., Gambacorti-Passerini, C., Calabretta, B. and Perrotti, D. (2002) hnRNP A1 nucleocytoplasmic shuttling activity is required for normal myelopoiesis and BCR/ABL leukemogenesis. Mol Cell Biol, 22, 2255-2266.
162. Zuker, M. (2003) Mfold web server for nucleic acid folding and hybridization prediction. Nucleic Acids Res, 31, 3406-3415.
163. Eberwine, J., Yeh, H., Miyashiro, K., Cao, Y., Nair, S., Finnell, R., Zettel, M. and Coleman, P. (1992) Analysis of gene expression in single live neurons. Proc Natl Acad Sci U S A, 89, 3010-3014.
164. R Development Core Team. (2005) R: A language and environment for statistical computing. R Foundation for Statistical Computing, Vienna, Austria. ISBN: 3-900051-07-0
165. Gentleman, R.C., Carey, V.J., Bates, D.M., Bolstad, B., Dettling, M., Dudoit, S., Ellis, B., Gautier, L., Ge, Y., Gentry, J. *et al.* (2004) Bioconductor: open software development for computational biology and bioinformatics. Genome Biol, 5, R80.
166. Lowry, O.H., Rosebrough, N.J., Farr, A.L. and Randall, R.J. (1951) Protein measurement with the Folin phenol reagent. J Biol Chem, 193, 265-275.
167. Shi, Y., Frost, P.J., Hoang, B.Q., Benavides, A., Sharma, S., Gera, J.F. and Lichtenstein, A.K. (2008) IL-6-induced stimulation of c-myc translation in multiple myeloma cells is mediated by myc internal ribosome entry site function and the RNA-binding protein, hnRNP A1. Cancer Res, 68, 10215-10222.
168. Dhamija, S., Doerrie, A., Winzen, R., Dittrich-Breiholz, O., Taghipour, A., Kuehne, N., Kracht, M. and Holtmann, H. (2010) IL-1-induced post-transcriptional mechanisms target overlapping translational silencing and destabilizing elements in IkappaBzeta mRNA. J Biol Chem, 285, 29165-29178.
169. Ichijo, H. (1999) From receptors to stress-activated MAP kinases. Oncogene, 18, 6087-6093.
170. Pickering, B.M. and Willis, A.E. (2005) The implications of structured 5' untranslated regions on translation and disease. Semin Cell Dev Biol, 16, 39-47.
171. Kozak, M. (2005) A second look at cellular mRNA sequences said to function as internal ribosome entry sites. Nucleic Acids Res, 33, 6593-6602.

172. Vagner, S., Galy, B. and Pyronnet, S. (2001) Irresistible IRES. Attracting the translation machinery to internal ribosome entry sites. EMBO Rep, 2, 893-898.
173. Sonenberg, N. and Hinnebusch, A.G. (2007) New modes of translational control in development, behavior, and disease. Mol Cell, 28, 721-729.
174. Proud, C.G. (2006) Regulation of protein synthesis by insulin. Biochem Soc Trans, 34, 213-216.
175. Proud, C.G. (2004) Role of mTOR signalling in the control of translation initiation and elongation by nutrients. Curr Top Microbiol Immunol, 279, 215-244.
176. Grivennikov, S.I., Greten, F.R. and Karin, M. (2010) Immunity, inflammation, and cancer. Cell, 140, 883-899.
177. Dougan, M. and Dranoff, G. (2009) Immune therapy for cancer. Annu Rev Immunol, 27, 83-117.
178. Zitvogel, L., Apetoh, L., Ghiringhelli, F. and Kroemer, G. (2008) Immunological aspects of cancer chemotherapy. Nat Rev Immunol, 8, 59-73.
179. Ammirante, M., Luo, J.L., Grivennikov, S., Nedospasov, S. and Karin, M. (2010) B-cell-derived lymphotoxin promotes castration-resistant prostate cancer. Nature, 464, 302-305.
180. Li, Y., Cai, L., Wang, H., Wu, P., Gu, W., Chen, Y., Hao, H., Tang, K., Yi, P., Liu, M. *et al.* (2011) Pleiotropic regulation of macrophage polarization and tumorigenesis by formyl peptide receptor-2. Oncogene, 30, 3887-3899.
181. Craig, M., Ying, C. and Loberg, R.D. (2008) Co-inoculation of prostate cancer cells with U937 enhances tumor growth and angiogenesis in vivo. J Cell Biochem, 103, 1-8.
182. Bingle, L., Brown, N.J. and Lewis, C.E. (2002) The role of tumour-associated macrophages in tumour progression: implications for new anticancer therapies. J Pathol, 196, 254-265.
183. Johnston, S.R., Saccani-Jotti, G., Smith, I.E., Salter, J., Newby, J., Coppen, M., Ebbs, S.R. and Dowsett, M. (1995) Changes in estrogen receptor, progesterone receptor, and pS2 expression in tamoxifen-resistant human breast cancer. Cancer Res, 55, 3331-3338.
184. Eferl, R. and Wagner, E.F. (2003) AP-1: a double-edged sword in tumorigenesis. Nat Rev Cancer, 3, 859-868.
185. Schmid, T., Bajer, M.M., Blees, J.S., Eifler, L.K., Milke, L., Rübsamen, D., Schulz, K., Weigert, A., Baker, A.R., Colburn, N.H. *et al.* (2011) Inflammation-induced loss of Pdcd4 is mediated by phosphorylation-dependent degradation. Carcinogenesis, 32, 1427-1433.
186. Yasuda, M., Schmid, T., Rübsamen, D., Colburn, N.H., Irie, K. and Murakami, A. (2010) Downregulation of programmed cell death 4 by inflammatory conditions contributes to the generation of the tumor promoting microenvironment. Mol Carcinog, 49, 837-848.
187. Mathews, M.B., Sonenberg, N. and Hershey, J.W.B. (2007) "Origins and Principles of Translational Control" In Mathews, M. B., Sonenberg, N. and Hershey, J. W. B. (eds.), Translational Control in Biology and Medicine. Cold Spring Harbor Laboratory Press, New York, pp. 1-40.
188. Komagata, S., Nakajima, M., Takagi, S., Mohri, T., Taniya, T. and Yokoi, T. (2009) Human CYP24 catalyzing the inactivation of calcitriol is post-transcriptionally regulated by miR-125b. Mol Pharmacol, 76, 702-709.

189. Velusamy, T., Shetty, P., Bhandary, Y.P., Liu, M.C. and Shetty, S. (2008) Posttranscriptional regulation of urokinase receptor expression by heterogeneous nuclear ribonuclear protein C. Biochemistry, 47, 6508-6517.
190. Hsieh, A.C., Liu, Y., Edlind, M.P., Ingolia, N.T., Janes, M.R., Sher, A., Shi, E.Y., Stumpf, C.R., Christensen, C., Bonham, M.J. *et al.* (2012) The translational landscape of mTOR signalling steers cancer initiation and metastasis. Nature, 485, 55-61.
191. Zauberman, A., Zipori, D., Krupsky, M. and Ben-Levy, R. (1999) Stress activated protein kinase p38 is involved in IL-6 induced transcriptional activation of STAT3. Oncogene, 18, 3886-3893.
192. Cuenda, A., Rouse, J., Doza, Y.N., Meier, R., Cohen, P., Gallagher, T.F., Young, P.R. and Lee, J.C. (1995) SB 203580 is a specific inhibitor of a MAP kinase homologue which is stimulated by cellular stresses and interleukin-1. FEBS Lett, 364, 229-233.
193. Yeh, C.H., Hung, L.Y., Hsu, C., Le, S.Y., Lee, P.T., Liao, W.L., Lin, Y.T., Chang, W.C. and Tseng, J.T. (2008) RNA-binding protein HuR interacts with thrombomodulin 5'untranslated region and represses internal ribosome entry site-mediated translation under IL-1 beta treatment. Mol Biol Cell, 19, 3812-3822.
194. Shi, Y., Frost, P., Hoang, B., Benavides, A., Gera, J. and Lichtenstein, A. (2011) IL-6-induced enhancement of c-Myc translation in multiple myeloma cells: critical role of cytoplasmic localization of the rna-binding protein hnRNP A1. J Biol Chem, 286, 67-78.
195. Shi, Y., Sharma, A., Wu, H., Lichtenstein, A. and Gera, J. (2005) Cyclin D1 and c-myc internal ribosome entry site (IRES)-dependent translation is regulated by AKT activity and enhanced by rapamycin through a p38 MAPK- and ERK-dependent pathway. J Biol Chem, 280, 10964-10973.
196. Faivre, S., Kroemer, G. and Raymond, E. (2006) Current development of mTOR inhibitors as anticancer agents. Nat Rev Drug Discov, 5, 671-688.
197. Van Eden, M.E., Byrd, M.P., Sherrill, K.W. and Lloyd, R.E. (2004) Demonstrating internal ribosome entry sites in eukaryotic mRNAs using stringent RNA test procedures. RNA, 10, 720-730.
198. Holcik, M., Graber, T., Lewis, S.M., Lefebvre, C.A., Lacasse, E. and Baird, S. (2005) Spurious splicing within the XIAP 5' UTR occurs in the Rluc/Fluc but not the betagal/CAT bicistronic reporter system. RNA, 11, 1605-1609.
199. Sherrill, K.W., Byrd, M.P., Van Eden, M.E. and Lloyd, R.E. (2004) BCL-2 translation is mediated via internal ribosome entry during cell stress. J Biol Chem, 279, 29066-29074.
200. Baranick, B.T., Lemp, N.A., Nagashima, J., Hiraoka, K., Kasahara, N. and Logg, C.R. (2008) Splicing mediates the activity of four putative cellular internal ribosome entry sites. Proc Natl Acad Sci U S A, 105, 4733-4738.
201. Komar, A.A. and Hatzoglou, M. (2005) Internal ribosome entry sites in cellular mRNAs: mystery of their existence. J Biol Chem, 280, 23425-23428.
202. Komar, A.A. and Hatzoglou, M. (2011) Cellular IRES-mediated translation: the war of ITAFs in pathophysiological states. Cell Cycle, 10, 229-240.
203. Sawicka, K., Bushell, M., Spriggs, K.A. and Willis, A.E. (2008) Polypyrimidine-tract-binding protein: a multifunctional RNA-binding protein. Biochem Soc Trans, 36, 641-647.

204. Pickering, B.M., Mitchell, S.A., Spriggs, K.A., Stoneley, M. and Willis, A.E. (2004) Bag-1 internal ribosome entry segment activity is promoted by structural changes mediated by poly(rC) binding protein 1 and recruitment of polypyrimidine tract binding protein 1. Mol Cell Biol, 24, 5595-5605.
205. Mitchell, S.A., Brown, E.C., Coldwell, M.J., Jackson, R.J. and Willis, A.E. (2001) Protein factor requirements of the Apaf-1 internal ribosome entry segment: roles of polypyrimidine tract binding protein and upstream of N-ras. Mol Cell Biol, 21, 3364-3374.
206. Kullmann, M., Gopfert, U., Siewe, B. and Hengst, L. (2002) ELAV/Hu proteins inhibit p27 translation via an IRES element in the p27 5'UTR. Genes Dev, 16, 3087-3099.
207. Meng, Z., Jackson, N.L., Choi, H., King, P.H., Emanuel, P.D. and Blume, S.W. (2008) Alterations in RNA-binding activities of IRES-regulatory proteins as a mechanism for physiological variability and pathological dysregulation of IGF-IR translational control in human breast tumor cells. J Cell Physiol, 217, 172-183.
208. Papadopoulou, C., Patrinou-Georgoula, M. and Guialis, A. (2010) Extensive association of HuR with hnRNP proteins within immunoselected hnRNP and mRNP complexes. Biochim Biophys Acta, 1804, 692-703.
209. Nagarajan, R., Svaren, J., Le, N., Araki, T., Watson, M. and Milbrandt, J. (2001) EGR2 mutations in inherited neuropathies dominant-negatively inhibit myelin gene expression. Neuron, 30, 355-368.
210. Thomas, S.E. and Gordon, D.S. (1986) Cyclosporine. South Med J, 79, 205-214.
211. Trepanier, D.J., Gallant, H., Legatt, D.F. and Yatscoff, R.W. (1998) Rapamycin: distribution, pharmacokinetics and therapeutic range investigations: an update. Clin Biochem, 31, 345-351.
212. Hudder, A. and Werner, R. (2000) Analysis of a Charcot-Marie-Tooth disease mutation reveals an essential internal ribosome entry site element in the connexin-32 gene. J Biol Chem, 275, 34586-34591.

8 Appendix

Table 8-1: Proteins identified to bind to EGR2-5'UTR of CM lysates only by MS

AccessionNo.	Gene	ΣCoverage	#Hits	# Unique Peptides
O95433	AHSA1	9,17	2	2
Q7L0Y3	MRRP1	8,93	2	2
P55735	SEC13	6,83	2	2
P24386	RAE1	1,99	2	1
O95425	SVIL	1,13	2	1
A4FU69	EFCB5	0,60	2	1

Table 8-2: Proteins identified to bind to EGR2-5'UTR of Ctr lysates only by MS

AccessionNo.	Gene	ΣCoverage	#Hits	# Unique Peptides
Q14258	TRI25	12,70	7	6
Q07021	C1QBP	12,06	3	2
Q9NSD9	SYFB	6,79	4	4
P17987	TCPA	5,94	2	2
P14618	KPYM	5,84	2	2
O60506	HNRPQ	4,98	4	3
P50990	TCPQ	4,56	2	2
Q86VP6	CAND1	4,31	4	4
P27694	RFA1	3,90	2	2
P55060	XPO2	3,50	2	2
Q8IXB1	DJC10	3,40	2	2
Q9P2N5	RBM27	2,36	2	2
Q92851	CASPA	1,34	11	1

Table 8-3: Proteins identified to bind to EGR2-5'UTR of CM and Ctr lysates by MS

AccessionNo.	Gene	ΣCoverage	#Hits	# Unique Peptides
P07437	TBB5	71,62	199	26
P68371	TBB2C	71,46	191	26
P78347	GTF2I	68,54	329	67
P60709	ACTB	66,67	121	22
P68363	TBA1B	65,63	176	25
Q71U36	TBA1A	62,53	171	23
P04350	TBB4	59,91	120	19
Q9BQE3	TBA1C	58,35	159	22

AccessionNo.	Gene	ΣCoverage	#Hits	# Unique Peptides
Q13885	TBB2A	55,96	152	21
Q12904	AIMP1	54,81	40	11
Q15233	NONO	52,02	35	17
P06748	NPM	51,70	71	13
P26599	PTBP1	51,60	64	16
Q96RQ3	MCCA	50,34	142	29
P04792	HSPB1	49,27	21	6
P50402	EMD	48,82	36	12
P58107	EPIPL	48,57	248	84
P11021	GRP78	46,64	62	26
Q9HCC0	MCCB	45,65	55	20
P10809	CH60	44,68	57	19
P54136	SYRC	42,58	67	28
Q9BRP8	WIBG	41,67	8	5
Q13085	ACACA	41,39	304	79
P42167	LAP2B	41,19	52	14
P0CG47	UBB	40,61	31	3
Q99623	PHB2	40,47	34	11
P11498	PYC	39,90	135	38
P68104	EF1A1	38,31	71	13
P05198	IF2A	38,10	41	10
P14868	SYDC	37,72	60	14
P05166	PCCB	37,66	45	14
P05165	PCCA	37,64	76	20
Q15149	PLEC1	35,85	273	142
P42166	LAP2A	35,16	59	19
P25705	ATPA	35,08	31	14
P35232	PHB	34,93	27	8
Q15365	PCBP1	34,27	36	8
P67809	YBOX1	34,26	11	5
Q96AG4	LRC59	33,88	34	10
P11142	HSP7C	33,13	81	20
Q15046	SYK	32,50	60	20
P23246	SFPQ	32,25	48	19
P62258	1433E	32,16	14	7
Q13509	TBB3	32,00	111	15
P41091	IF2G	31,99	60	12

AccessionNo.	Gene	ΣCoverage	#Hits	# Unique Peptides
P23396	RS3	31,69	12	6
Q7KZF4	SND1	31,32	42	20
Q13155	AIMP2	31,25	11	5
Q9NY65	TBA8	30,73	50	9
P61247	RS3A	30,68	14	8
P52272	HNRPM	30,68	46	15
P05388	RLA0	29,65	13	7
P09429	HMGB1	28,37	10	7
P36542	ATPG	27,85	16	7
P07814	SYEP	27,78	62	32
P31943	HNRH1	27,39	35	7
P63104	1433Z	27,35	12	6
P27348	1433T	27,35	6	5
O14579	COPE	26,95	6	4
P09651	ROA1	26,34	29	9
Q9UMS4	PRP19	26,19	23	7
Q9Y295	DRG1	25,61	25	7
P08195	4F2	25,40	50	13
P08238	HS90B	25,00	57	14
P47897	SYQ	24,90	24	17
P05141	ADT2	24,50	15	7
P41252	SYIC	24,41	55	23
Q14247	SRC8	24,00	18	10
P61981	1433G	23,89	7	5
Q86V81	THOC4	23,74	13	5
P08865	RSSA	22,03	13	4
Q12905	ILF2	21,79	12	5
Q99729	ROAA	21,69	11	6
Q04917	1433F	21,54	6	4
P19338	NUCL	21,41	45	13
P08107	HSP71	21,37	35	11
O75534	CSDE1	21,18	26	14
Q9Y446	PKP3	20,95	26	14
Q9BUF5	TBB6	20,63	50	9
Q96AE4	FUBP1	20,50	16	9
Q14257	RCN2	20,19	20	5
P51659	DHB4	20,11	17	10

AccessionNo.	Gene	ΣCoverage	#Hits	# Unique Peptides
P06576	ATPB	20,04	12	7
P17480	UBF1	20,03	23	11
P04406	G3P	20,00	7	4
Q8WXF1	PSPC1	19,89	16	9
Q9NXA8	SIRT5	19,68	15	6
P20042	IF2B	19,52	10	7
P31946	1433B	19,51	5	4
P48729	KC1A	19,29	7	5
P15924	DESP	19,16	74	38
P17844	DDX5	18,89	25	11
Q92522	H1X	18,78	11	3
P22626	ROA2	18,41	9	5
P42704	LPPRC	18,29	33	19
P02545	LMNA	18,07	20	9
P22087	FBRL	17,76	7	4
Q86UE4	LYRIC	17,53	19	7
P07900	HS90A	17,49	38	10
Q9P2J5	SYLC	17,35	27	15
P00338	LDHA	17,17	15	5
Q13283	G3BP1	17,17	12	5
Q07666	KHDR1	17,16	8	4
Q96CN7	ISOC1	17,11	6	4
P06493	CDK1	16,50	4	4
Q562R1	ACTBL	16,49	29	6
Q92945	FUBP2	16,46	16	7
Q14103	HNRPD	16,34	18	5
P55795	HNRH2	16,26	11	4
P11940	PABP1	16,19	13	7
Q9BY44	EIF2A	15,90	9	6
Q12849	GRSF1	15,63	6	4
Q15366	PCBP2	15,34	28	4
Q00577	PURA	15,22	3	2
O95793	STAU1	15,08	8	6
P09874	PARP1	14,79	20	11
P52597	HNRPF	13,73	25	3
Q01085	TIAR	13,33	5	3
Q00839	HNRPU	13,33	9	6

AccessionNo.	Gene	ΣCoverage	#Hits	# Unique Peptides
Q07065	CKAP4	13,29	7	5
Q8NC51	PAIRB	12,99	4	3
Q08211	DHX9	12,91	27	13
O00165	HAX1	12,90	8	2
P20700	LMNB1	12,63	5	4
Q96P11	NSUN5	12,59	6	4
Q13263	TIF1B	12,57	7	5
Q12906	ILF3	12,42	18	10
O95292	VAPB	12,35	4	2
P49327	FAS	12,35	45	22
P34931	HS71L	12,32	27	6
Q15773	MLF2	12,10	5	2
P04843	RPN1	12,03	8	5
P63244	GBLP	11,99	11	3
Q8WU90	ZC3HF	11,97	6	3
P26583	HMGB2	11,96	5	3
P18827	SDC1	11,94	3	2
Q9H9B4	SFXN1	11,80	6	3
O00571	DDX3X	11,78	18	6
P13010	XRCC5	11,61	8	6
P11387	TOP1	11,50	13	7
Q9Y285	SYFA	11,42	5	3
Q8WXX5	DNJC9	11,15	4	3
O43175	SERA	11,07	6	5
P19525	E2AK2	11,07	9	6
P12268	IMDH2	10,89	4	3
Q14008	CKAP5	10,88	22	17
Q99459	CDC5L	10,85	10	6
Q96I24	FUBP3	10,84	9	5
Q13151	ROA0	10,82	3	2
P16403	H12	10,80	9	2
Q6ZRV2	FA83H	10,77	17	8
Q8NE71	ABCF1	10,53	8	6
Q01813	K6PP	10,46	8	6
Q9NSI2	CU070	10,43	3	2
Q96CT7	CC124	10,31	3	2
P16401	H15	10,18	6	2

AccessionNo.	Gene	ΣCoverage	#Hits	# Unique Peptides
P12956	XRCC6	10,02	5	4
P17066	HSP76	9,95	19	5
P52907	CAZA1	9,79	6	2
P11586	C1TC	9,63	12	8
P40939	ECHA	9,31	5	4
P27824	CALX	9,29	7	4
P32322	P5CR1	9,09	4	2
P47755	CAZA2	9,09	5	2
P62424	RL7A	9,02	4	2
O60841	IF2P	9,02	19	7
P47756	CAPZB	8,66	4	2
P29692	EF1D	8,54	3	1
Q9Y4P3	TBL2	8,28	3	2
P09661	RU2A	8,24	3	2
P02786	TFR1	8,16	8	5
P61626	LYSC	8,11	36	1
P26196	DDX6	8,07	3	2
Q9BXS5	AP1M1	8,04	3	2
Q5T3I0	GPTC4	7,85	4	2
P61978	HNRPK	7,78	4	2
P46109	CRKL	7,59	4	2
P15927	RFA2	7,41	3	2
Q9Y5M8	SRPRB	7,38	4	2
Q3ZCQ8	TIM50	7,37	3	2
Q15717	ELAV1	7,36	8	2
P35250	RFC2	7,34	3	2
Q9Y6Q5	AP1M2	7,33	4	2
P12004	PCNA	7,28	2	1
Q96PK6	RBM14	7,17	6	3
O43290	SNUT1	7,12	4	3
Q9BPW8	NIPS1	7,04	5	2
Q9UJA5	TRM6	6,84	4	3
P50750	CDK9	6,72	3	2
Q01650	LAT1	6,71	4	2
P23258	TBG1	6,65	3	2
Q96HS1	PGAM5	6,57	5	2
Q9BW19	KIFC1	6,54	5	3

AccessionNo.	Gene	ΣCoverage	#Hits	# Unique Peptides
O15347	HMGB3	6,50	2	1
Q16891	IMMT	6,46	5	3
Q8WVV4	POF1B	6,45	5	3
Q7Z2W4	ZCCHV	6,32	5	4
P52292	IMA2	6,24	3	2
Q9UN86	G3BP2	6,22	4	2
Q14694	UBP10	6,02	4	3
O43395	PRPF3	6,00	6	3
O14979	HNRDL	5,95	8	3
Q86XZ4	SPAS2	5,87	3	2
Q08J23	NSUN2	5,87	4	3
P33993	MCM7	5,84	3	3
O00763	ACACB	5,82	50	11
Q01844	EWS	5,79	6	2
P17858	K6PL	5,77	5	3
Q9UJS0	CMC2	5,63	6	3
Q8NC56	LEMD2	5,57	3	2
Q9UJV9	DDX41	5,31	3	2
Q92499	DDX1	5,27	3	3
P26641	EF1G	5,26	3	2
Q9Y3F4	STRAP	5,14	2	1
Q9HC36	RMTL1	5,00	3	2
O43172	PRP4	4,98	3	2
Q9Y3I0	CV028	4,95	4	2
P62753	RS6	4,82	2	1
Q14444	CAPR1	4,80	4	3
Q13435	SF3B2	4,80	6	4
O15446	RPA34	4,71	2	1
Q00325	MPCP	4,70	6	2
P18124	RL7	4,44	2	1
Q9H3N1	TMX1	4,29	2	1
P48634	BAT2	4,27	5	4
P43243	MATR3	4,25	4	2
P13639	EF2	4,20	4	3
P51114	FXR1	4,19	3	2
O43852	CALU	4,13	3	1
Q9NVV4	PAPD1	4,12	3	2

AccessionNo.	Gene	ΣCoverage	#Hits	# Unique Peptides
P05023	AT1A1	4,11	5	3
P27816	MAP4	4,08	5	3
P23771	GATA3	4,06	2	1
O00338	ST1C2	4,05	2	1
P49368	TCPG	4,04	4	2
Q53H96	P5CR3	4,01	2	1
O95817	BAG3	4,00	3	2
P46940	IQGA1	3,98	6	4
O00139	KIF2A	3,97	3	2
P31153	METK2	3,80	3	1
Q5T280	CI114	3,72	2	1
P02768	ALBU	3,61	58	3
P78527	PRKDC	3,59	16	13
Q13724	MOGS	3,58	3	2
P62701	RS4X	3,42	2	1
P08237	K6PF	3,33	3	2
Q15427	SF3B4	3,30	2	1
Q6IN84	MRM1	3,12	2	1
Q12907	LMAN2	3,09	3	1
Q8N1G4	LRC47	3,09	2	1
Q5T0W9	FA83B	3,07	3	3
P14866	HNRPL	3,06	2	1
P35637	FUS	3,04	3	1
P27708	PYR1	2,79	6	4
Q96EY1	DNJA3	2,50	2	1
Q14157	UBP2L	2,21	4	2
Q08379	GOGA2	2,20	3	2
P49916	DNLI3	2,18	3	2
Q9Y230	RUVB2	2,16	2	1
Q8WXU2	DYXC1	2,14	5	1
Q96SB4	SRPK1	2,14	2	1
O94842	TOX4	2,09	2	1
Q9ULX6	AKP8L	2,01	2	1
P01833	PIGR	1,96	11	1
P55084	ECHB	1,90	2	1
Q92609	TBCD5	1,89	3	1
Q00610	CLH1	1,85	3	2

AccessionNo.	Gene	ΣCoverage	#Hits	# Unique Peptides
Q9BQG0	MBB1A	1,81	4	2
Q92896	GSLG1	1,78	3	2
P38646	GRP75	1,77	2	1
Q9Y6X9	MORC2	1,74	4	2
C9JN71	ZN878	1,69	38	1
Q9HCD5	NCOA5	1,55	2	1
Q99985	SEM3C	1,46	2	1
P55265	DSRAD	1,22	2	1
Q5D862	FILA2	0,96	7	2
Q0VF96	CGNL1	0,77	3	2
Q5S007	LRRK2	0,40	3	1

9 Publications

Articles

Rübsamen D., Blees J.S., Schulz K., Döring C., Hansmann M., Heide H., Weigert A., Brüne B., Schmid T. (2012) IRES-dependent translation of egr2 is induced under inflammatory conditions. RNA (accepted).

Blees J.S., Bokesch H.R., **Rübsamen D.**, Schulz K., Milke L., Bajer M.M., Gustafson K.R., Henrich C.J., McMahon J.B., Colburn N.H., Schmid T., Brüne B. (2012) Erioflorin stabilizes the tumor suppressor Pdcd4 by inhibiting the E3-ligase β-TrCP1. PlosOne (in revision).

Schulz K., Milke L., **Rübsamen D.**, Menrad H., Schmid T., Brüne B. (2012) HIF-1α protein is upregulated in HIF2α depleted cells via enhanced translation. FEBS Lett, 586, 1652-7.

Schmid, T., Bajer, M.M., Blees, J.S., Eifler, L.K., Milke, L., **Rübsamen, D.**, Schulz, K., Weigert, A., Baker, A.R., Colburn, N.H. Brüne B. (2011) Inflammation-induced loss of Pdcd4 is mediated by phosphorylation-dependent degradation. Carcinogenesis, 32, 1427-1433.

Yasuda M., Schmid T., **Rübsamen D.**, Colburn N.H., Irie K., Murakami A. (2010) Downregulation of programmed cell death 4 by inflammatory conditions contributes to the generation of the tumor promoting microenvironment. Mol Carcinog, 49, 837-48.

Poster Presentations

2nd UCT Science Day in Frankfurt/Main (2010): Identification of translationally deregulated proteins during inflammation-associated tumorigenesis.

EMBO Conference Series on Protein Synthesis and Translational Control in Heidelberg (2011): Identification of translationally deregulated proteins during inflammation-associated tumorigenesis.

10 Acknowledgement

Zum Schluss möchte ich allen Personen danken, die zum Gelingen dieser Arbeit beigetragen haben:

Bei Prof. Bernhard Brüne bedanke ich mich für die Möglichkeit meine Promotion in seinem Labor durchzuführen, für die Unterstützung während der gesamten Zeit sowie für die Begutachtung dieser Arbeit.

Ein besonderer Dank gilt außerdem Dr. Tobias Schmid für die Vergabe des Themas, seiner ständigen (und ausführlichen!) Diskussionsbereitschaft, die sehr engagierte Betreuung, aber auch für die Möglichkeit des selbstständigen Forschens.

Ich danke außerdem Dr. Claudia Döring für die Auswertung des Microarrays und Dr. Heinrich Heide für die Durchführung der Massenspektrometrie.

Des Weiteren danke ich allen Mitarbeitern der AG Brüne, die mir mit Hilfe und Ratschlägen zur Seite gestanden haben, insbesondere Johanna, Javier, Steffi und Kathrin sowie den ehemaligen Mitarbeitern Nico, Ann-Marie, Martina und Babsi.

Nicht zuletzt möchte ich mich bei meiner Familie bedanken, die mich fortwährend bei allem unterstützen und diese Arbeit mit Anteilnahme verfolgt haben.

Und natürlich danke ich Thomas, der immer an mich glaubt, mich aufbaut, meine Macken erträgt und der mir das außerlaborliche Leben so lebenswert macht!

11 Erklärung

Ich erkläre ehrenwörtlich, dass ich die dem Fachbereich Medizin der Johann Wolfgang Goethe-Universität Frankfurt am Main zur Promotionsprüfung eingereichte Dissertation mit dem Titel

“Identification of translationally deregulated proteins during inflammation-associated tumorigenesis”

am Institut der Biochemie 1 / Pathobiochemie unter Betreuung und Anleitung von Professor Dr. Bernhard Brüne mit Unterstützung durch Dr. Tobias Schmid ohne sonstige Hilfe selbst durchgeführt und bei der Abfassung der Arbeit keine anderen als die in der Dissertation angeführten Hilfsmittel benutzt habe. Darüber hinaus versichere ich, nicht die Hilfe einer kommerziellen Promotionsvermittlung in Anspruch genommen zu haben.

Ich habe bisher an keiner in- oder ausländischen Universität ein Gesuch um Zulassung zur Promotion eingereicht. Die vorliegende Arbeit wurde bisher nicht als Dissertation eingereicht.

Teile der vorliegenden Arbeit wurden in

> Rübsamen D., Blees J.S., Schulz K., Döring C., Hansmann M., Heide H., Weigert A., Brüne B., Schmid T. (2012) IRES-dependent translation of egr2 is induced under inflammatory conditions. RNA (accepted).

veröffentlicht.

Frankfurt am Main, den 15.08.2012